DEVELOPING RELEASABLE ANTIMICROBIAL PEPTIDE-POLYETHYLENE GLYCOL CONJUGATES BY TARGETING INFECTION SITE-ASSOCIATED HOST MATRIX METALLOPROTEINASES

by

Matthew Drayton

B.Sc., Thompson Rivers University, 2015

A THESIS SUBMITTED IN PARTIAL FULFILLMENT OF

THE REQUIREMENTS FOR THE DEGREE OF

MASTER OF SCIENCE

in

THE FACULTY OF GRADUATE AND POSTDOCTORAL STUDIES

(Chemistry)

THE UNIVERSITY OF BRITISH COLUMBIA

(Vancouver)

May 2021

The following individuals certify that they have read, and recommend to the Faculty of Graduate and Postdoctoral Studies for acceptance, a thesis entitled:

Developing Releasable Antimicrobial Peptide-Polyethylene Glycol Conjugates by Targeting Infection Site-Associated Host Matrix Metalloproteinases

submitted by Matthew Drayton in partial fulfillment of the requirements for

the degree of Master of Science

in Chemistry

Examining Committee:

Suzana K. Straus, Professor, Chemistry, UBC
Co-supervisor

Jayachandran N. Kizhakkedathu, Professor, Pathology and Laboratory Medicine, UBC
Co-supervisor

Stephen G. Withers, Professor, Chemistry/Biochemistry and Molecular Biology, UBC
Supervisory Committee Member

Russ W. Algar, Associate Professor, Chemistry, UBC
Supervisory Committee Member

Abstract

The rapid generation of multidrug-resistant (MDR) bacteria has caused bacterial infections to become a global health concern. Antimicrobial peptides (AMPs), or host defence peptides (HDPs), offer a viable solution to these pathogens due to their broad-spectrum activity and low generation of resistance. In addition, many AMPs possess immunomodulatory properties (e.g., anti-inflammatory activity) that may provide a more robust treatment of infection. However, high toxicity and short biological half-lives have greatly limited the production of clinically available AMP therapeutics. Conjugation of the peptides to delivery vehicles such as polyethylene glycol (PEG) has significantly improved these properties but has also been associated with large reductions in antimicrobial activity, making formulation challenging.

In this thesis, an enzymatically releasable PEG-AMP delivery system was developed by incorporating a cleavage sequence susceptible to matrix metalloproteinases (MMPs), enzymes released by the host during the inflammatory response to infection, onto an aurein 2.2-derived AMP. N- vs. C-terminal addition of the sequence found the former to best maintain the activity of the AMP after MMP cleavage, likely due to the maintenance of its amidated C-terminus and higher positive charge. Subsequent conjugation of the cleavable AMP to 2 kDa PEG significantly improved the AMP's blood biocompatibility *in vitro* but also eliminated its activity until cleaved by isolated human MMP. This activity was mimicked in an *in vivo* abscess model of high-density methicillin-resistant *Staphylococcus aureus* (MRSA) infection, where both free peptide and conjugate displayed strong activity confirmed to be dependent on the accumulation

of MMPs at the infection site, as non-cleavable D-isomeric counterparts of the compounds showed no activity.

Following this, the system was expanded to larger PEG molecules by incorporating a tetraglycine spacer between carrier and MMP cleavage sequence. This spacer enabled cleavage of the AMP when bound to 5, 10, and 22 kDa PEG, not possible for the initial peptide, allowing for further improvements in biocompatibility compared to the 2 kDa PEG-AMP conjugate. Altogether, the enzyme-releasable delivery system developed here may provide a suitable platform for the development of infection site-targeting AMP therapeutics where both high biocompatibility and activity can be achieved.

Lay Summary

If left unchecked, the rapid generation of multidrug-resistant bacteria will cause infection-related complications to skyrocket and become one of the top causes of death worldwide. Fortunately, antimicrobial peptides (AMPs) present a promising solution to these infections due to their ability to destroy bacteria with minimal resistance generation; however, few have been developed as clinical therapeutics as they require meticulous formulation to avoid toxic side effects and rapid degradation while still maintaining antimicrobial activity. Here, a delivery system specifically targeting infection sites was developed by linking an enzyme-cleavable AMP to a clinically approved, inert polymer. By doing so, the compatibility of the peptide may be improved until the system reaches an infection site, where the active peptide can then be released via matrix metalloproteinases, enzymes released locally by the body, to eradicate bacteria. Overall, this methodology presents a promising strategy for formulating safe and effective AMP therapeutics to combat multidrug-resistant pathogens.

Preface

All work described herein was conducted under the supervision of Dr. Suzana K. Straus and Dr. Jayachandran N. Kizhakkedathu. Ethics approval for the collection and use of human blood was received by The University of British Columbia Clinical Research Ethics Board (CREB, number H10-01896). Likewise, all animal experiments were performed in accordance with The Canadian Council on Animal Care (CCAC) and with approval by The University of British Columbia Animal Care Committee (protocol A19-0064).

A large portion of Chapter 1 has been published: M. Drayton; J. N. Kizhakkedathu; S. K. Straus. Towards Robust Delivery of Antimicrobial Peptides to Combat Bacterial Resistance. *Molecules*, **2020**, *25* (13), 3048. I performed the literature review and wrote the first draft, which was then edited by Dr. Suzana K. Straus and Dr. Jayachandran N. Kizhakkedathu. I was responsible for incorporating these edits as well as those from the reviewers.

A version of Chapter 2 has been submitted for publication. All peptides and conjugates were designed, synthesized, and purified by me. Dr. Evan F. Haney performed the peripheral blood mononuclear cell cytotoxicity assay, and Morgan A. Alford and Dr. Daniel Pletzer performed all *in vivo* studies. Dr. Suzana K. Straus performed the circular dichroism study, and ^{1}H NMR was performed by Dr. Maria Ezhova. Dr. Yoan Machado and Dr. Christopher M. Overall provided guidance on the development of the non-cleavable peptide. I designed and conducted all remaining experiments and performed the data analysis and presentation for each. Likewise, all work presented in Chapter 3 was performed solely by me with the exception of the macrophage polarization experiment, which was a joint project with Haiming D. Luo. Human

pro-MMPs used in both Chapter 2 and Chapter 3 were generously gifted by the lab of Dr. Christopher M. Overall.

Table of Contents

List of Tables

List of Figures

List of Symbols

c-	centi- (prefix)
Da	dalton
g	gram
g	times gravity
h	hour
k-	kilo- (prefix)
L	litre
m	metre
M	molar concentration
m-	milli- (prefix)
min	minute
n-	nano- (prefix)
s	second
α	alpha
β	beta
γ	gamma
μ-	micro- (prefix)
π	pi
%	percent
°C	degree Celsius

List of Abbreviations

AAC	Antibody-antibiotic conjugate
AEBSF	4-(2-aminoethyl)benzenesulfonyl fluoride hydrochloride
AMP	Antimicrobial peptide
ANOVA	Analysis of variance
APMA	4-aminophenylmercuric acid
APTT	Activated partial thromboplastin time
CCAC	The Canadian Council on Animal Care
CD	Circular dichroism
CFU	Colony forming units
CHCA	α-cyano-4-hydroxycinnamic acid
CPP	Cell-penetrating peptide
CREB	Clinical Research Ethics Board
D_2O	Deuterium oxide
DLS	Dynamic light scattering
DMEM	Dulbecco's Modified Eagle Media
DMF	*N,N*-dimethylformamide
DMSO	Dimethyl sulfoxide
DNA	Deoxyribonucleic acid
DSPE-PEG2000	1,2-distearoyl-sn-glycero-3-phosphoethanolamine-*N*-[amino(polyethylene glycol)-2000]

ECM	Extracellular matrix
EDT	Ethanedithiol
EDTA	Ethylenediaminetetraacetic acid
ELISA	Enzyme-linked immunosorbent assay
EPR	Enhanced permeability and retention
FBS	Fetal bovine serum
FDA	Food and Drug Administration
FITC	Fluorescein isothiocyanate
FRET	Fluorescence resonance energy transfer
HDP	Host defence peptide
HGT	Horizontal gene transfer
HPG	Hyperbranched polyglycerol
HPLC	High performance liquid chromatography
IFN-γ	Interferon gamma
IgG	Immunoglobulin
LB	Lysogeny broth
LDH	Lactate dehydrogenase
LPS	Lipopolysaccharide
mAB	Monoclonal antibody
MALDI-TOF MS	Matrix assisted laser/desorption ionization-time of flight mass spectrometry
MDR	Multidrug-resistant
MFI	Median fluorescence intensity

MIC	Minimum inhibitory concentration
MMP	Matrix metalloproteinase
mPEG	Methoxypolyethylene glycol
MRSA	Methicillin-resistant *Staphylococcus aureus*
MTS	3-[[4,5-dimethylthiazol-2-yl]-5-[3-carboxymethoxyphenyl]-2-[4-sulfophenyl]-2H-tetrazolium]
NLC	Nanostructured lipid carriers
NMR	Nuclear magnetic resonance
NP	Nanoparticle
OD	Optical density
PAGE	Polyacrylamide gel electrophoresis
PAMP	Pathogen associated molecular patterns
PBMC	Peripheral blood mononuclear cell
PBS	Phosphate buffered saline
PE	Phycoerythrin
PEG	Polyethylene glycol
PLGA	Poly(lactide-co-glycolide)
PMA	Phorbol 12-myristate 13-acetate
PPP	Platelet poor plasma
PRP	Platelet rich plasma
RBC	Red blood cell
RNA	Ribonucleic acid

ROS	Reactive oxygen species
SDS	Sodium dodecyl sulfate
SerP	Serine protease
SLN	Solid lipid nanoparticles
SMC	Smooth muscle cell
TES	Triethylsilane
TFA	Trifluoroacetic acid
TNF-α	Tumour necrosis factor-alpha
TRAP	Thrombin receptor activating peptide
UV	Ultraviolet
VSMC	Vascular smooth muscle cell
WTA	Wall teichoic acid

Acknowledgements

I would first like to express my gratitude to Dr. Suzana K. Straus and Dr. Jayachandran N. Kizhakkedathu for the opportunity to work in their labs on such a multidisciplinary, collaborative project. I thank them for all their support and guidance along the away and for the chance to learn and explore fields of research previously unfamiliar to me.

I would also like to sincerely thank our collaborators from the Overall and Hancock labs who made this work possible. In particular, I thank Dr. Parker Jobin, Dr. Reinhild Kappelhoff, and Dr. Yoan Machado for their generosity and insight, and I thank Dr. Daniel Pletzer, Dr. Evan F. Haney, and Morgan A. Alford for their tireless work and determination. I also acknowledge with gratitude all current and past Straus and Kizhakkedathu lab members as well as the supportive work community set up by the Centre for Blood Research.

Finally, I owe a debt of gratitude to my family for their unending support and to the friends I made both in and out of the lab during my time here. More specifically, I thank Julie McNutt, Haiming D. Luo, Morgan A. Alford, Sreeparna Vappala, Chanel La, Kevin Gonzalez, and Dr. Erika Siren, whose encouragement will forever be appreciated.

Chapter 1: Introduction

1.1 Antimicrobial Resistance

1.1.1 History and Generation

The discovery of antibiotic agents has been deemed one of the most impactful advances in modern medicine. Indeed, the administration of penicillin, first discovered by Sir Alexander Fleming in 1928, in the 1940s began what is known as the "era of antibiotics", where once-deadly infections caused even by a small cut in the skin could now be effectively treated[1]. The period of rapid antibiotic discovery that occurred shortly thereafter (termed the 1950s "golden era") contributed to the pivotal role of these agents in medicine and surgery today.

However, specific resistance of the infectious bacteria to these drugs emerged rapidly. In fact, one of the factors initiating the large-scale discovery of antibiotics in the golden era was the need to combat infections by penicillin-resistant bacteria[2,3], which were identified even before the widespread administration of penicillin in World War II[2]. Importantly, β-lactams—a family of chemically modified penicillin derivatives resistant to cleavage by penicillinases, or beta-lactamases—were developed during this period. To date, resistance has been identified for nearly all developed antibiotics[3]. Even bacteria resistant to vancomycin, a promising antibiotic used for the treatment of methicillin-resistant *Staphylococcus aureus* (MRSA) that displayed very little resistance generation in a laboratory setting, were identified only 7 years after the introduction of the drug into clinical practice in 1972[3].

Once the traditional approach of modifying existing antibiotics began to lose its efficacy against these multidrug-resistant (MDR) organisms, many large pharmaceutical companies began to abandon antibiotic discovery programs in the 1980s for other avenues promising greater

profits[4]. Stricter regulatory barriers by, e.g., the United States Food and Drug Administration (FDA) exacerbated the issue, with significant reductions in the number of antibiotics being approved between 1983 and 2007 meaning even effective antibiotics could be rejected for commercial use[3]. As such, the number of novel antibiotics approved by the FDA each year has greatly decreased[3]. Promisingly, though, the approval of 9 new drugs between 2018 and 2019, a significant increase from previous years, suggests this may improve in the near future[5].

Nevertheless, the slow development and approval of effective antibiotics means bacterial infections are once again posing a serious threat to global human health. Experts in the field have estimated that, if left unchecked, these antibiotic resistant-pathogens could cause infection-related deaths to rise to levels observed during the Victorian era or cost 10 million lives per year by 2050[6], which some suggest might actually be an underestimate[7]. Further, on a topical note, many are concerned that the recent COVID-19 pandemic may exacerbate resistance and increase this number, as antibiotics are being heavily overprescribed to COVID-19 patients even when only a small proportion (estimated to be 6.9%[8]) also display bacterial coinfection[8–10]. As such, it is of utmost importance and urgency to develop novel treatments for these infections, as well as more tightly regulate the current excessive use of antibiotics in healthcare and other fields, such as agriculture, that facilitate resistance generation[2,3].

1.1.2 Bacterial Membrane Composition

A key characteristic of an effective antibiotic is its ability to selectively target bacterial cells. Thus, it is important to understand the makeup of these organisms and how they differ from eukaryotic cells. A particularly indispensable understanding is required of the bacteria cell wall, which is potentially the most influential component in regards to antibiotic efficacy and is additionally the target of many antimicrobial peptides (AMPs), introduced in Chapter 1.2.

Bacteria are generally categorized into one of two groups based on the composition of their cell walls. These are termed Gram-positive and Gram-negative bacteria, the namesakes of which derive from the bacteriologist Hans Christian Gram, who developed the staining technique used to differentiate between the two[11]. Gram-negative bacteria, unlike Gram-positive, contain an outer membrane that is key in protecting the cell from the environment (Figure 1.1)[12]. Unlike the cell membrane, this membrane contains fewer phospholipids, which themselves are restricted to the inner leaflet, and instead is made up mainly of glycolipids. Of particular note is the glycolipid lipopolysaccharide (LPS), which promotes the secretion of pro-inflammatory cytokines by immune cells[12]. Theses cytokines are responsible for coordinating the body's innate defence against infection; however, when released in sudden, large amounts, they can result in sepsis, leading to tissue and organ damage that may be fatal[12,13].

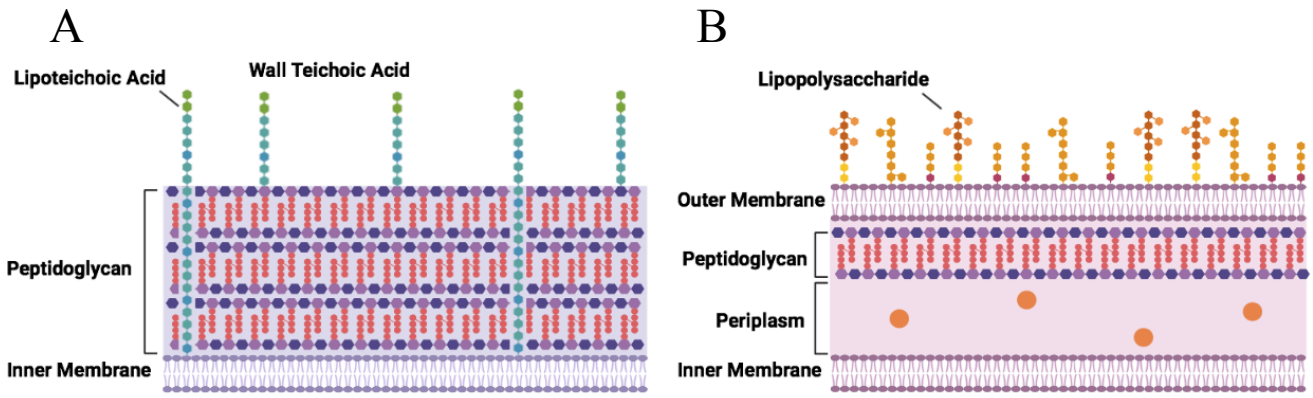

Figure 1.1. Structures of Gram-positive (A) and Gram-negative (B) cell walls. Figure created using BioRender.com and Adobe Illustrator.

Below the outer membrane of Gram-negative bacteria is a thin, rigid layer of peptidoglycan, a polymer consisting of alternating amino sugars called N-acetylglucosamine and N-acetylmuramic acid[12]. Together, the outer membrane and peptidoglycan wall stabilize the

inner membrane, preventing lysis by maintaining the high osmotic pressure found within the cell. In addition to protecting the organism, the outer membrane of Gram-negative bacteria also establishes the periplasm, a viscous space between the inner and outer membranes that is responsible for housing enzymes responsible for cell wall maintenance and for sequestering destructive enzymes, such as RNAse[12].

Conversely, Gram-positive bacteria do not contain an outer membrane (Figure 1.1). Instead, a much thicker layer of peptidoglycan surrounds their inner membrane[12]. Unique to Gram-positive bacteria, this layer also contains anionic glycopolymers that account for a large proportion of the wall's mass and play important roles in, among others, membrane stability, membrane function and intercellular interactions[12,14]. One major group of these polymers is teichoic acids, which can be further categorized into lipoteichoic acids and wall teichoic acids (WTAs) depending on their anchoring to lipids of the inner membrane or to peptidoglycan, respectively[14]. These acids impart a generalized negative charge to the surface of the bacteria, a unique feature that is importantly not displayed by eukaryotic cells[15]. Gram-negative bacteria likewise have an overall negative charge due to the phosphate groups present in LPS[16].

1.1.3 Mechanisms of Resistance

The unique physiological characteristics of bacterial cells can be taken advantage of in the development of antibiotics. In particular, there are five major targets conventionally exploited by antibiotics: the bacterial cell membrane, the peptidoglycan cell wall, nucleic acid synthesis, protein synthesis, and metabolic pathways[17,18].

However, as previously mentioned, many bacteria have quickly developed methods to resist the action of conventional antibiotics. Resistance can be intrinsic, i.e., arising from the inherent structural features of a bacterial species, such as efflux pumps that can remove drugs

from the cytosol, absent targeting structures, and differences in cytoplasmic membrane structures (especially between Gram-positive and Gram-negative bacteria, as discussed earlier); or acquired/developed, either through the acquisition of genetic material from other bacterial species (horizontal gene transfer, HGT) or by mutations in their own chromosomal DNA[19,20]. In fact, the discovery of this genetic mechanism of acquired resistance, first posited in the mid 1950s, completely transformed the field of microbiology and resulted in a much better understanding of the generation and treatment of MDR pathogens[2].

In general, three main mechanisms of acquired antibiotic resistance have been identified: 1. reduction of intracellular antibiotic concentration via drug efflux and/or decreased membrane penetration; 2. modification of antibiotic targets, either genetically or by post-translational modification; and 3. inactivation of the antibiotic itself by degradation (e.g., hydrolysis) or by biochemical modification (e.g., acetylation and phosphorylation)[19,20]. Figure 1.2 summarizes these mechanisms below.

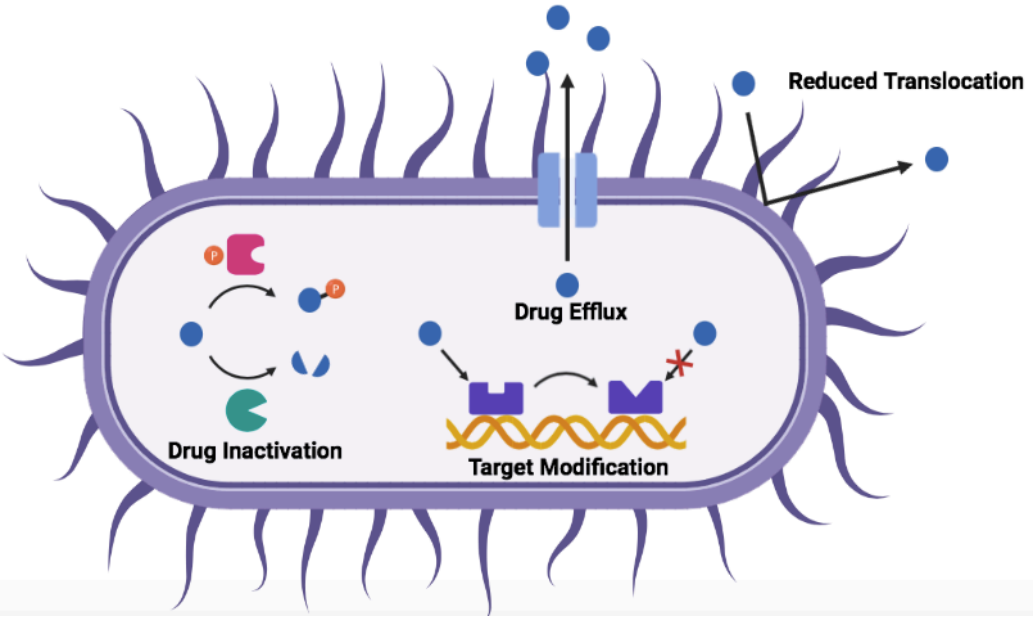

Figure 1.2. Mechanisms of acquired antibiotic resistance by bacteria. Drug represented in dark blue. Figure created using BioRender.com.

Due to the limited availability of small molecule antibiotics and their restricted mechanisms of action and activity spectra, there has been great interest in identifying novel antibiotic alternatives for the treatment of existing and emerging MDR bacteria[21]. In recent years, the development of novel antibiotics has exhibited a shift towards the discovery of novel bacterial targets (e.g., new binding sites in bacterial ribosomes, the cell wall, metabolic pathways, etc.) and towards the development of non-traditional approaches to combat infections (e.g., antivirulent, adjunctive, preventative, microbiota-modulating, and immunomodulating strategies)[4,21,22]. Interestingly, a large fraction of the agents currently in preclinical development focus on pathogen-specific treatment, which has not generally been prevalent in antibiotic history[4]. One particular promising family of compounds that has garnered much interest as both direct acting and immunomodulating therapies against infection is AMPs, discussed below.

1.2 Antimicrobial Peptides as Antibiotic Alternatives

1.2.1 Introduction

Since their first discovery, AMPs, otherwise known as host defence peptides (HDPs), have been identified as key compounds in the host defence systems of virtually all organisms across the three domains of life[23]. In addition to displaying activity against a broad spectrum of bacteria and other pathogenic species[24,25], many AMPs also favourably modulate the host's immune and inflammatory responses to infection[23,26]. Moreover, AMPs have been associated with slower resistance generation compared to conventional antibiotics and have also been found to be effective against biofilm-associated bacteria[21,23]. These properties highlight clear advantages of AMPs over conventional small-molecule antibiotics, but their success in being translated into clinical practice has been low due to a number of inherent biocompatibility shortcomings, as discussed in Section 1.3.1.

1.2.2 Structures and Classes

In nature, AMPs are produced both ribosomally and nonribosomally, with the majority of the latter being synthesized by bacterial species[27]. AMPs synthesized by ribosomal translation of mRNA are found more widely, from bacteria to higher order life forms, and have been found to play critical roles in the innate immunity of these organisms. In humans and other mammals, many ribosomal AMPs are stored within immune cells, specifically in the granules of neutrophils, where they are can be released locally at sites of infection and inflammation; or they are released in skin and mucosal secretions[27]. Their production is also often tightly regulated, with many being expressed as inactive precursors and later activated by proteolytic cleavage[27]. Expression can be constitutive (e.g., in neutrophils, as discussed), or induced by the presence of

pathogen associated molecular patterns (PAMPs) or cytokines during, e.g., inflammation and infection[27].

Generally speaking, AMPs are short polypeptide sequences ranging from 12–50 amino acids with an overall positive charge (generally ≥ +2) and high hydrophobic character (typically 30–50%)[27,28]. As such, they often possess a large number of tryptophan, lysine, and arginine residues. These structural features are responsible for the antimicrobial activity of the compounds: the positive charge enables targeting of bacteria via electrostatic interactions with negatively-charged bacterial membranes (see Section 1.1.2), while the hydrophobicity facilitates interactions with the phospholipid membrane, which can result in disruption of its integrity or can allow for translocation of the peptide into the cytosol where it can target intracellular processes[27].

A common classification system of AMPs utilizes the peptide's secondary structure—that is, their propensity to form α-helical, β-sheet or random-coil/extended structures, the first two of which are most common in nature[27]. In general, α-helical AMPs are unstructured in solution but form amphiphilic structures when in contact with a biological membrane, whereas β-sheet peptides are more structured in solution due to the presence of disulphide bonds, leading to smaller conformational changes upon interaction with lipid membranes. Though extended AMPs often possess no secondary structure, they also fold into amphiphilic structures upon membrane interaction and often contain a high number of proline and histidine residues in addition to arginine and tryptophan[27].

1.2.3 Mechanisms of Action

Facilitated by their amphiphilic and cationic structures, many AMPs directly destroy bacteria through initial interactions with the bacterial membrane[27]. This key electrostatic

interaction forms between the AMP's cationic amino acids and the negatively charged components of bacterial membranes, such as anionic phospholipids (phosphatidylglycerol, cardiolipin, and phosphatidylserine) found in both Gram-positive and Gram-negative bacterial membranes; and teichoic acids and LPS present in the cell wall and outer membrane of Gram-positive and Gram-negative bacteria, respectively[27]. In contrast, mammalian cell membranes possess mainly zwitterionic phospholipids, with negatively charged phospholipids facing the cytoplasm in the inner leaflet of the membrane, if present at all. This difference imparts some selectivity onto the AMP between bacterial and mammalian cells. Interestingly, the loss of this asymmetry in inner and outer leaflets in cancer cells that results in negatively charged phosphatidylserine being found on the outer leaflet is partially responsible for the anticancer activity of some AMPs[29]. In addition to electrostatic interactions, certain AMPs, such as nisin and mesenterecin, also interact with the bacterial membrane through receptor-mediated interactions[29].

The initial interaction with the bacterial membrane is imperative for the direct killing of bacteria by AMPs, which occurs through physical perturbation of the membrane itself and/or through disruption of intracellular processes (e.g., DNA/RNA synthesis, protein synthesis and folding, enzymatic activity, cell wall synthesis, etc.) after translocation through the membrane[27]. Once in contact with the membrane, the AMPs form amphiphilic structures (if not present already, as discussed in Section 1.2.2)—the cationic domains of the peptide interact with the hydrophilic/negatively charged phospholipid head groups, while the hydrophobic domains associate with the hydrophobic fatty acid tails of the lipid bilayer core[27]. Once a sufficient peptide concentration is reached, the AMPs self-assemble at the bacterial membrane, causing membrane permeability either through pore formation (as in the "barrel-stave" and "toroidal

pore" models) or through formation of micelles via detergent-like effects (as in the "carpet" model)[27,29]. This membrane permeabilization ultimately leads to leakage of ions and metabolites, which causes depolarization of the transmembrane potential resulting in impaired membrane function (e.g., osmotic regulation) that eventually leads to membrane rupture and lysis[27]. It can also allow for translocation of AMPs into the cytoplasm for intracellular targeting, as previously mentioned. Many AMPs likely function through multiple complementary actions, which may be partially responsible for the minimal resistance generated by bacteria toward the compounds[27].

In addition to direct bacterial action, many AMPs have been shown to regulate a broad range of immunomodulatory activities that can enhance the host's response to infection. These activities include suppression of pro-inflammatory cytokines and anti-endotoxin activity, which can prevent abnormal and harmful inflammatory conditions (as present in, e.g., sepsis); stimulation of chemotaxis; and immune cell differentiation and activation, which facilitates clearance of bacteria by the host[26,27,29]. In this way, AMPs are thought to provide a more robust treatment of infection through combined antibacterial activity and immune system modulation.

1.2.4 Aurein Peptides

The aurein peptides are AMPs secreted on the skin of Australian southern bell frogs *Litoria aurea* and *Litoria raniformis*[30]. These cationic AMPs form five aurein families, ranging from short and active peptides (Families 1– 3) to longer, typically inactive peptides (Families 4 and 5), which can be further categorized into subfamilies based on length and sequence similarity, denoted by an additional number (e.g., aurein 1.2). Families 1–3 have been particularly well studied, displaying broad-spectrum activity with particularly high potency against Gram-positive bacteria[30]. Our lab has extensively studied the structures and mechanisms of action of two aurein peptides, aurein 2.2 and 2.3, consisting of 16 amino acids with a net

charge of +2 and an amidated C-terminus[30–34]. These AMPs are proposed to function by adopting highly α-helical structures in the membranes of bacteria, forming toroidal pores and causing selective leakage of potassium, magnesium, and iron, which disrupts the transmembrane potential of the bacterial membranes[30–33]. Notably, truncation of aurein 2.2 by three residues from the C-terminus (aurein 2.2-Δ3) has been shown not to hinder its antimicrobial activity[34,35], suggesting it arises mainly from the peptide's N-terminal region.

Previously, our lab generated novel peptides derived from aurein 2.2-Δ3, namely 73 and 77, with 8-fold improved activity by substituting the basic and hydrophobic residues of the peptide with arginine and tryptophan, respectively (Table 1.1)[36]. These residues were chosen as they have been shown to facilitate electrostatic interactions between the AMP and the bacterial membrane (in the case of arginine) and to mediate peptide-lipid interactions (in the case of tryptophan)[37,38]. Furthermore, both amino acids have been shown to improve peptide-membrane interactions by the formation of cation-π interactions[38,39]. The two peptides possess a net charge increase of +1 and a slightly higher mean hydrophobic moment than aurein 2.2-Δ3, with two cation-π interactions between arginine and tryptophan residues possible when in their α-helical forms[30].

Table 1.1. Sequences of aurein 2.2 derivatives. Substituted residues with respect to aurein 2.2-Δ3 are underlined.

Peptide	Sequence[a]	C-terminus	Net Charge (pH 7.4)
aurein 2.2-Δ3	GLFDIVKKVVGAL	-$CONH_2$	+2
73	RLWDIVRRWVGWL	-$CONH_2$	+3
77	RLWDIVRRVWGWL	-$CONH_2$	+3

[a]One letter amino acid codes are as follows: A, alanine; D, aspartic acid; F, phenylalanine; G, glycine; I, isoleucine; K, lysine; L, leucine; P, proline; R, arginine; V, valine; W, tryptophan.

Interestingly, though both peptides displayed improved bactericidal activity against *Staphylococcus aureus*, they possessed less α-helicity than aurein 2.2 in model membranes and caused less membrane perturbation as determined by membrane depolarization and ion leakage[30]. Altogether, these results suggest peptides 73 and 77 likely function by permeabilizing through the cell membrane and interacting with other targets, such as those involved in cell wall biosynthesis, as other arginine- and tryptophan-rich peptides do[30], though further studies are required to determine the exact mechanism of action. Unfortunately, these improved variants also displayed stronger cytotoxicity than aurein 2.2, as determined by hemolysis and cell viability assays[36], necessitating formulation strategies if they were to ever be translated as therapeutic agents.

1.3 Formulating Antimicrobial Peptides for Drug Delivery

1.3.1 Challenges Associated with Antimicrobial Peptides

Despite their promising properties, AMPs suffer from a number of fundamental weaknesses that make their translation into effective antibiotic agents challenging. Firstly, they are inherently susceptible to protease degradation due to the L-amino acids that make up their structure, severely limiting their bioavailability and circulation time when administered to the body (due to, in particular, the presence of blood and stomach proteases)[40]. Furthermore, their small size results in quick removal from the body by kidney filtration and the reticuloendothelial system[27]. Secondly, many AMPs display cytotoxicity towards host cells, which can result in systemic toxicity[41]. This is thought to be largely due to the hydrophobic faces of the AMP, a common characteristic often required for antimicrobial activity, which can enable insertion into mammalian cell membranes. Peptides 73 and 77 display higher toxicity than the parent peptide aurein 2.2 likely due to this reason[36]. Finally, the activity of AMPs can be highly dependent on

environmental factors such as pH, salt concentration, and the presence of proteins/proteases or host cells found in the physiological environment, which can be difficult to model *in vitro*[26,42,43]. Peptide aggregation is likely one of the main factors influencing the activity and toxicity of AMPs in these environments[37].

Indeed, toxicity and low efficacy resulting in non-superiority over conventional antibiotics have been reported repeatedly as reasons for failure in Phase III clinical trials[21]; as such, the majority of AMPs being tested clinically are for topical application, where concerns regarding degradation and widespread toxicity are lessened[21,43]. To minimize these disadvantages, a variety of chemical modifications and delivery vehicles (discussed herein) have been harnessed with the aim of translating safe and efficacious AMP therapies, particularly as systemic agents, into clinical practice.

1.3.2 Formulation Strategies

A number of strategies have been utilized to improve the properties of AMPs. These methods are generally harnessed to improve peptide stability and reduce toxicity profiles, but some also focus on improving their efficacy and specificity. AMP modulations can be categorized into two main families: internal modification (i.e., chemical alteration) and external modification (i.e., delivery vehicle conjugation/encapsulation). In the case of the latter, which is the focus of this thesis, attachment to a delivery vehicle can greatly improve the AMP's biocompatibility and protease stability, but is often accompanied by a decrease in the peptide's activity. As such, release mechanisms may be incorporated to allow for infection-site release of the AMP, improving efficacy and decreasing systemic toxicity. Various formulation strategies and release mechanisms are detailed below (summarized in Figure 1.3).

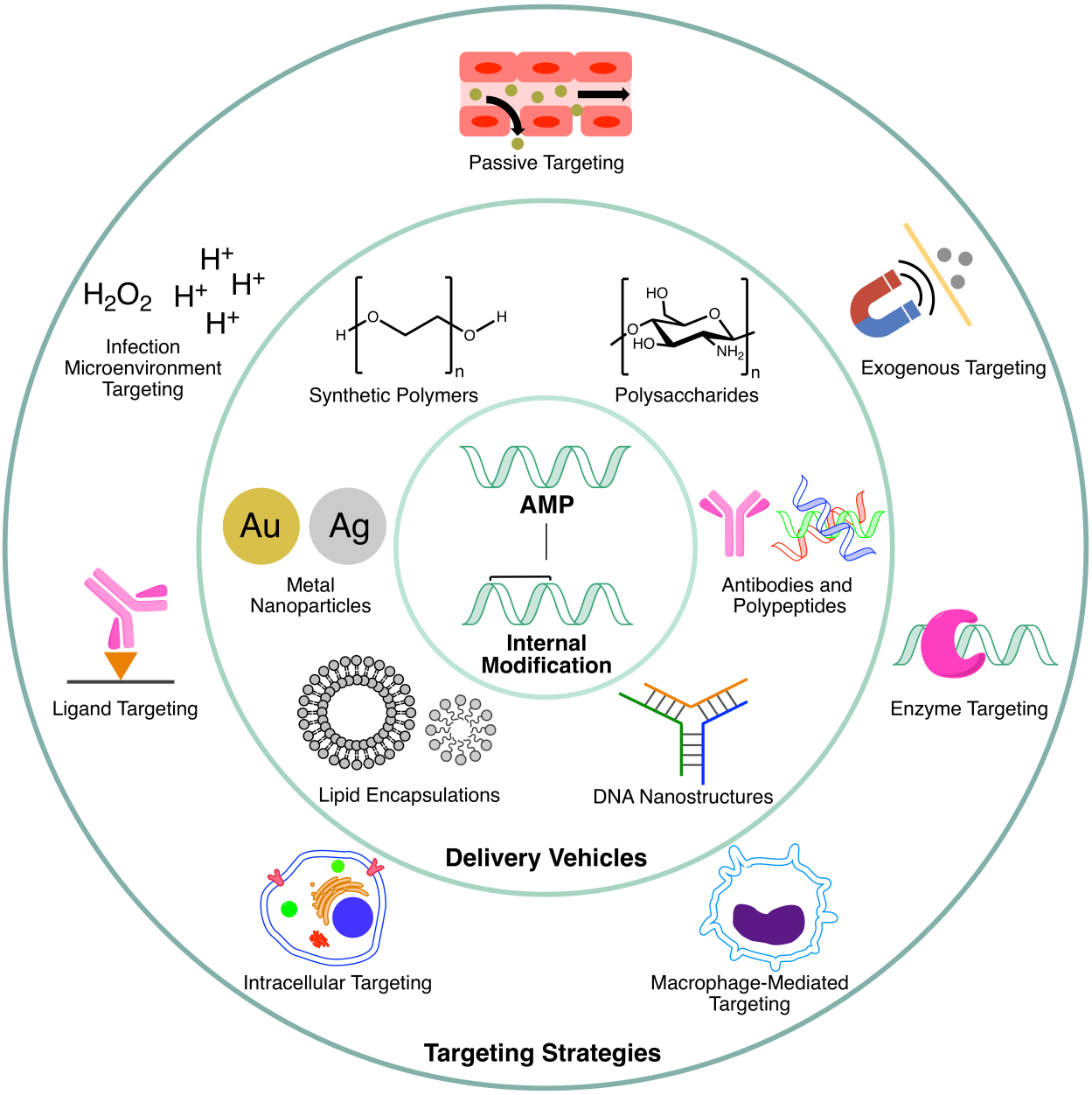

Figure 1.3. Summary of the formulation strategies harnessed in the development of AMP therapeutics.

1.3.2.1 Chemical Modification

One of the most common methods to improve the proteolytic stability of AMPs is isomerization—that is, replacing one or more of the L-amino acids with D-amino acids. This prevents stereospecific proteolysis, which can not only greatly improve *in vivo* circulation time

but can also prolong the activity of these peptides in the presence of proteases (e.g., in blood)[29]. Further, incorporation of D-amino acids does not often negatively affect the antimicrobial activity; in fact, it often improves the AMP's activity, potentially due to resistance to bacterial proteases[29,44,45]. However, D-peptide synthesis is quite costly[46], which presents a major hurdle for translating this approach into clinical practice.

Another common method to improve peptide stability is cyclization. This is generally accomplished by incorporating disulphide bridges via cysteine residues, a motif displayed by human defensins[47], or by introducing hydrocarbon staples between i, i + 4 or i + 7 residues, often by sulfur and nitrogen arylation of cysteine and lysine residues, respectively[48,49]. These staples lock the peptide into an α-helical structure with twisted amide bonds, which are less susceptible to degradation by proteases[46,50]. These staples are not without drawbacks, however: they are often accompanied by unpredictable, often negative effects on antimicrobial activity, cytotoxicity, and solubility[46,50]. Recently, though, Mourtada et al. were able to develop an algorithm for the *in silico* design of stable, nontoxic stapled AMPs (StAMPs) by studying the structure-function-toxicity relationship of 58 StAMPs using magainin II[46]. They determined that staple placement within the peptide's already established hydrophobic face had minimal negative effects on hemolytic activity, while placement in a region that lengthened the entire hydrophobic face substantially increased this activity. This new understanding will undoubtedly be beneficial in the future development of StAMPs.

Finally, many researchers have utilized peptidomimetic approaches to generate AMP alternatives that display improved stability and *in vivo* half-life. These peptide mimics generally imitate the amphiphilic structure of AMPs by using modified amino acids or amino acid-like subunits that alter the chemical composition of the backbone, thereby protecting the structure

from protease degradation[51,52]. A number of these compounds have shown success in clinical trials, such as the defensin mimetic brilacidin[53,54]. Further, Luther et al. recently developed a family of peptidomimetic structures consisting of two linked macrocycles made up of both natural amino acids and synthetic building blocks[55]. A number of the compounds showed low cell toxicity, maintenance of activity in human serum, and strong activity in several mouse models of infection accompanied by good tolerability and pharmacokinetics, suggesting strong potential for success in clinical trials.

1.3.2.2 Delivery Vehicles

Delivery vehicles are a popular strategy used in drug delivery to improve the biocompatibility, stability, and pharmacokinetics of bound drugs. They are particularly promising for AMP formulation as these peptides are often limited to topical applications due to their toxicity and rapid degradation, as previously described. Below, a number of the delivery vehicles showing strong potential for AMP formulation are discussed.

1.3.2.2.1 Lipid Encapsulations

Lipid encapsulation is potentially one of the most common delivery vehicles used for AMP formulation. These lipid encapsulations, which range from liposomes and micelles to nanostructured lipid carriers (NLCs) and solid lipid nanoparticles (SLNs), are generally desired for their high biocompatibility, biodegradability, and safety[56,57]. Further, they can allow for facile encapsulation of both hydrophobic and hydrophilic compounds, particularly important for amphiphilic AMPs. Interestingly, certain lipid nanostructures, such as liposomes and reconstituted lipoproteins, are also being used as "nanodecoys" to trap and detain pathogens and virulence factors to treat infectious diseases[58], thus providing another potential benefit for AMP formulation. Recently, our labs utilized polymeric micelles composed of 1,2-distearoyl-sn-

glycero-3-phosphoethanolamine-*N*-[amino(polyethylene glycol)-2000] (DSPE-PEG2000) lipids as a delivery vehicle for a number of aurein 2.2-derived AMPs[59]. The encapsulated peptides showed marked decreases in hemolytic activity and improved biocompatibility. Furthermore, the most promising peptide showed strong antimicrobial activity in an *in vivo* mouse abscess model at 5 mg/kg, reducing abscess size by 85% and bacterial count 510-fold. However, controlled and/or targeted release of encapsulated drugs can be difficult to achieve with these lipid-based formulations.

1.3.2.2.2 Metal Nanoparticles

Metal nanoparticles have also gained great interest as delivery vehicles for AMPs due to their large surface area-to-volume ratio, which enables multiple molecules to be loaded onto their surface, and their innate antimicrobial activity[60]. Further, their unique magnetic, electrical, and thermal properties can easily facilitate exogenous targeting techniques, as discussed in Section 1.3.2.4.4. The two metal nanoparticles that have been most explored for AMP conjugation are gold nanoparticles (AuNPs) and silver nanoparticles (AgNPs). In general, AgNPs display stronger innate antimicrobial activity but are accompanied by high toxicity, whereas AuNPs exhibit relatively higher biocompatibility and lower toxicity. In fact, some researchers have actually utilized surface peptide conjugation to decrease the cytotoxicity of AgNPs[61,62]. Notably, a number of AMP-AuNP conjugates have used DNA aptamers to increase cellular uptake for targeting intracellular bacteria[63,64]. These conjugates displayed strong efficacy both *in vitro* and *in vivo* alongside low toxicity. However, the generally high toxicity of metal nanoparticles compared to other delivery vehicles as well as concerns regarding non-biodegradability and unknown interactions with cellular functions limit their usefulness as AMP delivery vehicles.

1.3.2.2.3 Synthetic Polymers

Synthetic water-soluble polymers are one of the most popular delivery vehicles for drug formulation, as they have been shown to greatly improve the biocompatibility, stability, and circulation time of the payload[65]. In the case of polyethylene glycol (PEG), potentially the most well-studied water-soluble polymer, this is accomplished by steric repulsion, whereby the drug is shielded from opsonization and enzymatic degradation within the biological environment[65]. Other water-soluble polymers likely confer the same protection in this way. In regards to AMP formulation, a number of polymeric structures have been harnessed, falling into three main categories: linear polymers (e.g., PEG), dendrimer-like polymers (e.g., hyperbranched polyglycerol, HPG), and polymeric nanoparticles (e.g., poly(lactide-co-glycolide), PLGA).

As mentioned, PEGylation is one of the most popular synthetic polymers used for drug delivery and has had the best success in clinical trials thus far[65]. It has been used in AMP conjugation to substantially reduce the cytotoxicity of a number of AMPs, including tachyplesin I[66], a magainin 2 derivative[67], the heparin cofactor II fragment KYE28[68], the synthetic AMP CaLL[69], and, more recently, the disulphide-rich AMP cryptdin[70]. However, in each case, the antimicrobial activity of the peptide was significantly reduced upon PEG conjugation, once again highlighting the necessity for release mechanisms to maintain activity while still allowing for improved biocompatibility. Moreover, PEG itself has some drawbacks, including non-biodegradability, high intrinsic viscosity, and mono-/bi-functionality[29].

PLGA nanoparticles have been used heavily for AMP encapsulation due to their ability to confer prolonged drug release and protection of the payload from the biological environment. Further, PLGA itself has a number of properties that make it promising for AMP formulation: it is biodegradable, which lessens worries regarding bioaccumulation[71]; and it displays wound

healing properties, which is an area where AMPs are often utilized[72]. Indeed, the latter has been explored by Vijayan et al., who conjugated an AMP to growth factor-encapsulating PLGA nanoparticles for the co-delivery of these two therapeutic agents for wound healing, where they displayed moderate antimicrobial activity alongside sustained growth factor release[73]. Notably, PLGA nanoparticles have been shown to improve the efficacy and delivery of the AMP plectasin against *S. aureus*-infected bronchial epithelial cell monolayers[74]. Additionally, poly(vinyl alcohol)-coated PLGA nanoparticles improved the transport of encapsulated AMP esculentin-1 through an artificial lung mucus and bacterial barrier, and displayed 4- to 17-fold enhancement of activity in an *in vivo* lung infection mouse model[75]. These results suggest PLGA-AMP nanoparticles could be useful for the treatment of bacterial infection in cystic fibrosis patients.

Our labs have worked heavily on the application of the dendrimer-like polymer HPG for a variety of biomedical applications, including cell surface engineering, organ preservation, macromolecular therapeutics, and the delivery of therapeutic agents, including AMPs[76]. Indeed, HPG is a promising water-soluble polymer that has gained much attention in recent years due to its high biocompatibility, multi-functionality and tunability, and stability[76]. Furthermore, synthesis of HPG is easy and can be made biodegradable by the incorporation of moieties like acid-sensitive linkages to prevent bioaccumulation[77].

Concerning AMP conjugation, our groups first demonstrated that covalently attaching aurein 2.2 to moderate molecular weight (44 kDa) HPG significantly improved its biocompatibility in blood and cell culture[78]. However, the conjugates displayed significantly lower *in vitro* activity against *S. aureus* and *Staphylococcus epidermidis*. It was suggested that this decrease in activity might be due to interactions of the AMP with the polymer or from reductions in peptide-membrane contact due to the large size of the complex. Promisingly, the

efficacy and biocompatibility of the conjugates were dependent on peptide density, which ranged from 7–18 AMPs per polymer, highlighting the favourable ability to tune HPG properties for optimizing drug delivery. This tunability was further studied by conjugating peptide 77 to HPG of different molecular weights (22–105 kDa)[36]. These conjugates once again displayed strong biocompatibility, and they also conferred resistance to trypsin degradation. The most promising conjugate, a 22 kDa HPG containing 7–8 AMPs, displayed moderate *in vitro* activity against *S. aureus*, with an MIC of 50 μg/mL (roughly 6-fold higher than peptide 77); unfortunately, however, the *in vivo* activity of the peptide in a mouse abscess model was completely lost upon conjugation (data not published), highlighting a clear case where AMP release would be beneficial. In another case, mixing HPG polymers containing a hydrophobic core surrounded by carboxylic acid-functionalized PEG groups with the synthetic AMP IDR-1018 was used to significantly reduce the aggregation of the peptide both *in vitro* and *in vivo* without affecting the immunomodulatory activity of the peptide[79]. This formulation proved more efficacious than others using hyaluronic acid and cellulose derivatives.

1.3.2.3 Natural Biomolecules

As alternatives to synthetic polymers and metallic nanoparticles, natural biomolecules have garnered interest in recent years as AMP carriers primarily due to their innate biocompatibility and biodegradability. Below, a number of these biomolecules are discussed.

1.3.2.3.1 Polysaccharides

Chitosan is a popular polysaccharide used for AMP delivery. It is a linear sugar made up of glucosamine and *N*-acetylglucosamine subunits, and in addition to its high biocompatibility and biodegradability, it also displays bioadhesive, wound healing, and mild antibacterial properties[80]. These properties can be extensively tuned by molecular weight and by chemical

modification of amine groups by, e.g., deacetylation. A number of papers have detailed the utilization of chitosan to improve the biocompatibility of AMPs[80–84]. For example, Hou et al. developed short chain chitosan-polylysine AMP nanoparticles displaying low hemolytic activity alongside strong, broad-spectrum activity *in vitro* and *in vivo*, and improved selectivity[83]. However, concerns remain regarding inconsistent characteristics based on source and unpredictable degradation profiles of chemically modified chitosan, which is often required to maintain uniform physiochemical properties[85].

1.3.2.3.2 Polypeptides

Interestingly, cell penetrating peptides (CPPs), short peptides with similar structures and often similar antimicrobial activities to AMPs, have been attached to AMPs to improve their activity and specificity, particularly against Gram-negative bacteria[86,87]. These peptides often negligibly affect the cytotoxicity of the AMP. Similarly, short polycationic hexa-arginine polypeptides have recently been conjugated to vancomycin to bypass multiple modes of vancomycin resistance in bacterial strains while simultaneously increasing antimicrobial activity 1000-fold *in vitro*[88]. The conjugates were efficacious *in vivo*, exhibited improved biodistribution and excretion profiles compared to free vancomycin, and displayed no cytotoxicity in blood or cell culture.

Furthermore, certain AMPs have been structurally manipulated to form dendritic structures that display strong antimicrobial activity, improved serum stability, and reduced hemolysis[89]. These structures are formed by a branching lysine core, off which peptide branches can form via reactions with the lysine amine groups. Tetrabranched AMP oligodendrimers, sometimes referred to as multiple antigen peptides, have likewise displayed these properties[90,91]. The tetrabranched AMP M33-L displayed strong antimicrobial activity, which translated well in

mouse sepsis models, high serum stability, and lower toxicity compared to the clinically used peptide colistin[91]. Isomerization of the dendrimer further improved the AMP's activity, potentially by increasing resistance to bacterial proteases[92].

1.3.2.3.3 Antibodies

Due to their innate bacteria/toxin targeting and neutralizing activities, many human monoclonal antibody (mAb) therapies are currently being developed and tested in clinical trials for the treatment of bacterial infection[93]. These antibodies generally exhibit long half-lives, slow host clearance, and high biocompatibility[94]. Further, their pathogenic specificity can prevent native microbiome disruption and provide a targeting mechanism for conjugated drugs. As such, antibodies have garnered great interest as delivery vehicles for conventional antibiotics as compounds called antibody-antibiotic conjugates (AACs). Notably, Lehar et al. developed an AAC composed of a rifamycin analogue bound to an antibody specific to the β-*N*-acetylglucosamine residues of WTAs[95]. Upon uptake of AAC-opsonized *S. aureus* by immune cells, the antibiotic was released from the antibody by phagolysosomal cathepsins, which recognized the dipeptide cleavage sequence between the two molecules. These AACs displayed strong *in vitro* activity against intracellular bacteria, and also showed strong efficacy against MRSA in a mouse bacteraemia model.

There are a limited number of published examples of antibody-AMP conjugates to date. The first comes from Franzma et al., who conjugated the AMP SMAP28 to rabbit immunoglobulin (IgG) antibodies specific to a strain of *Porphyromonas gingivalis*[96]. Though the conjugate showed strong activity against the targeted strain *in vitro*, its specificity decreased at higher concentrations. More recently, Touti et al. conjugated cathelicidin-derived macrocyclic AMPs to antibodies specific for *E. coli* strains[97]. The antibody chosen targeted core LPS glycans

present on the surface of bacteria in high density in hopes this would facilitate interaction of the bound AMP with the cell surface. Conjugation of peptide to AMP was accomplished enzymatically via sortase A donor and acceptor peptide tags found on the AMP and antibody, respectively. The most promising conjugates displayed minimal hemotoxicity and strong bactericidal activity against certain strains of *E. coli*, though this specificity was once again diminished at higher concentrations. To note, half of the studied conjugates displayed no activity, highlighting the difficulties that can arise in the development of non-releasing antibody-AMP conjugates.

Although antibodies possess a number of advantages relating to clinically relevant applications, they also suffer from some drawbacks. Firstly, their high specificity (i.e., narrow spectrum) can be a disadvantage in the treatment of polymicrobial infections. Secondly, they often require extensive and costly optimization[93]. And thirdly, their targeting can be hindered by cell-wall components such as WTAs that can conceal cell surface epitopes[98].

1.3.2.3.4 DNA Nanostructures

Recent advances in the development and chemistry of DNA nanostructures has made them particularly promising for a wide variety of biomedical applications. In particular, these structures are appealing for drug delivery as they are small in size, highly soluble and biocompatible, biodegradable, and responsive to stimuli[99,100]. Furthermore, they can be extensively tuned to allow for very precise attachment of multiple therapeutics and targeting ligands. Recently, Mela et al. showed the capability of DNA nanostructures to combat bacteria at infection sites by functionalizing lysozyme-containing DNA origami nanostructures with aptamers targeting both Gram-positive and Gram-negative bacteria[101]. Similarly, Obuobi et al. developed DNA hydrogels for the topical release of an AMP upon degradation by nuclease-

secreting MRSA[100]. These AMP-loaded nanostructures enabled sustained release of the peptide in response to environmental nucleases, which substantially decreased the toxicity of the peptide against cultured dermal cells. Further, the hydrogel maintained good antibacterial activity in an *in vivo* porcine skin model with a single application and improved the wound healing rates due to anti-inflammatory properties thought to have arisen from the DNA nanostructures themselves, highlighting another potential advantage of these nanostructures for AMP delivery.

1.3.2.4 Release Mechanisms

In most cases where delivery vehicles are utilized for drug delivery, the payload is directly conjugated to or encapsulated in the vehicle as a means to improve the drug's biocompatibility, stability, and circulation time. However, without a release mechanism, this formulation strategy can often hinder the activity of the bound drug, which is particularly relevant for AMPs that require access to the bacterial membrane surface for their activity. In some cases, non-specific release (e.g., hydrolytic release) has been harnessed for prolonged release of the drug, but this can raise concerns regarding off-site toxicity[65]. As such, there has been great interest in developing targeting mechanisms that release the payload at the diseased site. For targeting the site of infection in AMP delivery, three main release mechanisms can be utilized: passive targeting, endogenous targeting (i.e., targeting the biochemical microenvironment of infection), and exogenous targeting (i.e., using extrinsic guidance and release by external stimuli).

1.3.2.4.1 Passive Targeting

As mentioned, hydrolytic release is a commonly utilized approach for continuous release of payloads over days to months[65], accomplished by ester[65] or ketal[77] moieties between the delivery vehicle and drug. However, this not only raises concerns regarding off-site toxicity, but

can also necessitate higher doses of the drug to maintain suitable concentration at the disease site. For infection site targeting, a phenomenon known as the enhanced permeability and retention (EPR) effect can also be utilized as a means of passive targeting. This effect results from an increase in vascular permeability and lymphatic retention arising from inflammation and activation of immune cells by the release of toxic bacterial agents (e.g., LPS and lipoteichoic acid) at the site of infection[102–104]. Nanoparticles such as PEG-coated liposomes have been shown to accumulate in mouse tissue infection by *S. aureus* in this way[105–107].

1.3.2.4.2 Endogenous Targeting

The unique microenvironment of the infection site can also be exploited for targeting. Vancomycin[108,109], antibodies[110], aptamers[63,64], and lectins[111,112] have all been used in nanoparticle formulation to target infection-associated ligands or structures on the bacterial surface. However, ligand-based targeting strategies can be limited by a lack of target accessibility and by the structural heterogeneity of targets[113].

In addition, pH, redox gradients, and enzymes associated with the infection site can be utilized for targeted delivery of AMPs. As the pH of infection sites can reach as low as 4.5 in the case of biofilms due to anaerobic fermentation and inflammation[113–116], pH-sensitive linkers (e.g., hydrazone, aconityl, and acetal/ketal linkages) that are stable in blood but hydrolyze at low pH can potentially be harnessed for infection site release of antibiotics. These can also be useful in targeting specific tissues that bacteria often inhabit, such as the gastrointestinal tract and skin[114]. Additionally, targeting pH is beneficial for polymicrobial infections as well as broad-spectrum bacterial treatment, as it does not discriminate between bacteria type. Notably, Radovic-Morena et al. developed pH-responsive poly(D,L-lactic-co-glycolic acid)-b-poly(L-histidine)-b-PEG nanoparticles encapsulating vancomycin for pH-sensitive binding to

bacteria[114]. Protonation of surface histidines at low pH was used to generate strong electrostatic interactions between the nanoparticles and the negatively charged bacterial membrane.

Similar to pH, the local redox environment is also altered locally at infection sites due to the accumulation of reactive oxygen species (ROS) in inflamed tissue[113,117], thereby providing a potential means for targeting infection via redox-sensitive linkers. No reports have been published thus far utilizing this mechanism for AMP release. Additionally, enzyme-cleavable linkers can be harnessed to target enzymes (e.g., proteases, lipases, and glycosidases) secreted by the bacteria and/or released by the host in response to infection[113]. Protease targeting is particularly useful for AMP formulation as these cleavage sequences can be directly adjoined to the peptide termini during chemical synthesis or peptide expression. Notably, matrix metalloproteinases (discussed in Section 1.4), which are secreted in large amounts by the host in response to infection-associated inflammation[118], provide a promising target here.

1.3.2.4.3 Intracellular Targeting

The body's first response to pathogenic bacteria is the innate immune system. Within minutes, immune cells such as macrophages, neutrophils, and phagocytic cells engulf invading bacteria and destroy them via fusion of acidic lysosomes, which contain digestive enzymes, bactericidal proteins (e.g., lysozyme), ROS, and reactive nitrogen species[118–120]. However, it has fairly recently been discovered that a number of bacterial species, such as *Escherichia coli* and *S. aureus*, have developed ways to withstand this process, resulting in immune cells housing pathogenic bacteria for prolonged periods of time and disseminating them to other tissues throughout the body[95,121]. These intracellular bacteria are thought to be key players in chronic infections and can be particularly difficult to treat due to their location within the cell, where

they can avoid non-membrane passing antibiotics and enter into dormant states (e.g., small colony variants and persister cells) that alter their susceptibility to antibiotics[94].

Fortuitously, the intracellular bacterial environment provides a number of means by which antibiotics can be released upon cellular uptake or fusion with acidic endosomes and lysosomes[65,113]. Firstly, the cytosol is a highly reducing environment, which can allow for cleavage of disulphide linkers. Uptake in acidic phagolysosomes can also enable cleavage of the acid-sensitive linkers previously mentioned and cleavage of linkers susceptible to lysosomal proteases, such as cathepsin B.

The uptake of bacteria by phagocytic cells provides another unique method of nonspecific infection targeting. Xiong et al. utilized conjugated mannosyl ligands to delivery vancomycin-loaded nanogels to macrophages, which possess many cell surface mannose receptors, in order to take advantage of their innate bacteria scavenging abilities[122]. Upon being engulfed by the macrophages, the bacteria were then destroyed by vancomycin, which was released from the nanogel's polyphosphoester core by degradation from bacterially produced phosphatase or phospholipase. In another case, Hou et al. enhanced cultured macrophages using vitamin A lipid nanoparticles containing mRNA encoding an AMP-cathepsin B conjugate[123]. After translation in the cytosol, the resulting protein-peptide conjugate was delivered to the lysosome due to its cathepsin-B tag and subsequently cleaved by the enzyme to release the broad-spectrum AMP. These lysosomally enhanced macrophages were able to destroy intracellular MDR *E. coli* and *S. aureus*; furthermore, they facilitated immune system recovery in septic mice.

1.3.2.4.4 Exogenous Targeting

Unlike endogenous targeting, exogenous targeting utilizes stimuli outside the body to guide the responsive carrier to the infection site and/or to provide localized release of the bound drug. Temperature changes, electric or magnetic fields, light, and lasers are all examples of externally applied stimuli used for this purpose[113,124]. For example, Meeker et al. developed photoactivatable gold nanocages conjugated with *S. aureus*-targeting antibodies that released daptomycin in response to near-infrared light irradiation[110]. These nanoparticles eradicated both planktonic and biofilm-associated *S. aureus*, in part due to the localized bactericidal photothermal effects of the irradiation. The authors suggest these particles, with development, could show great promise in the treatment of orthopedic infections, where surgeons have direct access to the site of infection. Thermo-responsive polymers[125] as well as magnetic-responsive chitosan microbeads[126] and iron oxide nanoparticles[127] have also been explored for the controlled release of alamethicin, vancomycin, and cecropin mellitin, respectively.

1.4 Matrix Metalloproteinases as Targets in Infection

1.4.1 Structure, Classification, and Distribution

Since the first discovery of matrix metalloproteinase (MMP) activity initially identified in 1962 as collagenolytic activity in metamorphosing tadpoles[128], 28 vertebrate MMPs have been identified[129]. These proteases are multidomain, zinc (Zn^{2+})-dependent metalloproteinases that process and degrade a number of extracellular membrane (ECM) components, including collagen and gelatin[129]. MMPs are highly homologous, specifically to collagenase-1 (MMP-1), so not unexpectedly, they share a common core structure consisting of: a propeptide domain, which prevents MMP activity by occupying the active site of the enzyme and is removed upon activation; a catalytic domain, which contains the Zn^{2+}-binding motif and mediates substrate

proteolysis; a linker peptide domain of variable length; and a hemopexin domain, which is thought to facilitate protein-protein interactions and generate substrate specificity[129,130]. The activation of MMPs from their inactive (pro-MMP) to active (MMP) forms is mediated by the propeptide domain's cysteine-switch motif, which chelates the Zn^{2+} in the active site until cleaved by other proteolytic enzymes, such as serine proteases or other MMPs[129]. The large family of MMPs can be further broken down into smaller groups based on the substrates and structural features of the enzymes, as listed in Table 1.2**.**

Table 1.2. Categorizations of MMPs and their distributions in the human body.[129,131]

Family	MMP	Sources (Cells and/or Organs/Tissues)
Collegenases	MMP-1	*skin* endothelial cells, fibroblasts, keratinocytes, platelets, SMCs, macrophages
	MMP-8	macrophages, neutrophils
	MMP-13	*skin* macrophages, SMCs, fibroblasts, keratinocytes, osteoblasts, osteoclasts
Gelatinases	MMP-2	*skin* endothelial cells, platelets, polymorphonuclear leukocytes, osteoblasts, osteoclasts, fibroblasts, keratinocytes
	MMP-9	*skin* endothelial cells, VSMCs, polymorphonuclear leukocytes, macrophages, fibroblasts, keratinocytes, osteoblasts, osteoclasts
Stromelysins	MMP-3	*skin* endothelial cells, epithelial cells, VSMCs, platelets, fibroblasts, keratinocytes
	MMP-10	*skin* epithelial cells, fibroblasts, keratinocytes
	MMP-11	*uterus, placenta, brain*

Family	MMP	Sources (Cells and/or Organs/Tissues)
Matrilysins	MMP-7	*skin* endothelial cells, glandular skin epithelial cells, VSMCs
	MMP-26	*uterus, placenta, kidney*
Membrane-Type (MT) MMPs	MMP-14	*skin* fibroblasts, keratinocytes, osteoblasts, osteoclasts, VSMCs, platelets
	MMP-15	*placenta, brain, heart* fibroblasts, leukocytes
	MMP-16	*lung, kidney, spleen, heart, reproductive tissue* leukocytes
	MMP-17	*brain, reproductive tissue* leukocytes
	MMP-24	*lung, kidney, brain* leukocytes
	MMP-25	*lung, spleen, kidney,* leukocytes
Others	MMP-12	SMCs, fibroblasts, macrophages
	MMP-19	*liver, kidney, lung, brain, heart, reproductive tissue, skin* fibroblasts, keratinocytes, leukocytes
	MMP-20	*dental tissue*
	MMP-21	*placenta, kidney, liver* fibroblasts, macrophages
	MMP-23	*reproductive tissue*
	MMP-27	*heart, kidney, bone* leukocytes, macrophages
	MMP-28	*skin, brain, lung, heart, kidney, pancreas* keratinocytes

SMCs: smooth muscle cells; VSMCs: vascular smooth muscle cells

1.4.2 Roles in the Human Body

MMPs are expressed by a large array of tissues and cells throughout the body, including fibroblasts, endothelial cells, and vascular cells, as well as by the macrophages, neutrophils, and lymphocytes of the immune system (Table 1.2)[129,131]. Though MMPs have historically been known to chiefly play major roles in ECM remodeling, their functions have since expanded to a number of other important processes, including cell proliferation and differentiation, angiogenesis, and wound healing; additionally, they have been associated with immune modulation by facilitating leukocyte recruitment, cytokine processing, and defensin activation[129,132]. When not controlled, however, the overexpression of MMPs may contribute to a number of harmful pathologies, including cancer (e.g., tumor progression), inflammation, and tissue invasion[129]. As such, MMPs are tightly regulated by a number of mechanisms. For one, aside for MMP-8 and MMP-9, they are generally not stored within cells and require gene transcription for secretion, upon which they are held in close proximity to the cell[132]. Furthermore, as previously mentioned, they are secreted as pro-enzymes that must undergo proteolytic cleavage in order to become activated. And lastly, their activity is regulated by inhibitors called tissue inhibitors of metalloproteinases, secreted by the host[132].

1.4.3 Presence During Bacterial Infection

An essential mechanism of the innate immune system's initial response to bacterial infection is inflammation, whereby the release of chemoattractants, inflammatory cytokines and chemokines, and histamine, and the presence of PAMPs such as LPS mediate the recruitment of inflammatory cells (e.g., leukocytes) to the site of infection[133]. Many of these cells must migrate from the blood stream through the endothelium and, in many cases, across mucosal and epithelial barriers in order to reach the site, which requires the breakdown of the basement

membrane[132,133]. Released MMPs are partially responsible for this process, degrading the components of the ECM and modulating the activity of present cytokines and chemokines to regulate chemoattraction[132]. Neutrophils, the most abundant leukocyte and the first to arrive at infection sites, are then able to fight invading bacteria through direct phagocytosis and by the release of additional MMPs (mainly MMP-8 and MMP-9) as well as toxic components such as ROS, lysozyme, and AMPs[118,133] As such, MMP expression is markedly increased during inflammatory processes like infection[133], thereby providing a targeting mechanism by which AMPs or antibiotics may be released at infection sites.

1.5 Thesis Rationale, Hypotheses, and Aims

In the fight against the increasingly pressing global health crisis of MDR pathogens, it is imperative to generate novel antimicrobial therapeutics both for the current treatment of resistant organisms and for the prevention of further generation of resistance. AMPs promise an exciting solution in this regard due to their broad range of activity, strong efficacy against MDR bacterial strains, and low resistance generation. Furthermore, many AMPs can also beneficially modulate the host's response to infection, providing a potentially more robust and comprehensive approach for treatment.

Unfortunately, however, the translation of AMPs into clinical practice has been limited, with only cyclic, lipo- and/or glycopeptides currently being available commercially[134]. This is likely due to a number of inherent drawbacks of exogenously applied AMPs, including protease degradation (e.g., in serum), aggregation leading to activity loss and toxicity, short biological half-life, and nonspecific or systemic toxicity. Indeed, the majority of commercially available AMPs have cyclic structures, which generally have higher biological stabilities compared to linear AMPs, and some are used solely as last-resort intravenous treatments (e.g., colistin) or as

topical treatments (e.g., bacitracin and gramicidin) due to high host toxicities[134,135]. Furthermore, a large proportion of the AMPs—particularly the synthetic linear AMPs—currently in clinical trials are limited to topical applications, where these concerns are minimized[134].

As such, appropriate strategies are needed in order to formulate safe and effective AMP therapeutics. The use of delivery vehicles, particularly biocompatible polymers, has been heavily explored for improving the biocompatibility of bound AMPs, but this is often accompanied by significant losses in activity compared to the free peptide. Previous work in our labs detailing the conjugation of aurein 2.2 and its derivative 77 to HPG certainly displayed this trend. To address this issue, it was hypothesized that incorporating an enzymatically cleavable linker between the polymer and the AMP sensitive to proteases expressed largely at sites of infection (e.g., MMPs) could marry the improved stability and biocompatibility conferred by the polymer with the unhindered activity of the free peptide. Thus, the aims of my thesis were to: 1. develop and characterize a bioconjugation system incorporating PEG and a new AMP consisting of peptide 73 and a cleavage site targeting infection site-related MMPs; and 2. explore methods to modify and translate the system to improve its overall biocompatibility. These will be described in Chapter 2 and Chapter 3, respectively, as outlined below.

1.5.1 Developing an Enzyme-Releasing Peptide-Polymer Delivery System for Infection Site Delivery of Antimicrobial Peptides

Previous work on conjugating aurein 2.2. and peptide 77 to HPG has demonstrated the substantial advantages of utilizing biocompatible polymers to improve the toxicity and stability profiles of AMPs. However, losses in antimicrobial activity (particularly *in vivo*) suggest a mechanism enabling release of the AMP from the polymer in the presence of infection is necessary for maintaining efficacy. In Chapter 2, the development and characterization of a

protease-cleavable bioconjugate incorporating the AMP 73 and PEG is detailed. I hypothesized that incorporating a linker sequence targeting enzymes concentrated locally at infection sites, namely MMPs, between AMP and polymer would reduce the toxicity of the bound AMP without substantially reducing its activity *in vivo.* Accordingly, the aims of Chapter 2 were to:

1. explore how incorporation of an MMP cleavage sequence onto the N- or C-terminus of peptide 73 affected its activity, both before and after cleavage;
2. determine whether the developed peptides—Linker73 (L73) and 73Linker (73L)—were susceptible to cleavage when conjugated to low molecular weight PEG and whether this cleavage occurred in a biologically relevant scenario;
3. characterize the blood compatibility and toxicity of free peptide and conjugate *in vitro*; and
4. test the efficacy and toxicity of free peptide and conjugate in a clinically relevant mouse abscess model of high-density MRSA infection.

1.5.2 Translating the Enzyme-Cleavable Platform to Larger Polymers for Improved Biocompatibility

The selection of delivery vehicle can greatly impact the resulting conjugate's stability, biocompatibility, and pharmacokinetic properties, but the identity of the vehicle and, in the case of polymers, their molecular weight can often prevent access of the enzyme to the cleavage site, preventing drug release. In Chapter 3, the conjugation of the MMP-releasable AMP developed in Chapter 2 to larger molecular weight PEG is detailed. I hypothesized that incorporating a flexible glycine spacer between polymer and AMP would allow the targeted MMP sufficient access to the cleavage site, while the larger PEG would provide greater improvements in the biocompatibility of the conjugate. In addition, I hypothesized that the developed compounds

could display immunomodulatory properties, as these have been associated with a number of AMPs/HDPs. With that stated, the aims of Chapter 3 were to:

1. synthesize the MMP-cleavable AMP developed in Chapter 2 with a tetraglycine spacer between the N-terminal cysteine used for PEG conjugation and the MMP cleavage site;
2. conjugate the new cleavable AMP to larger molecular weight PEG and determine if it remained susceptible to MMP cleavage; and
3. determine the *in vitro* biocompatibility of the new conjugates and explore the anti-inflammatory properties of the top candidates from Chapter 2 and Chapter 3.

Chapter 2: Matrix Metalloproteinase-Cleavable Antimicrobial Peptides and their Conjugation to Polyethylene Glycol for Treatment of Infection

2.1 Synopsis

The extremely rapid development of antimicrobial resistance has necessitated the development of novel treatments for bacterial infection. AMPs have become increasingly promising for this purpose due to their high activity, slow resistance generation, and multimodal functionalities (e.g., direct bacteria killing and immunomodulation) that may provide more robust protection of the host against infection. However, off-site toxicity due to mammalian membrane disruption and rapid removal from the body (i.e., short half-lives) have hindered the translation of AMPs into clinical practice. Conjugation to water-soluble polymers, e.g., PEG, can greatly improve these properties but is commonly associated with a reduction or abolishment of antimicrobial activity. Indeed, peptide 73, a derivative of the AMP aurein 2.2 with improved activity but high toxicity, was previously conjugated to HPG to substantially improve its biocompatibility. As expected, however, this also resulted in reductions in *in vitro* activity and elimination of *in vivo* activity.

In this chapter, I detail the synthesis of enzyme-cleavable bioconjugates for treatment of infection, accomplished by the incorporation of an MMP-cleavable linker sequence at the N- or C-terminus of peptide 73 and the subsequent conjugation of the AMP to low molecular weight PEG. As outlined in Chapter 1, MMPs (particularly the gelatinase MMP-9) are expressed in high amounts during the inflammatory response to infection and should thus provide a mechanism by which the infection site can be targeted. The enzymatic cleavage of the compounds in response

to MMP *in vitro* and *ex vivo* is detailed, as is their activity and biocompatibility before and after cleavage both *in vitro* and in an *in vivo* abscess model. Ultimately, the integration of a release mechanism targeting the site of infection aims to provide a means in which the biocompatibility and stability of the polymer carrier can be combined with the unaltered activity of the free peptide.

2.2 Methods

2.2.1 Materials

Unless otherwise stated, all reagents were purchased from Sigma-Aldrich Canada Co. (Oakville, ON). Maleimide-functionalized methoxyPEG (mPEG) was purchased from Advance Polymers Inc. (Montreal, QC). Recombinant human tumour necrosis factor-α (TNF-α) was purchased from Abcam (Toronto, ON), and fluorescently conjugated antibodies used for platelet activation experiments were purchased from BD Biosciences (San Jose, CA, USA). All human pro-MMPs were expressed, purified, and validated by the Overall Lab (Vancouver, BC), as detailed elsewhere[136].

2.2.2 Ethics Statement

All blood used in this study was collected from consenting, unmedicated, healthy donors at the Centre for Blood Research (Vancouver, BC) following a protocol approved by The University of British Columbia Clinical Research Ethics Board (CREB, number H10-01896). All animal experiments were performed in accordance with The Canadian Council on Animal Care (CCAC) and approved by The University of British Columbia Animal Care Committee (protocol A19-0064).

2.2.3 Peptide Synthesis and Purification

All peptides were synthesized using solid-phase Fmoc peptide synthesis using a peptide synthesizer (CS Bio Co., Menlo Park, CA, USA) as previously described[36]. Briefly, Fmoc-protected amino acids were coupled to each other from C- to N-terminus. Rink resin was used for peptides with amidated termini, while Wang was used for carboxylated peptides (Table 2.1). Fmoc protecting groups were removed by the addition of piperidine for sequential coupling. After synthesis, the resin and side chain protecting groups were removed by trifluoroacetic acid (TFA) in a cocktail mixture also containing phenol, ethanedithiol (EDT), and triethylsilane (TES). The resulting peptide mixture was concentrated via rotary evaporation and precipitated using cold diethyl ether. The vacuum filtrated peptide was dissolved in water, lyophilized, and purified by reverse-phase high performance liquid chromatography (HPLC, Waters 600 System, Mississauga, Ontario, Canada) using a semi-preparative C4 column and UV detector set at 214 and 229 nm. A buffer gradient containing 0.1% TFA and varying concentrations of water and acetonitrile was used[36]. Peptides were identified using matrix-assisted laser desorption/ionization-mass spectrometry (MALDI-TOF MS; Voyager-DE STR Mass Spectrometer, Applied Biosystems). The final purity of the peptides was ≥ 95%.

For MALDI-TOF mass spectrometry, the compound was dissolved in water at a concentration of 0.1–1 mg/mL and mixed with 10 mg/mL α-cyano-4-hydroxycinnamic acid (CHCA) in a 1:1 volumetric ratio. For subsequent cleavage assays, the buffered cleavage mixture or acidified acetonitrile extract was mixed directly with the CHCA matrix, as indicated. The resulting solution was then spotted at 1 µL on the MALDI-TOF MS plate and left to dry, after which the samples were run.

2.2.4 Conjugation of Peptides to Polyethylene Glycol

N- or C-terminal cysteine-containing peptides were dissolved in anhydrous *N,N*-dimethylformamide (DMF) and mixed with mPEG-maleimide (2 kDa or 5 kDa) dissolved in anhydrous acetonitrile. The reaction was set up in a 1:1 molar ratio (approximately 3 mM) and stirred for 16–24 h under argon. The conjugates were then purified using HPLC as described above. Characterization of the conjugates was completed using MALDI-TOF MS (Figure A1) and ^{1}H NMR (Figure A2).

2.2.5 Circular Dichroism for Determination of Peptide Secondary Structure

Solution circular dichroism (CD) experiments were carried out using a JASCO J-815 spectropolarimeter (Victoria, BC) at room temperature, as previously described[30]. Briefly, the spectra were obtained over a wavelength range of 190–250 nm. A continuous scanning mode was used with a response of 1 s with 0.5-nm steps, bandwidth of 1.5 nm, and a scan speed of 50 nm/min. Three scans were used to improve the signal-to-noise ratio. Each spectrum was corrected by subtracting the background (either 750 μM phosphate buffer or 10 mM sodium dodecyl sulfate (SDS) in 750 μM phosphate buffer, pH 7.4) from the sample spectrum. Solution CD samples (100 μM peptide or conjugate in phosphate or SDS/phosphate buffer) were placed in a cell (0.1 cm in length) in 200 μL portions. The cells were rinsed with 600 μL of phosphate buffer (or 10 mM SDS in phosphate buffer) and 100 μL of the sample prior to each run.

2.2.6 Measurement of Particle Size by Dynamic Light Scattering

Test compounds were dissolved in PBS at a concentration of 1 mg/mL and measured using the Zetasizer Nano ZS (Malvern Panalytical, Montreal, QC) at 25 °C to determine their average hydrodynamic diameter. Each sample was run once with three subruns; a representative figure is displayed in Appendix A.

2.2.7 Enzymatic Cleavage of Peptides and Conjugates

2.2.7.1 *In Vitro* Cleavage by Matrix Metalloproteinases

Human pro-MMP-2, pro-MMP-8, pro-MMP-9, and pro-MMP-12 catalytic domain were activated via incubation with 1 mM 4-aminophenylmercuric acid (APMA) for 40 min at 37 °C. The peptide/conjugate to be tested was dissolved in 20 mM Tris, 50 mM NaCl, 100 mM $CaCl_2$ at pH 7.4 and incubated with activated 10 μg/mL MMP for 30 min at 37 °C. Cleavage was assessed using MALDI-TOF MS. For subsequent MIC assays, the cleavage mixture was purified by HPLC to collect the enzymatically cleaved fragments.

2.2.7.2 *Ex Vivo* Cleavage by Activated Neutrophils

To mimic the enzymatic cleavage of the compounds that would occur within the body, the peptides/conjugates were incubated with the cell-free supernatant of activated neutrophils. Whole human blood was collected in 1 mM EDTA tubes (Becton, Dickinson and Company, Franklin Lakes, NJ, USA). Neutrophils were isolated from whole blood using the EasySEP™ Direct Human Neutrophil Isolation Kit (STEMCELL Technologies, Vancouver, BC). Isolated neutrophils were resuspended in RPMI 1640 media supplemented with 10% fetal bovine serum (FBS) and 1% penicillin/streptomycin and plated at 1 x 10^6 cells/well in a 48-well tissue culture plate. The cells were then treated with 10 ng/mL TNF-α for 1 h at 37 °C under 5% CO_2 to induce activation as previously described[137]. The suspensions were centrifuged, and the resulting cell-free supernatant was incubated with 1 mM APMA for 45 min at 37 °C to activate pro-MMPs, as neutrophils release MMP-8 and MMP-9 in their inactivated forms[138,139]. The relative levels of endogenous activated MMPs were determined by withholding APMA in control incubations. To confirm peptide cleavage resulted from MMP activity, 10 μM marimastat (MMP inhibitor) or 1 mM 4-(2-aminoethyl)benzenesulfonyl fluoride hydrochloride (AEBSF; serine protease inhibitor)

was added for 5 min to some samples. To each supernatant, the peptides/conjugates were added at 100 μg/mL and incubated for 1–2 h at 37 °C. The peptide fragments were extracted from the supernatant by adding 2 volume equivalents of acetonitrile with 0.1% TFA and centrifuging to remove pelleted proteins. The peptide cleavage was then characterized using MALDI-TOF MS.

2.2.8 Minimum Inhibitory Concentration Assay

Following a previously described protocol[78], lysogeny broth (LB) was inoculated with *S. aureus* (strain C622, ATCC® 25923™), MRSA (USA 300 LAC) or *Pseudomonas aeruginosa* (PA01) and incubated overnight at 37 °C with shaking (200 rpm). The culture was then diluted in LB (or in Mueller-Hinton Broth, in the case of *P. aeruginosa*) to 10^5 to 10^6 CFU/mL for the assay, as determined by optical density at 600 nm (OD_{600}). Stock solutions of the compounds to be tested were prepared in water and added to a 96-well round-bottom polypropylene plate, where they were serially diluted 2-fold in LB in a Corning™ 3879 96-well round-bottom polypropylene plate (Corning, Glendale, AZ, USA) to achieve a concentration series across the plate (50 μL total). To each well, 50 μL of the bacterial culture was then aliquoted. The plate was incubated at 37 °C overnight, and the minimum inhibitory concentration (MIC) was determined visually by identifying the well with the lowest concentration of compound that inhibited bacterial growth (i.e., resulted in no bacterial pellet formation).

2.2.9 Blood Compatibility

2.2.9.1 Red Blood Cell Lysis

Donated blood was collected in 3.8% sodium citrate tubes (Becton, Dickinson and Company, Franklin Lakes, NJ, USA) to prevent clotting. The blood was centrifuged at 1000 *g* for 5 min to generate packed red blood cells (RBCs), which were then washed three times with phosphate buffered saline (PBS) to yield an 80% hematocrit suspension. RBCs were prepared at

10% hematocrit and treated with peptide/conjugate prepared in PBS for 1 h at 37 °C. A positive control generating 100% RBC lysis was prepared using ~10% Extran™ 300 Detergent solution; a negative control was prepared using PBS. The percent lysis was determined using the Drabkin method following our previous publications[140,141]. Briefly, 5 μL of the treated RBC mixture was added to 250 μL of Drabkin solution. The remaining mixture was centrifuged to pellet the RBCs, and 10 μL of the supernatant was added to 250 μL of Drabkin solution. The absorbance of the solutions, proportional to the amount of released haemoglobin, was measured using a SpectraMAX Multi-Mode M3 Plate Reader (Molecular Devices, LLC, San Jose, CA, USA) at 540 nm.

2.2.9.2 Peripheral Blood Mononuclear Cell Cytotoxicity

To assess cytotoxicity towards peripheral blood mononuclear cells (PBMCs), cells were isolated by density centrifugation using blood collected from healthy volunteers. Briefly, blood was collected in sodium heparin tubes, diluted 1:1 in PBS, layered on Lymphoprep™ density gradient medium (STEMCELL Technologies, Vancouver, Canada) and spun at ~350 *g* for 20 min without brakes in an Allegra 6 centrifuge (Beckman Coulter, Brea, CA, USA). PBMCs were collected from the buffy coat, rinsed twice in PBS, and then resuspended to a density of 2 x 10^6 cells/mL in RPMI 1640 media containing L-glutamine and supplemented with 10% FBS. Fifty microliters of this cell suspension was added to the wells of a 96-well flat-bottom tissue culture treated microplate and the cells were rested for 1 h in an incubator at 37 °C with 5% CO_2. After resting, 40 μL of 10% RPMI 1640 media was added to each well followed by 10 μl of a peptide or polymer solution (prepared in endotoxin free water) at 10x the final concentration being evaluated. The microplate was incubated for 20–22 h at 37°C with 5% CO_2. Following incubation, Triton X-100 was added to the positive control wells to a final concentration of 2%

and mixed thoroughly by aspirating the media numerous times with a pipet. The plates were centrifuged at ~400 *g* for 5 minutes in an Allegra 6 centrifuge, and the supernatants were transferred to a sterile 96-well polypropylene microplate. Peptide-induced cytotoxicity was assessed using the Cytotoxicity Detection Kit, which quantifies the lactate dehydrogenase (LDH) activity released from damaged cells. The assay was performed on the collected cell supernatants according to the manufacturer's instructions. Vehicle treated samples and cells lysed with 2% Triton X-100 served as the negative (0%) and positive (100%) controls, respectively.

2.2.9.3 Platelet Activation

Platelet activation was measured based on protocols published by our labs[142]. Blood collected in 3.8% sodium citrate tubes was centrifuged at 156 *g* for 12 min to generate platelet rich plasma (PRP). After collection of the PRP, the remaining blood was centrifuged at 2000 *g* for 20 min to generate platelet poor plasma (PPP). Peptide or conjugate prepared in PBS was added to PRP, and the resulting solution was incubated for 1 h at 37 °C. A PBS buffer control was prepared, as was a positive control inducing platelet activation by incubating 0.1 mM thrombin receptor activating peptide (TRAP) with PRP and incubating for 15 min at room temperature. In the interim, the tagging mixtures were prepared by adding fluorescently labeled antibodies to PPP at a 1:19 volumetric ratio: anti-CD42-fluorescein isothiocyanate (FITC) to label all platelets and ensure population purity; anti-CD62P-phycoerythrin (PE) to label activated platelets; and anti-human IgG-FITC and IgG-PE to measure nonspecific binding. Following incubation, the treated PRP was added to the corresponding antibody-containing PPP solutions at a 1:10 volumetric ratio, which were then incubated for 15 min at room temperature away from light. The solutions were then run on a 3-Laser CytoFLEX Flow Cytometer (Beckman Coulter Life Sciences, Indianapolis, IN, USA). Using the CD42-gated platelets, 1 x 10^4 events were

counted for each measurement. Platelet activation was assessed by PE median fluorescence intensity associated with presentation of the glycoprotein CD62P.

2.2.9.4 Blood Coagulation by Activated Partial Thromboplastin Time Assay

Blood was collected in 3.8% citrate tubes, and PPP was collected as described above. The activated partial thromboplastin time (APTT) assay was performed following protocols found in literature from our labs[78,142]. Briefly, peptide or conjugate prepared in PBS was added to PPP in a 1:9 volumetric ratio. An equivalent volume of actin FSL was added to the solution, which was placed in a cuvette strip with a steel ball and incubated for 3 min at 37 °C. Pre-warmed 0.025 M $CaCl_2$ was added to the cuvette solutions to initiate clotting, and the time taken for clot formation was measured on a ST4 Coagulation Analyzer (Diagnostica Stago, France).

2.2.10 Cell Viability

Cell viability assays were performed following published protocols with slight modifications[36,78]. EA.hy926 ATCC® CRL-2992™ endothelial and NIH/3T3 ATCC® CRL-1658™ fibroblast cell lines were maintained in Dulbecco's Modified Eagle Media (DMEM) supplemented with 10% FBS and 1% penicillin/streptomycin (passage number ≤ 30). For the cell viability assay, 5 x 10^3 cells were plated per well in a 96-well tissue culture plate. Following attachment, the cells were treated with peptide or conjugate solutions prepared in 1% or 10% FBS DMEM for 48 h at 37 °C under 5% CO_2. Controls corresponding to 100% growth (no treatment), 0% growth (treatment with dimethyl sulfoxide, DMSO) and background signal (cell-free media) were also included. The cells were then washed with PBS and the 3-[[4,5-dimethylthiazol-2-yl]-5-[3-carboxymethoxyphenyl]-2-[4-sulfophenyl]-2H-tetrazolium] (MTS) reagent was added to each well as specified by the kit instructions (CellTiter 96® AQ_{ueous} One

Solution Cell Proliferation Assay, Promega Corporation, Madison, WI, USA). After 40 min incubation, the absorbance of each well was read at 490 nm.

2.2.11 Mouse Abscess Infection Model

Female outbred CD-1 mice were purchased from Charles River Laboratories, Inc. (Wilmington, MA, USA) and were 7–9 weeks of age, 25 ± 2 g in mass. Abscess formation and treatment was performed as previously described[143]. Briefly, *S. aureus* (USA300) LAC was subcultured at 37 °C with shaking (250 rpm) to an OD_{600} of 2.0 in LB. Cells were washed twice with sterile PBS and resuspended to a final OD_{600} of 2.0. Bacteria were injected (50 µL, ~5.0 x 10^7 CFU) subcutaneously into the right dorsum of shaved mice under anaesthesia (2.5% isofluorane). After 1 h, 50 µL of the test or control compounds was injected subcutaneously at the infection site. Abscess formation proceeded for 72 h and disease progression was monitored daily. At the experimental endpoint, mice were euthanized with CO_2 followed by cervical dislocation. Abscess lesion size or visible dermonecrosis was measured using a caliper. Abscesses were harvested in PBS and homogenized using a Mini-Beadbeater (BioSpec Products, Bartlesville, OK, USA) and serially diluted for bacterial enumeration on LB agar plates. Experiments contained 2–5 mice each and were performed with 2–3 independent replicates. Prior to efficacy testing, compounds were tested for toxicity by assessing dermonecrosis and/or peptide aggregation following subcutaneous injection.

To monitor the recruitment of MMPs to the abscess in real time, the commercially available MMP-activatable fluorescent probe MMPSense™ 750 FAST (~4.3 kDa; PerkinElmer, Waltham, MA, USA) was used. Abscesses were formed as described above and 100 µL of the probe (2 nmol) was injected intravenously 1 h later. MMPs that were recruited to the site of infection were imaged for up to 72 h (60 s exposure, medium binning, 750 nm excitation and 780

nm emission) using a Lumina *in vivo* imaging system (IVIS; PerkinElmer, Waltham, MA, USA) and analyzed using Living Image software v3.1 (PerkinElmer, Waltham, MA, USA).

2.2.12 Statistical Analysis

All statistical analyses were performed using GraphPad Prism (GraphPad Software, Inc., La Jolla, CA, USA). Significance is denoted according to *P* value following this notation: ns = not significant; * $P \leq 0.05$; ** $P \leq 0.01$; *** $P \leq 0.001$; **** $P \leq 0.0001$. The statistical tests used for each data set are stated in the figure captions.

2.3 Results and Discussion

2.3.1 Synthesis of Matrix Metalloproteinase-Cleavable Peptides and Characterization of Activity

To confer MMP susceptibility onto peptide 73, the cleavage sequence GPLG↓VRGK was appended to either the N- or C-terminus of the peptide to generate peptides L73 and 73L, respectively (Table 2.1). This sequence has been shown to be cleaved by a wide array of MMPs, particularly the gelatinases MMP-2 and MMP-9[144–147]. MMP-9 is acutely associated with bacterial infection, where it is released by neutrophils and macrophages, immune cells that are particularly important during the early stages of infection[119,148,149]. Thus, increased local presence of host MMPs should allow for cleavage of the peptide, permitting release of the active peptide fragment after the AMP is conjugated to PEG (Figure 2.1). As shown Figure 2.2, both peptides were cleavable by isolated human MMP-9, confirming that the parent peptide sequence did not negatively impact the susceptibility of the sequence to enzymatic cleavage.

Previously, it was shown that the activity of aurein 2.2 depended largely on its N-terminus[35], suggesting addition of amino acids onto this end could negatively impact its activity. Conversely, appending the cleavage sequence onto the C-terminus of 73 would result in the

removal of its amidated terminus upon enzymatic cleavage, resulting in an overall decrease of charge by 1 (Table 2.1) and thus likely reducing antimicrobial activity. Furthermore, cleavage on the N-terminus would leave behind an arginine and a lysine on the peptide, increasing the overall charge of 73 to a final charge of +5 (Table 2.1). Thus, it was important to test both versions for their activity before and after MMP cleavage to determine which would be best suited for PEGylation.

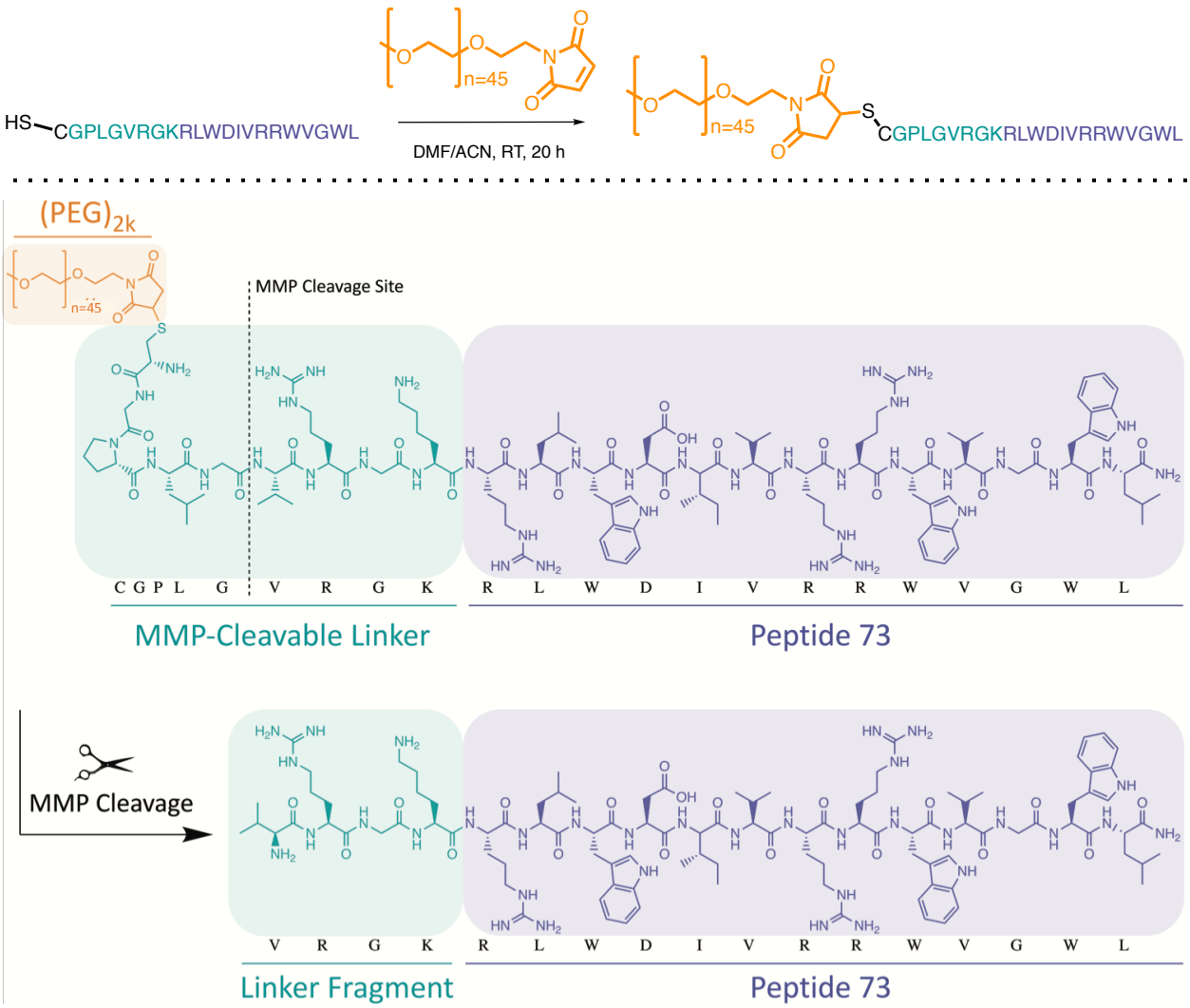

Figure 2.1. Schematic representation of the enzymatic cleavage of N-terminus PEGylated L73 by targeted host MMPs. The reaction scheme for the conjugation of L73 to 2 kDa PEG is shown above.

Table 2.1. The sequences of the developed peptides and conjugates developed in this chapter.

Compound	Amino Acid Sequence[d]	C-terminus	Net Charge (pH 7.4)
Synthesized Peptides			
73	**RLWDIVRRWVGWL**	$CONH_2$	+3
L73[a]	GPLGVRGK**RLWDIVRRWVGWL**	$CONH_2$	+5
D-L73[b]	GPlGvRGK**RLWDIVRRWVGWL**	$CONH_2$	+5
cL73[c]	CGPLGVRGK**RLWDIVRRWVGWL**	$CONH_2$	+5
D-cL73[b]	CGPlGvRGK**RLWDIVRRWVGWL**	$CONH_2$	+5
73L	**RLWDIVRRWVGWL**GPLGVRG	$CONH_2$	+4
73Lc	**RLWDIVRRWVGWL**GPLGVRGC	$CONH_2$	+4
linker fragment	GPLG	COOH	0
Synthesized Peptide Conjugates			
$(PEG)_{2k/5k}$-cL73	$(PEG)_{2k/5k}$-CGPLGVRGK**RLWDIVRRWVGWL**	$CONH_2$	+5
$(PEG)_{2k}$-D-cL73[b]	$(PEG)_{2k}$-CGPlGvRGK**RLWDIVRRWVGWL**	$CONH_2$	+5
73Lc-$(PEG)_{2k/5k}$	**RLWDIVRRWVGWL**GPLGVRGC-$(PEG)_{2k/5k}$	$CONH_2$	+4
Peptide Fragments Generated by *In Vitro* MMP-9 Cleavage			
cleaved L73	VRGK**RLWDIVRRWVGWL**	$CONH_2$	+5
cleaved 73L	**RLWDIVRRWVGWL**GPLG	COOH	+2

[a] L73 stands for MMP cleavable Linker + peptide 73 (in bold)

[b] In D-L73 and D-cL73, two amino acids in the linker are D-amino acids (indicated by lower case letters).

[c] Cysteine is added to the sequence to allow for conjugation to maleimide-functionalized mPEG.

[d] One letter amino acid codes are as follows: C, cysteine; D, aspartic acid; G, glycine; I, isoleucine; K, lysine; L, leucine; P, proline; R, arginine; V, valine; W, tryptophan.

Peptides L73 and 73L both displayed negligible activity *in vitro* against *S. aureus* (strain C622) as determined by MIC assays (125 μg/mL each, Table 2.2). However, following MMP-9 cleavage, the purified peptide fragment of 73L only displayed a 2-fold increase in activity at an MIC of 63 μg/mL, whereas that of L73 displayed a 16-fold increase at an MIC of 8 μg/mL, comparable to 73. A similar trend in activity was obtained against the clinical MRSA isolate USA300 LAC. This is likely due to the lower positive charge of cleaved 73L (+2) compared to cleaved L73 (+5), partially a result of the lost amidated C-terminus. Though both uncleaved and cleaved L73 possess the same net charge, the lower activity of the former may be the result of a lower overall hydrophobic moment when adopting an α-helix (Figure A3), a feature that can be important for AMP activity[30]. Interestingly, both full length L73 and 73L displayed activity against the Gram-negative pathogen *P. aeruginosa* (16 μg/mL), but where the activity improved for L73 upon MMP-9 cleavage, the activity of 73L decreased 4-fold, further supporting the importance of the amidated C-terminus.

Table 2.2. MICs of generated peptides and conjugates against a variety of pathogenic bacteria. Data is reported as the mode from *n*=3 independent experiments. An MIC of ≥125 μg/mL is considered inactive.

	MIC (μg/mL)		
Compound	***S. aureus* C622**	**MRSA USA300 LAC**	***P. aeruginosa* PA01**
Parent Peptides			
aurein 2.2	31	-	-
73	4	8	16
N-terminus MMP-Cleavable Peptides and Conjugates			
L73	125	>125	16
cleaved L73	8	16	8
D-L73	31	63	16
cL73	>125	>125	-
$(PEG)_{2k}$-cL73	>125	>125	63
$(PEG)_{5k}$-cL73	>125	>125	-
$(PEG)_{2k}$-D-cL73	>125	>125	63
C-terminus MMP-Cleavable Peptides and Conjugates			
73L	125	63	16
cleaved 73L	63	31	63
73Lc	>125	>125	-
73Lc-$(PEG)_{2k}$	>125	>125	63
73Lc-$(PEG)_{5k}$	>125	>125	-

2.3.2 Conjugation to Low Molecular Weight Polyethylene Glycol

To determine if MMP cleavage was hindered by conjugation to PEG and whether this depended on PEG size, both L73 and 73L were synthesized with an N- or C-terminal cysteine, respectively, and conjugated to maleimide-modified 2 kDa or 5 kDa mPEG (size denoted herein as subscript). The purity of the bioconjugates was confirmed by HPLC repurification (Figure A1) and ^{1}H NMR (Figure A2). Conjugation further decreased the activity of both peptides *in vitro* (Table 2.1), but this was not worrisome due to the designed enzymatic release mechanism.

Indeed, the MIC of MMP-cleaved $(PEG)_{2k}$-cL73 matched that of cleaved L73. Interestingly, PEGylation of both L73 and 73L did not influence the secondary structures of the peptides either in buffer or in SDS micelles, where they adopted α-helical structures consistent with previous work on 73[30] (Figure A4). This suggests the reductions in antimicrobial activity were not a result of perturbations in peptide secondary structure upon interaction with lipid membranes.

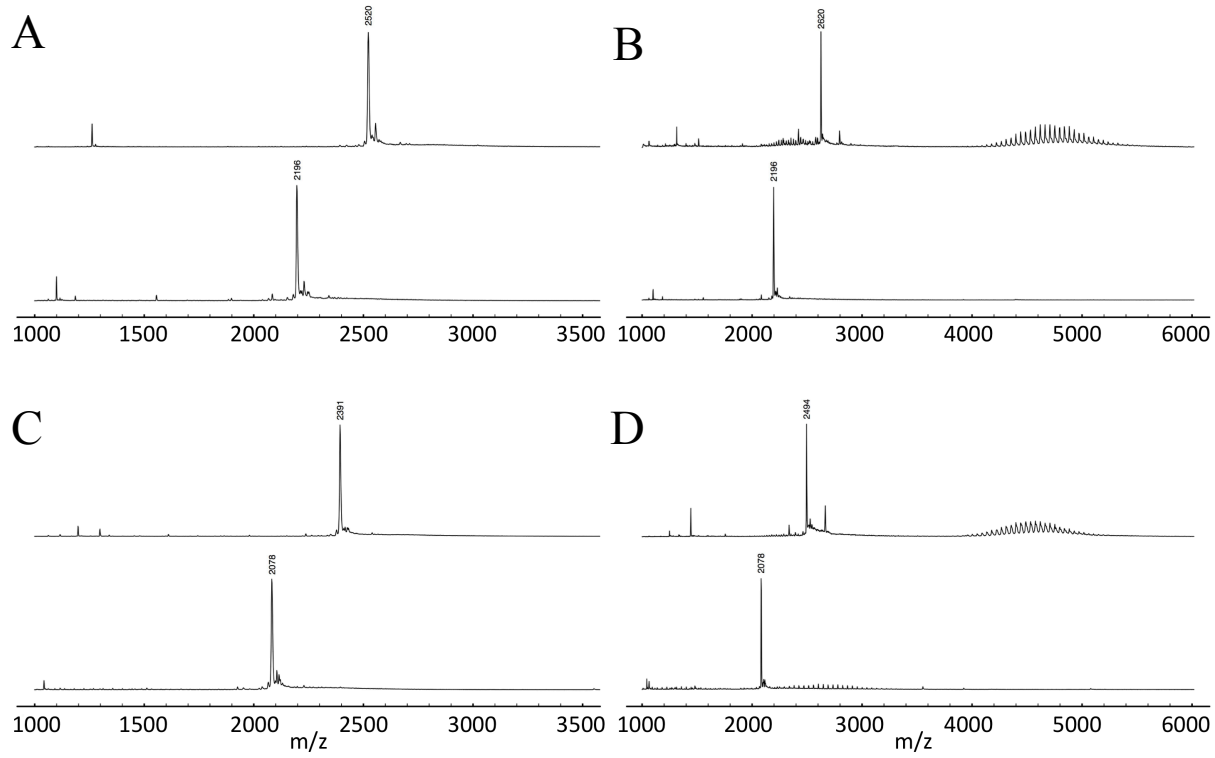

Figure 2.2. Characterization of the cleavage of developed compounds by activated MMP-9. MALDI-TOF mass spectra are displayed for (A) L73, (B) $(PEG)_{2k}$-cL73, (C) 73L, and (D) 73Lc-$(PEG)_{2k}$ before (top) and after (bottom) incubation with activated MMP-9. Cleaved peptide fragments can be seen at m/z=2196 $[M + H]^+$ for both (A) and (B) and at m/z=2078 $[M + H]^+$ for both (C) and (D) (sequences can be found in Table 2.1).

Interestingly, both $(PEG)_{2k}$ conjugates maintained susceptibility to isolated MMP-9, but cleavage of the $(PEG)_{5k}$ conjugates seemed to be dependent on N- versus C-terminus

conjugation, as the $(PEG)_{5k}$-cL73 conjugate did not display cleavage (Figure A5). This could potentially be due to a lack of accessibility of the enzyme to the cleavage site owing to the sterically bulky polymer shielding or wrapping around the beginning of the cleavage sequence. It is possible that cleavage prevention could occur at some point between 2 and 5 kDa PEG, but this was not tested here. Nevertheless, the strong activity (and high water solubility) of cleaved L73 made it and its $(PEG)_{2k}$-cL73 conjugate the top candidates for future studies. Non-cleavable versions of both peptide and conjugate were also synthesized by substituting D-isomers of leucine and valine in the MMP cleavage sequence (confirmed by incubation with activated MMP-9, Figure A6).

2.3.3 Characterizing the Top Candidates in a Model of Neutrophil-Mediated Matrix Metalloproteinase-9 Cleavage

Neutrophils are one of the most potent sources of MMPs in the body, particularly storing a large amount of MMP-9 in cytosol-contained granules that are released upon stimulation[137,150,151]. During infection, endothelial cells capture dormant neutrophils circulating within the blood and guide them through endothelial cell linings to the site of infection[148]. Once there, the activated neutrophils destroy microorganisms through a number of processes, including phagocytosis, release of extracellular traps, and degranulation[148,151]. The latter results in the release of granular contents, such as microbicidal agents (e.g., AMPs and ROS) and MMPs, to help fight infection[149,151]. Furthermore, the released MMPs are harnessed here to regulate the chemoattraction of the inflammatory infiltrate[152,153]. As such, it was hypothesized that neutrophils isolated from whole human blood could be utilized as an *ex vivo* model to mimic the enzymatic cleavage that the developed compounds would experience in a biological setting.

As shown in Figure 2.3, both L73 and $(PEG)_{2k}$-cL73 displayed the targeted peak at m/z=2196 $[M + H]^+$ corresponding to MMP-9 cleavage when incubated with the cell-free supernatant of TNF-α-activated neutrophils. A small amount of cleavage was also observed in untreated neutrophils, likely due to background activation caused by isolation and handling of the cells. To confirm this cleavage was not a result of other proteases, two additional conditions were included using marimastat, a broad-spectrum MMP inhibitor, and AEBSF, a serine protease inhibitor. When marimastat was introduced into the cell-free supernatant, the peptide peak at m/z=2196 $[M + H]^+$ disappeared, confirming that released MMPs were responsible for the cleavage of the free peptide and conjugate (Figure 2.3). Moreover, cleavage was maintained in the presence of AEBSF, suggesting serine proteases did not play a role in the cleavage. In addition, both the lead peptide and conjugate were also susceptible to cleavage by isolated MMP-8 and MMP-12 (Figure A7), which are released largely by neutrophils and macrophages, respectively[129,154,155]. Altogether, these results provide an idea of the cleavage that the compounds would display in a biological environment where activated neutrophils and macrophages are present (e.g., at an infection site).

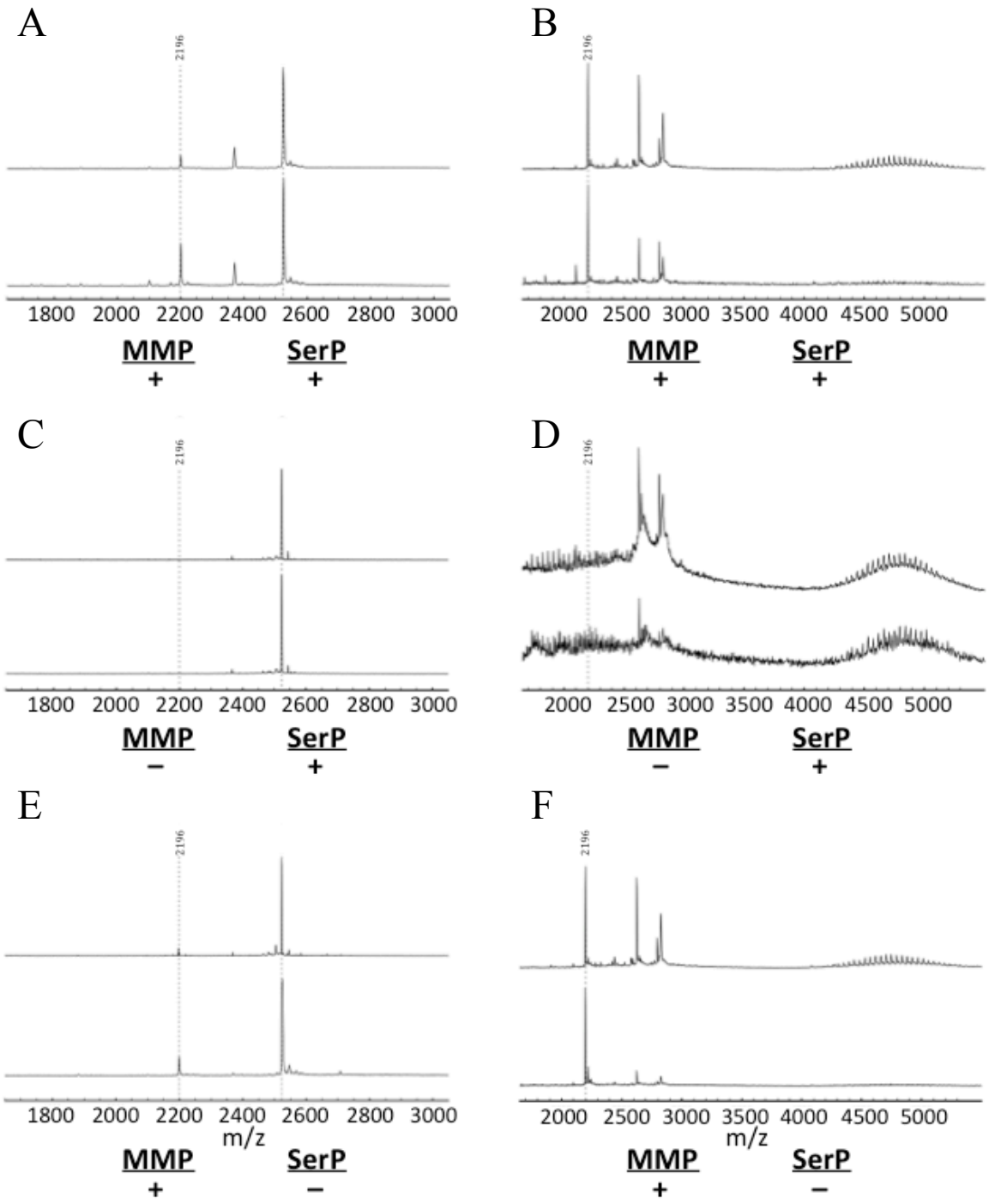

Figure 2.3. *Ex vivo* characterization of the enzymatic cleavage of the compounds after exposure to the cell-free supernatant of isolated neutrophils. MALDI-TOF mass spectra are displayed for L73 (left column: A, C, E) and $(PEG)_{2k}$-cL73 (right column: B, D, F). Top and bottom spectra in each display cleavage of the compound in the cell-free supernatant of untreated or TNF-α-activated neutrophils, respectively. In (A) and (B), no enzyme inhibitors are present. In (C) and (D), marimastat, a broad-spectrum MMP inhibitor, is present. In (E) and (F), AEBSF, a serine protease (SerP) inhibitor, is present.

2.3.4 *In Vitro* Biocompatibility of Top Candidates

2.3.4.1 Blood Compatibility

Blood compatibility is an important factor to be considered in the development of therapeutic agents, particular those being developed for systemic administration, as it is important to be aware of how the compounds affect the processes and cells housed in the blood. To start, the synthesized compounds were tested for their ability to lyse red blood cells. As shown in Figure 2.4A, both L73 and the non-cleavable D-L73 displayed a large amount of hemolysis at all tested concentrations, similar to 73. As expected, PEGylation of L73 resulted in substantially improved compatibility compared to the free peptide at all tested concentrations up to 125 μg/mL, or 16x the MIC of cleaved L73 (with respect to *S. aureus* C622) ($P \leq 0.001$). A less obvious improvement was observed at the high concentration of 250 μg/mL ($P < 0.05$). Interestingly, the non-cleavable $(PEG)_{2k}$-D-cL73 conjugate displayed even less hemolysis than its cleavable counterpart, particularly at 250 μg/mL.

Additionally, the $(PEG)_{2k}$-cL73 conjugate was less cytotoxic than L73 against isolated human PBMCs over a large concentration range (Figure 2.4B). Specifically at 63 and 125 μg/mL, a significant improvement ($P \leq 0.05$) was observed for the conjugate over free peptide. This protection was not observed when the two individual components, i.e., L73 and $(PEG)_{2k}$, were added together, confirming the reduced cytotoxicity was a result of covalent conjugation to the polymer. Analogous results were obtained for $(PEG)_{2k}$-D-cL73 (Figure A8).

Platelets play an important role in hemostasis, rapidly arresting blood loss in injured blood vessels by clumping together and initiating the formation of blood clots[156]. Previous work has shown that certain cationic peptides and polymers can activate platelets[157], which may lead to serious thrombotic complications such as vessel occlusions preventing blood flow through the

body. Thus, L73 and the $(PEG)_{2k}$-cL73 conjugate were tested for their influence on platelet activation by measuring the expression of the transmembrane glycoprotein CD62P on the platelet surface by flow cytometry (Figure 2.4C). Fortunately, no activation was observed by either compound up to a peptide concentration of 250 μg/mL.

Furthermore, the compounds were tested for their ability to influence blood coagulation via the APTT assay, a clinical coagulation assay which measures the time it takes for fibrin clot formation via the intrinsic coagulation pathway (Figure 2.4D). Both L73 and $(PEG)_{2k}$-cL73 presented no influence on coagulation time up to 63 μg/mL, but above this concentration, onset of coagulation was delayed for both compounds, though less so for the conjugate ($P \leq 0.01$). Altogether, the results in this section indicate the conjugate displayed good blood compatibility, with reductions in cytotoxicity relative to free peptide.

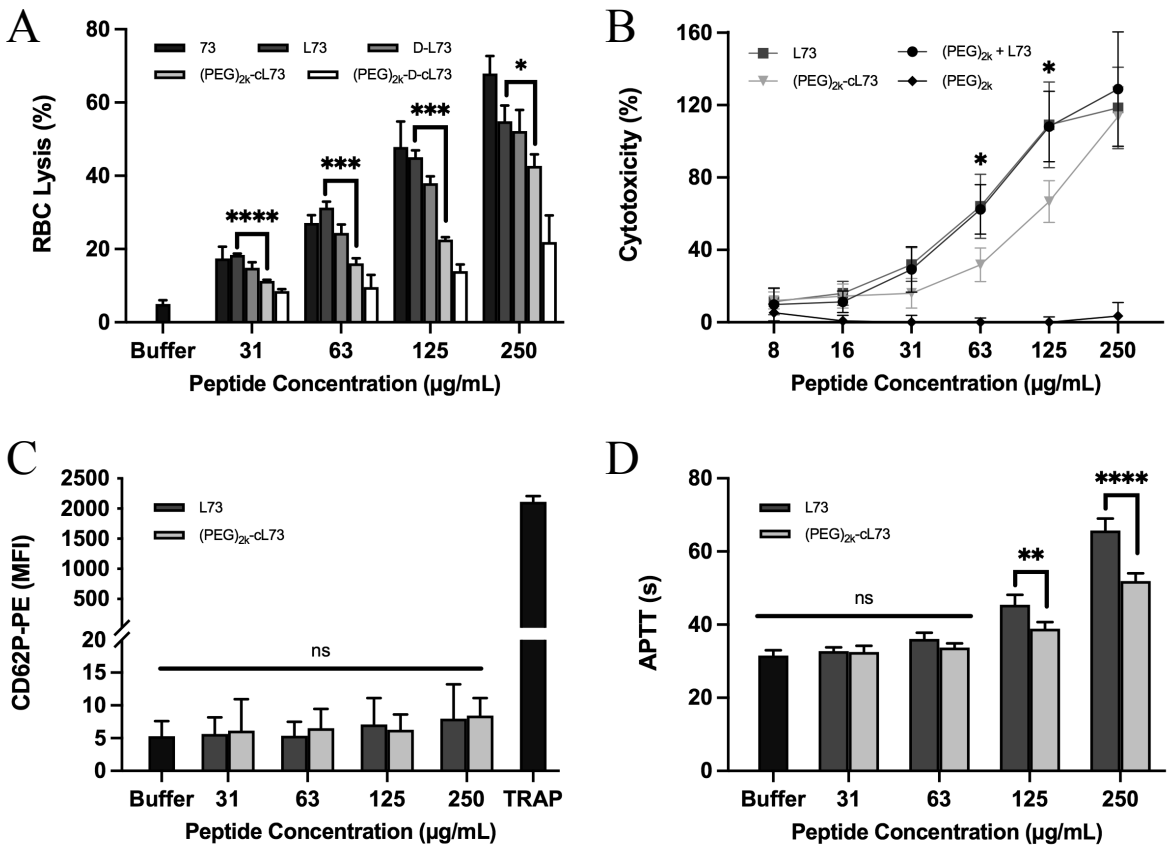

Figure 2.4. Blood compatibility and cytotoxicity of developed peptides and conjugates. (A) Lysis of red blood cells induced by peptides or conjugates. (B) PBMC cytotoxicity after exposure to developed compounds. (C) Activation of platelets in response to incubation with compounds as quantified by the expression of CD62P, a marker associated with platelet activation. Median fluorescent intensity (MFI) was standardized against background platelet fluorescence. TRAP was used as a positive control. (D) Influence of the developed peptide and conjugate on coagulation time. Statistical analysis: ns = not significant; * $P \leq 0.05$; ** $P \leq 0.01$; *** $P \leq 0.001$; **** $P \leq 0.0001$ according to unpaired t-test (A and B) or one-way ANOVA with Tukey test for multiple comparisons (C and D). Data is presented as mean ± standard deviation for n=3–5 independent experiments (i.e., 3–5 separate donors). PBMC cytotoxicity was performed by Dr. Evan F. Haney.

2.3.4.2 Influence on Cell Viability

In addition to blood compatibility assays, the biocompatibility of L73 and its conjugate was assessed by measuring the cell viability of treated fibroblast and endothelial cell lines. Interestingly, in contrast to hemolysis, both free AMP and conjugate displayed similar toxicities

against both cell lines at all tested concentrations in 10% FBS media (Figure 2.5A and B). It was hypothesized that some cleavage could be occurring due to background stimulation of the cells resulting in MMP release, but no differences in viability were identified between the conjugate and its non-cleavable counterpart at the tested concentrations (Figure A9). It is possible that the small size of the conjugated PEG relative to peptide (2 vs. 2.62 kDa, respectively) did not fully prevent the bound peptide from interacting with the cell membrane, or that serum or cell-secreted proteases were breaking down the peptide over this long treatment period. Forde *et al.* likewise found that conjugation of 2 kDa PEG to a 23-residue peptide of 2.64 kDa did not reduce the peptide's toxicity against host cystic fibrosis bronchial epithelial cells[158,159]. Nevertheless, here the conjugate displayed high compatibility up to 16 μg/mL in endothelial and 31 μg/mL in fibroblast cell lines, corresponding to 2x or 4x the MIC of cleaved L73 (with respect to *S. aureus* C622), respectively.

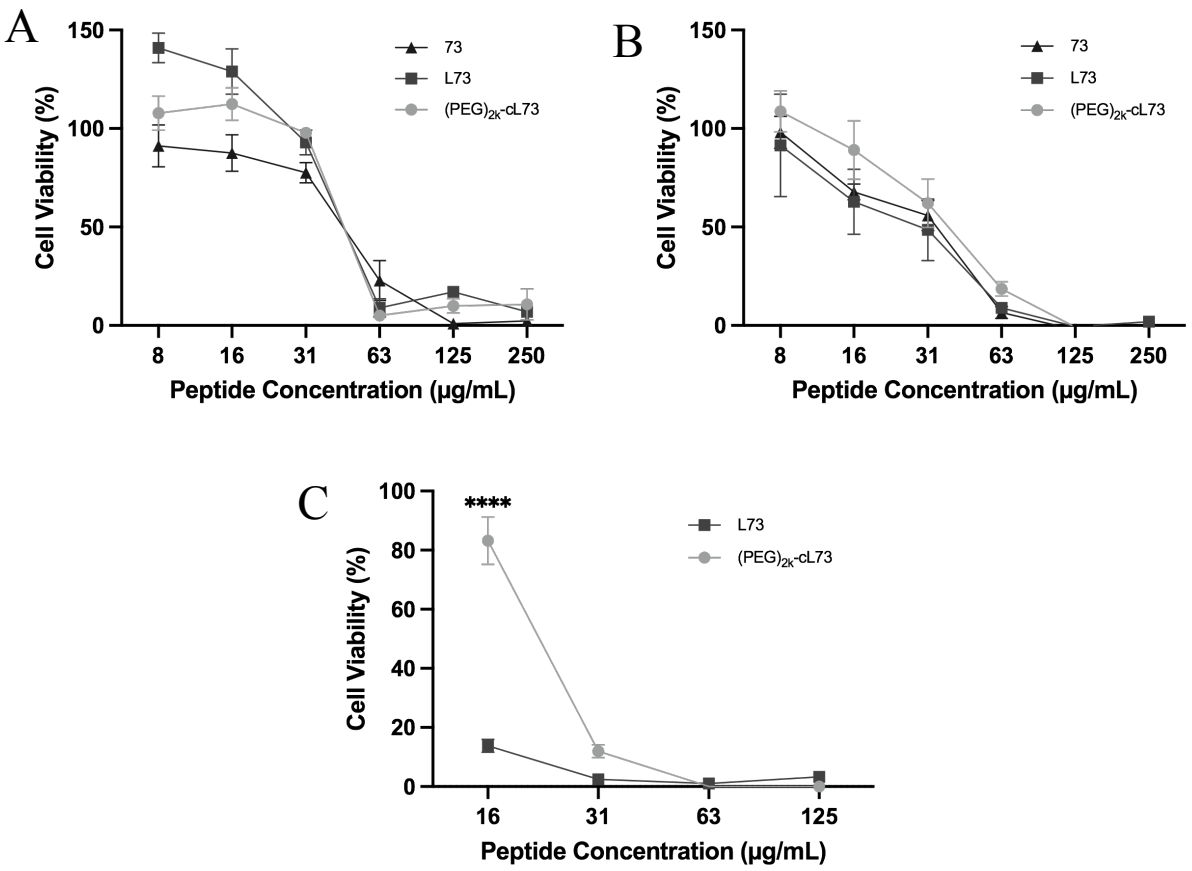

Figure 2.5. Cell viability of EA.hy926 endothelial cells and NIH/3T3 fibroblasts when treated with developed compounds. Plots (A) and (B) display cell viability of NIH/3T3 and EA.hy926 cells, respectively, after 48 h treatment in high serum (10% FBS) conditions; plot (C) displays cell viability of EA.hy926 cells after 48 h treatment in low serum (1% FBS) conditions. Values above 100% viability may indicate increased metabolic activity due to cellular stress or induced cell proliferation. Statistical analysis: **** $P \leq 0.0001$ according to unpaired t-test (C). Data is presented as mean ± standard deviation for n=5 replicates.

Interestingly, repeating the assay in low serum (1% FBS) conditions revealed a substantial difference in endothelial cell viability between conjugate and free peptide at 16 µg/mL ($P \leq 0.0001$) along with a sharper decline in viability with concentration relative to the previous high serum conditions (Figure 2.5C). This may suggest that interactions between free L73 and the cellular membrane are more strongly perturbed by the presence of serum due to,

e.g., binding of the peptide with serum-associated proteins (e.g., albumin), which has been reported for a number of cationic AMPs[160,161].

2.3.5 Investigating the Safety and Efficacy of the Top Candidates in a Mouse Infection Model

It can be difficult to fully assess how a developed drug behaves when administered to the body solely based on *in vitro* assays. This is particularly true for AMPs, whose activities and biocompatibility are greatly influenced by factors of the host milieu, such as salts, pH levels, and proteases[26]. Moreover, the activities of the compounds detailed in this chapter depend on the response of the host to infection, which cannot be fully mimicked *in vitro.* Thus, the developed compounds were studied *in vivo* using a mouse abscess model of high-density MRSA infection[143].

Abscess formation is a common condition associated with bacterial infection, most commonly by community associated MRSA[162]. These abscesses are generally difficult to treat as high bacterial loads, low pH, and large amounts of debris reduce the efficacy of many common antibiotics[163,164]. Previously our labs showed strong activity of aurein 2.2 and 73 in MRSA-infected mouse abscesses, suggesting the MMP-cleavable compounds developed here could similarly be effective if cleaved by targeted enzymes within the abscess.

To start, the efficacy of free L73 was tested using the model. In addition to L73, the non-cleavable counterpart D-L73, the MMP-cleaved L73 fragment and the short linker fragment liberated upon MMP cleavage (Table 2.1) were included. None of these compounds displayed any toxicity toward the mice up to 7.5 mg/kg, as determined by preliminary assessments of peptide aggregation and dermonecrosis following subcutaneous injection. At 15 mg/kg, L73 induced minor lesioning and aggregation under the skin (Figure A10). To compare to previous

work with 73, a concentration resulting in 5 mg/kg of MMP-liberated peptide was chosen for the studies.

As shown in Figure 2.6A, a single injection of L73 at 5.7 mg/kg (0.14 ± 0.01 mg) significantly reduced abscess size by 84.6% and bacterial load 79-fold. Similar activity was observed for MMP-cleaved L73 (administered at 5.0 mg/kg, or 0.13 ± 0.01 mg, to replicate the amount corresponding to 100% cleavage of L73), with 89.3% reduction in abscess size and 15-fold reduction in bacterial load. The short linker fragment did not display any activity relative to the saline control. The low *in vitro* activity of L73 suggests the strong activity observed here arises from the cleavage of the AMP in the presence of MMPs; this was further supported by the complete lack of activity displayed by the non-MMP cleavable D-L73 (Figure 2.6A).

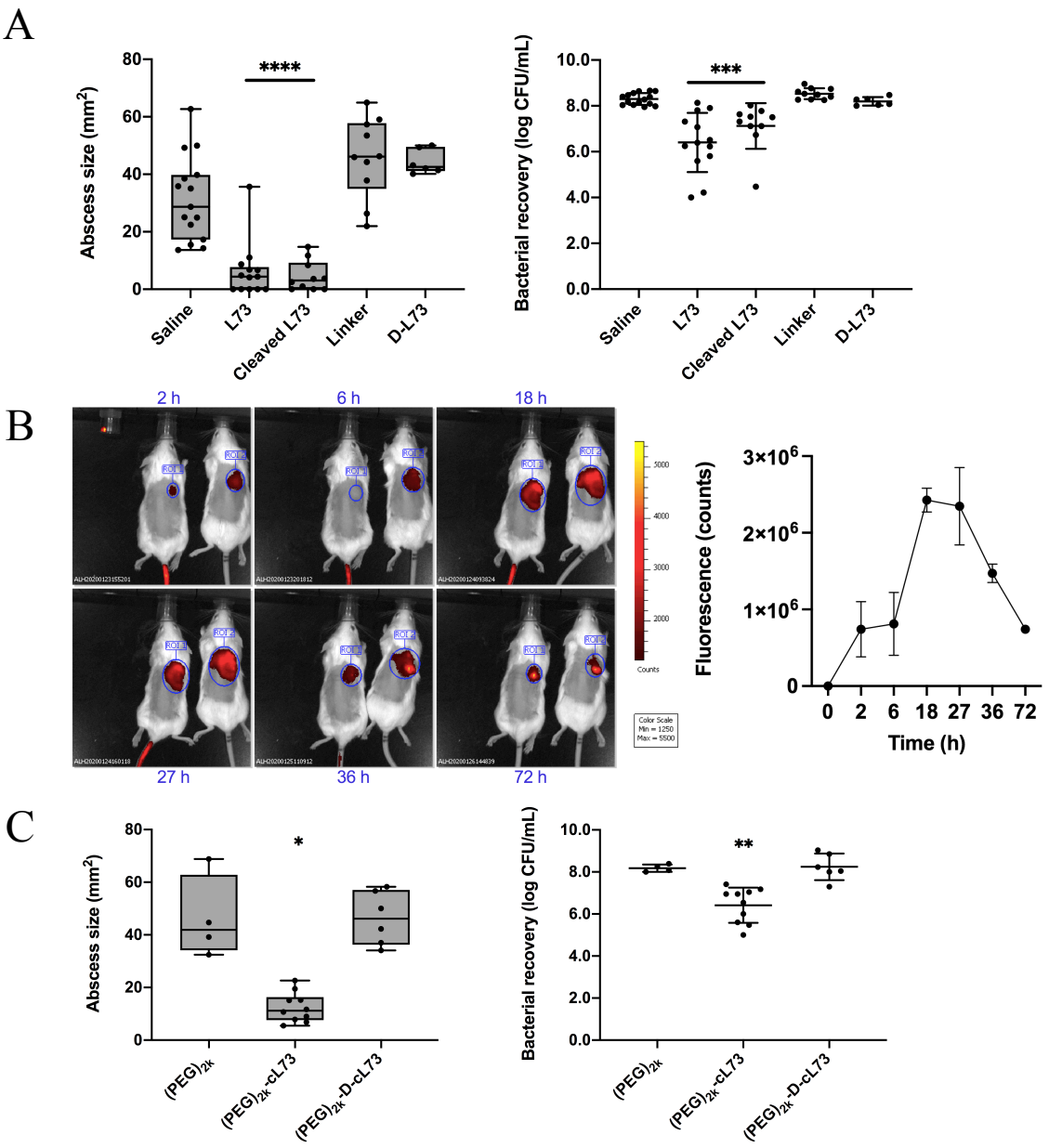

Figure 2.6. Activity of MMP-cleavable and -resistant peptides and conjugates and recruitment of MMPs to *S. aureus* USA300 LAC abscess infection in a murine cutaneous infection model. (A) Plots of abscess size (left) and bacterial load (right) in mice treated with saline or developed AMPs. (B) MMP recruitment to the site of infection, monitored up to 72 h post-infection in real time using the fluorescent probe MMP FAST™ 750. (C) Plots of abscess size (left) and bacterial load (right) in mice treated with PEG alone or developed PEG-HDP conjugates. Statistical analysis: * $P \leq 0.05$; ** $P \leq 0.01$; *** $P \leq 0.001$; **** $P \leq 0.0001$ according to Kruskal-Wallis nonparametric test relative to saline or PEG alone. Box and whisker plots show median, minimum and maximum of abscess sizes. Bacterial recovery is presented as geometric mean ± standard deviation. Data for 2–3 independent experiments containing 2–5 biological replicates each are shown (n = 4–16). Experiments were performed by Morgan A. Alford and Dr. Daniel Pletzer.

To confirm that MMPs were being recruited to the abscess site, MMP activity was monitored in real-time using a fluorescent MMP probe delivered intravenously 1 h after abscess formation (Figure 2.6B). As hypothesized, MMP activity increased steadily following bacterial inoculation, peaking at 18 h post-infection and decreasing thereafter. To note, the cleavage sequence of the probe (PLG↓VR) is the same utilized in L73, and the half-life of the probe is 24 h, meaning the observed decrease in MMP activity may be due to the degradation of the probe itself rather than a loss of MMP activity at the abscess site. This also provides some evidence regarding the capability of using MMPs to provide targeted release at sites of infection.

Next, the efficacy of the $(PEG)_{2k}$-cL73 conjugate and its non-cleavable counterpart were tested in the model. An initial study performed at a 28 mg/kg peptide concentration (one 0.70 ± 0.06 mg dose) indicated that the conjugate displayed some reduction in both abscess size and bacterial load (Figure A11), but due to the high solubility and non-toxicity of the compound up to a high concentration of 250 mg/kg (or 142 mg/kg peptide), the remaining studies were performed at this higher concentration. The reduction in toxicity relative to free L73 may be attributed to the prevention of peptide aggregation in the physiological environment by PEG, as *in vitro* dynamic light scattering (DLS) studies indicated that 74% of L73 formed large aggregates with a hydrodynamic size (diameter) of 170 ± 45 nm in PBS, whereas $(PEG)_{2k}$-cL73 displayed a singular form with a diameter of 134 ± 18 nm (Figure A12), a trend similarly observed when 73 was encapsulated in PEGylated phospholipid micelles[59]. In the abscess model, the conjugate displayed strong activity, reducing abscess size by 73.3% and bacterial load 58-fold compared to 2 kDa PEG alone (Figure 2.6C). As before, the non-cleavable version did not produce any reductions in abscess size or bacterial load even at this high concentration, further supporting the notion that MMP-release was necessary for activity.

2.4 Summary

In this chapter, the development of an enzymatically releasable PEG-AMP system was detailed. N- and C-terminal addition of an MMP-recognized cleavage sequence onto peptide 73 determined that N-terminus modification was optimal for maintaining the activity of the AMP after cleavage. The uncleaved peptide, termed L73, displayed minimal activity *in vitro*. The peptide's susceptibility to MMP cleavage was maintained after conjugation to low molecular weight (2 kDa) PEG, though 5 kDa PEGylation prevented cleavage entirely, likely as a result of the polymer's steric bulkiness. The resulting $(PEG)_{2k}$-cL73 conjugated displayed good blood compatibility, significantly reducing hemolysis, cytotoxicity, and coagulation time relative to free peptide.

Furthermore, both free L73 and $(PEG)_{2k}$-cL73 displayed strong activity against MRSA in a mouse abscess model of high-density infection when administered as a single dose. MMPs were shown to localize at the abscess site throughout the timeframe of the experiment, providing a means by which the active peptide fragment could be released. Indeed, non-cleavable versions of both free peptide and conjugate containing two substituted D-amino acids in the cleavage site did not display any efficacy in the mouse model, confirming MMP release was required for activity. Moreover, the PEGylated peptide was highly water-soluble and displayed no toxicity toward the mice up to a high concentration of 250 mg/kg. Altogether, the results presented in this chapter demonstrate the potential of harnessing MMP-cleavable AMP-polymer conjugates for site-specific targeting of infection.

Chapter 3: Modifying the Matrix Metalloproteinase-Cleavable Polyethylene Glycol-Antimicrobial Peptide Platform to Larger Molecular Weight Polyethylene Glycol Carriers for Improved Biocompatibility

3.1 Synopsis

The success of a therapeutic agent does not solely depend on its efficacy. The drug's biocompatibility, biostability, biodegradability, and pharmacokinetics must all also be considered, as they determine how the drug behaves within the body. Indeed, two of the major factors limiting the development of AMP therapeutics are their high toxicity and rapid degradation/kidney clearance within the body. For this reason, many of the current AMPs in clinical trials are prepared for topical application, where these concerns are much less prominent.

In Chapter 2, an MMP-releasable PEG-AMP platform was developed to provide a means by which these bioconjugates could target infection sites, thereby limiting off-site toxicity. Though the developed conjugate displayed strong activity and biocompatibility *in vivo*, only moderate reductions in toxicity profiles were observed *in vitro,* potentially due to the small size of the polymer relative to the peptide. With biocompatibility concerns remaining, the applicability of the system is limited.

In this Chapter, I detail the translation of the MMP-cleavable bioconjugate platform to larger molecular weight PEG with the focus of reducing *in vitro* toxicity profiles. To do this, the developed N-terminus MMP-releasable AMP was synthesized with a flexible tetraglycine spacer to facilitate enzymatic cleavage once bound to these larger polymeric groups. After confirming enzymatic cleavage by isolated MMP-9, the bioconjugates were assessed for their *in vitro*

activity, toxicity, and blood compatibility. Finally, the anti-inflammatory activities of some of the most promising compounds from Chapter 2 and Chapter 3 were assessed in the first study exploring the immunomodulatory properties of peptide 73 derivatives.

3.2 Methods

3.2.1 Synthesis of Peptides and Polyethylene Glycol Conjugates

The AMP cL73 was synthesized with a tetraglycine N-terminal spacer, termed cG4-L73, using solid-phase Fmoc peptide synthesis as described in Chapter 2.2.3. Purification was likewise completed using semi-preparative HPLC with characterization by MALDI-TOF MS. Conjugation of cG4-L73 to 5, 10, and 22 kDa mPEG-maleimide was performed as in Chapter 2.2.4. Purity of the conjugates was confirmed by HPLC repurification (Figure B1).

3.2.2 *In Vitro* Cleavage by Matrix Metalloproteinase-9

Human pro-MMP-9 was activated by incubation with 1 mM APMA for 30 min at 37 °C. Peptide or PEG-peptide bioconjugates were dissolved in 50 mM Tris buffer with 100 mM NaCl and 10 mM $CaCl_2$ (pH 7.4) and incubated at a final peptide concentration of 0.1 mg/mL with activated MMP-9 for 30 min. Cleavage was confirmed by sodium dodecyl sulfate-polyacrylamide gel electrophoresis (SDS-PAGE).

For SDS-PAGE, the cleavage mixture was diluted in 5x loading buffer (62.5 mM Tris-HCl, 30% w/v glycerol, 0.04% w/v bromophenol blue, 2% w/v SDS, 6.25% β-mercaptoethanol, pH 6.8), and 1 μg of peptide was loaded onto a 4-20% Mini-PROTEAN® TGX™ Precast Protein Gel (Bio-Rad Laboratories, Inc., Hercules, California, USA). The gel was run at 150 V for 50–60 min in 1x running buffer (19.2 mM Tris-HCl, 192 mM glycine, 0.1% w/v SDS, pH 8.3), after which it was washed for 15 min in deionized water. The washed gel was then stained with EZBlue™ Gel Staining Reagent for 60 min. The stained gel was washed overnight in deionized

water and imaged using an Odyssey® Classic Infrared Imager (LI-COR Biosciences, Lincoln, NE, USA).

3.2.3 Blood Compatibility and Toxicity Assays

All blood compatibility assays—RBC lysis, platelet activation, and APTT—were performed as described in Chapter 2.2. Blood was collected from consenting unmedicated donors following an approved protocol by the University of British Columbia CREB (number H10-01896). Cell viability assays were likewise performed as described in Chapter 2.2.10.

3.2.4 Anti-Inflammatory Assay using Polarized Macrophages

Macrophage polarization was performed following a previous protocol[165]. Briefly, THP-1 ATCC® TIB-202™ monocytes were seeded at 3.2 x 10^4 cells/well in a 96-well tissue culture plate in RPMI 1640 supplemented with 10% FBS, 1% penicillin/streptomycin and 2 mM L-glutamine (M0 media) and treated with 100 nM phorbol 12-myristate 13-acetate (PMA) for 72 h to induce differentiation into resting (M0) macrophages. Then, the media was replaced with M0 media containing 100 ng/mL LPS and 20 ng/mL interferon gamma (IFN-γ) with or without peptide/conjugate for polarization of the M0 macrophages into M1 phenotype. L73 and $(PEG)_{2k}$-cL73 were supplemented at 8 μg/mL peptide concentration, while cG4-L73 and $(PEG)_{5k}$-cG4-L73 were supplemented at 16 μg/mL. Controls showing no TNF-α release were also included by incubating the M0 macrophages in M0 media or in M2-polarizing media (M0 media with 20 ng/mL interleukin 4 (IL-4)). After 24 h incubation, the supernatant of each well was collected, and the amount of released TNF-α was quantified by enzyme-linked immunosorbent assay (ELISA) following the manufacturer's protocol (Thermo Fisher Scientific Inc., Waltham, MA, USA).

3.3 Results and Discussion

3.3.1 Synthesis and Characterization of Antimicrobial Peptides and Higher Molecular Weight Polyethylene Glycol-Antimicrobial Peptide Conjugates

In Chapter 2, PEGylation of cL73 by 5 kDa PEG prevented the cleavage of the peptide by the targeted enzyme, MMP-9. In order to translate the enzyme-cleavable mechanism to larger molecular weight PEG as well as to other potential carriers in the future, it was hypothesized that a chemical spacer between carrier and cleavage site could provide sufficient space between the two components to allow for cleavage. Consequently, a tetraglycine spacer was added to the N-terminus of the peptide (termed cG4-L73, Table 3.1). Glycine spacers are commonly employed in therapeutics due to their flexibility, inertness, and lack of secondary structure, which is particularly important for protein therapeutics[166–168]. Furthermore, they can be easily incorporated into AMPs through synthesis or expression, circumventing the need for additional modification steps after initial AMP production.

As hoped, the addition of the tetraglycine spacer enabled MMP-9 cleavage of 5, 10, and 22 kDa PEG-cG4-L73 conjugates, as shown by the disappearance of the conjugate band and appearance of the cleaved peptide band in SDS-PAGE after exposure to the enzyme (Figure 3.1). The larger PEGylated peptides migrated through the gel less than what would be expected for a protein of similar molecular weight, but this is consistent with previous reports[169,170]. Though the tetraglycine spacer permitted enzymatic cleavage here, it is possible that a shorter sequence would have also been sufficient. As before, both free cG4-L73 and its PEGylated conjugates were inactive against *S. aureus* C622 *in vitro* (MIC >125 μg/mL), but activity was recovered upon cleavage by MMP-9 (MIC 8 μg/mL, Table 3.1).

Table 3.1. Sequences of the peptides and conjugates studied in this chapter and their *in vitro* activity against *S. aureus* C622. Data is reported as the mode from *n*=3 independent experiments. An MIC of ≥125 μg/mL is considered inactive.

Compound	Amino Acid Sequence[d]	C-terminus	MIC (μg/mL) *S. aureus* C622
Synthesized Peptides			
L73[a]	GPLGVRGK**RLWDIVRRWVGWL**	$CONH_2$	125
cL73[b]	CGPLGVRGK**RLWDIVRRWVGWL**	$CONH_2$	>125
cG4-L73[c]	CGGGGGPLGVRGK**RLWDIVRRWVGWL**	$CONH_2$	>125
Synthesized Peptide Conjugates			
$(PEG)_{2k}$-cL73	$(PEG)_{2k}$-CGPLGVRGK**RLWDIVRRWVGWL**	$CONH_2$	>125
$(PEG)_{5k/10k/22k}$-cG4-L73	$(PEG)_{5k/10k/22k}$-CGGGGGPLGVRGK**RLWDIVRRWVGWL**	$CONH_2$	>125
Peptide Fragments Generated by *In Vitro* MMP-9 Cleavage			
cleaved L73/cG4-L73	VRGK**RLWDIVRRWVGWL**	$CONH_2$	8

[a] L73 stands for MMP cleavable Linker + peptide 73 (in bold).

[b] Cysteine is added to the sequence to allow for conjugation to maleimide-functionalized mPEG.

[c] cG4-L73 incorporates four glycine residues after the N-terminal cysteine and before the rest of L73.

[d] One letter amino acid codes are as follows: C, cysteine; D, aspartic acid; G, glycine; I, isoleucine; K, lysine; L, leucine; P, proline; R, arginine; V, valine; W, tryptophan.

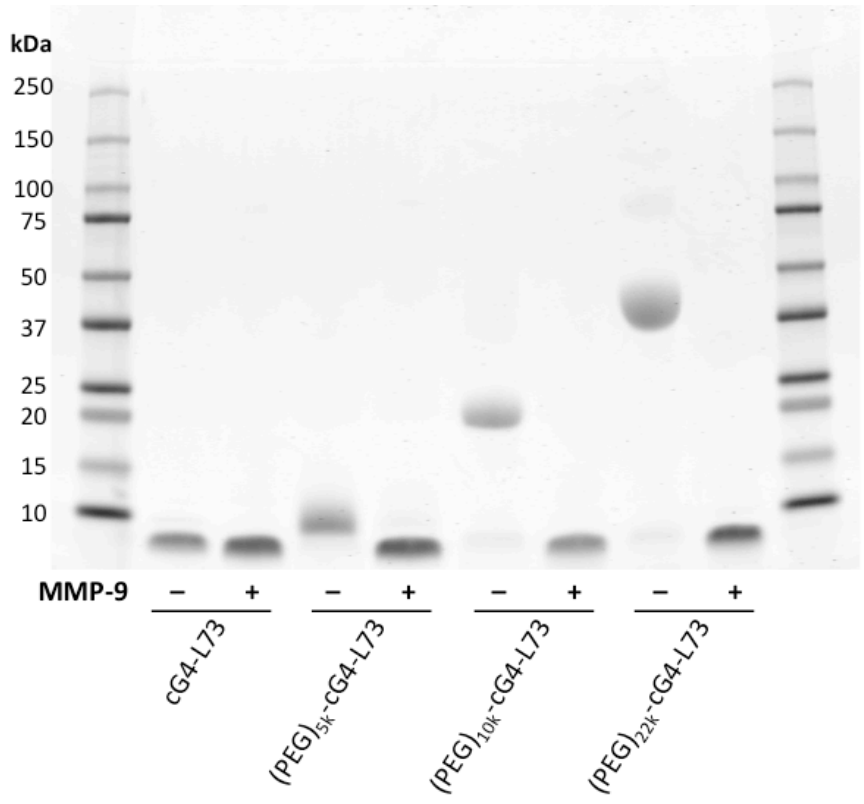

Figure 3.1. Visualization of the cleavage of cG4-L73 and its larger PEG conjugates by activated human MMP-9 through SDS-PAGE.

3.3.2 *In Vitro* Biocompatibility of Higher Molecular Weight Conjugates

As in Chapter 2, the novel conjugates and AMP were first assessed for cytotoxicity through an RBC lysis assay. As displayed in Figure 3.2A, all three PEG conjugates resulted in large reductions in lysis compared to free cG-L73 at all concentrations above 63 μg/mL ($P \leq 0.01$). In fact, the conjugates displayed 18 ± 1% lysis at most even at 250 μg/mL (or 31x the MIC of MMP-cleaved cG4-L73), roughly 2.4-fold less than that displayed by $(PEG)_{2k}$-cL73 at the same concentration (43 ± 3%, Figure 2.4A). Furthermore, no significant difference in lysis between buffer and any of the three conjugates up to 125 μg/mL was found. Interestingly, all three conjugates seemed to reduce lysis by the same level irrespective of PEG size, perhaps

suggesting the protective effects of PEG plateau somewhere at a lower molecular weight (i.e., between 2 and 5 kDa).

A similar trend was displayed when determining the cell viability of endothelial cells after 48 h treatment with the developed AMP and its conjugates (Figure 3.2B). All three conjugates did not decrease cell viability up to a peptide concentration of 63 μg/mL, at which a significant improvement over free cG4-L73 was observed ($P \leq 0.0001$). This was an improvement over the previously developed $(PEG)_{2k}$-cL73, which almost completely abolished cell viability at 63 μg/mL under the same conditions (Figure 2.5B).

In addition, the conjugates displayed no influence on platelet activation up to 250 μg/mL (Figure 3.2C) or on clotting time up to 63 μg/mL (Figure 3.2D), consistent with $(PEG)_{2k}$-cL73. Interestingly, the conjugates did produce an increase in clotting time above this concentration, which the free peptide did not (Figure 3.2C). This was not influenced by unconjugated PEG (data not shown) and is inconsistent with cysteine-free L73 (Figure 2.4D), perhaps suggesting the ability of the free peptide to form dimers via disulphides prevents interactions with the clotting pathway.

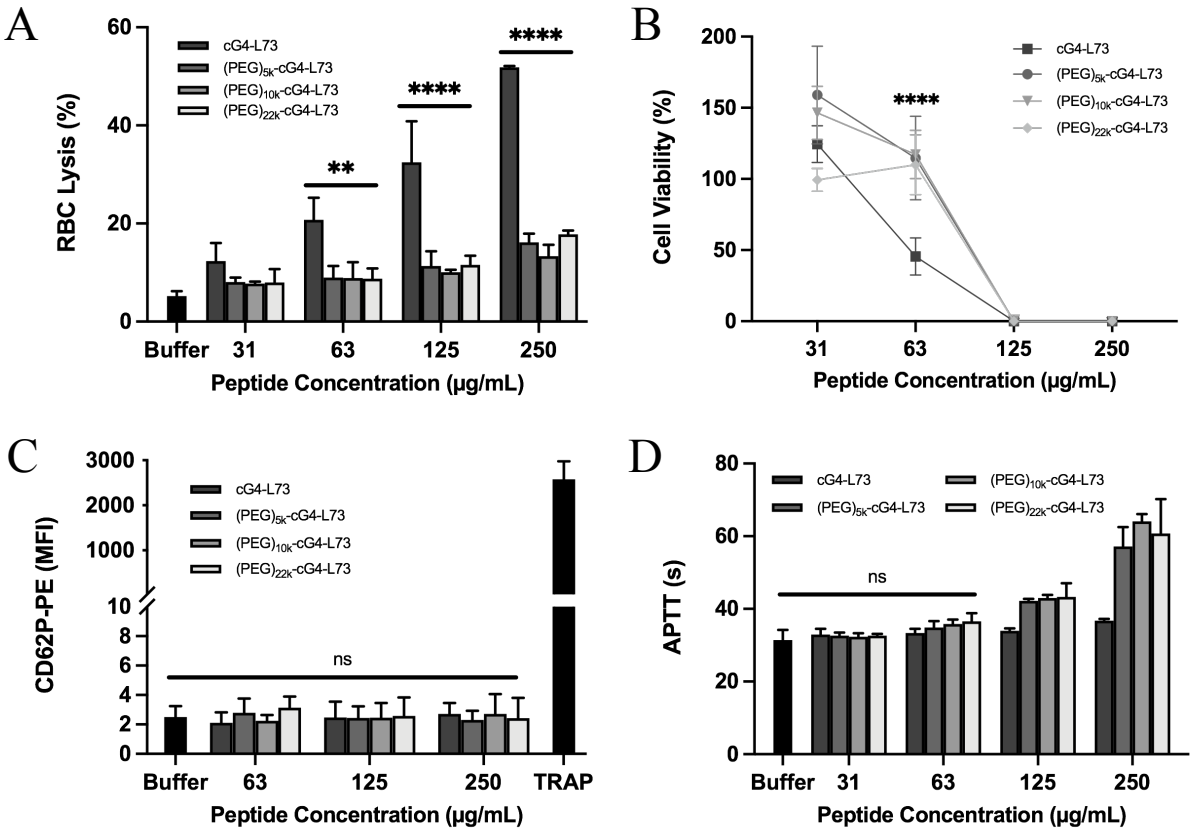

Figure 3.2. *In vitro* biocompatibility of cG4-L73 and its larger molecular weight PEG conjugates. (A) Lysis of red blood cells by tested compounds. (B) Cell viability of EA.hy926 endothelial cells after 48 h treatment with compounds in high serum (10% FBS) conditions. Values above 100% viability may indicate increased metabolic activity due to cellular stress or induced cell proliferation. (C) Activation of platelets in response to incubation with compounds as quantified by the expression of CD62P, a marker associated with platelet activation. MFI values were standardized against background platelet fluorescence. TRAP was used as a positive control. (D) Influence of the developed peptide and conjugate on coagulation time. Statistical analysis: ns = not significant; ** $P \leq 0.01$; **** $P \leq 0.0001$ according to one-way ANOVA with Tukey test for multiple comparisons. Data is presented as mean ± standard deviation for n=3 independent experiments (i.e., 3 separate donors) for blood assays and n=5 replicates for cell viability.

3.3.3 A Glimpse into the Anti-Inflammatory Activity of L73 and its Counterparts

As mentioned briefly in Chapter 1.2.3, many AMPs/HDPs also possess immunomodulatory capabilities that can help mediate the body's fight against infection[26,27,29]. As

no previous work has yet been done studying the immunomodulatory properties of peptide 73, some of the MMP-cleavable peptides and conjugates from Chapters 2 and 3 were assessed for anti-inflammatory activity using a model that measures the release of the inflammatory cytokine TNF-α by LPS-stimulated human macrophages[165].

As shown in Figure 3.3, both cG4-L73 and $(PEG)_{5k}$-cG4-L73 significantly reduced the release of TNF-α by LPS-stimulated macrophages over a 24 h period at a low peptide concentration of 16 μg/mL ($P \leq 0.05$). The 5 kDa PEG conjugate was chosen here as a representative of the larger molecular weight PEG conjugates as they all displayed identical *in vitro* biocompatibility. This observed anti-inflammatory activity may be a result of the compounds binding with LPS, a common action exhibited by AMPs/HDPs that prevents macrophage stimulation[171,172]. L73 and its 2 kDa conjugate also seemed to display some anti-inflammatory activity, though not as strongly as the new peptide/conjugate (ns compared to untreated macrophages). This may partially be due to the lower concentration tested here (8 vs. 16 μg/mL), which was chosen to ensure maintenance of biocompatibility.

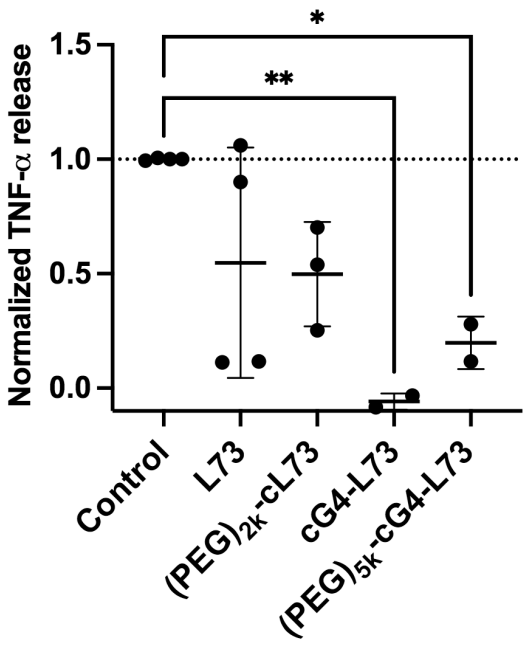

Figure 3.3. TNF-α release by LPS-stimulated THP-1 macrophages with or without treatment of developed compounds. TNF-α release was quantified via ELISA and normalized to the release by untreated LPS-stimulated THP-1 macrophages (M1 control). Statistical analysis: * $P \leq 0.05$; ** $P \leq 0.01$ according to one-way ANOVA with Dunnett's test for multiple comparisons.

3.4 Summary

In this chapter, the MMP-cleavable PEG-AMP system developed for infection site targeting in Chapter 2 was translated to larger molecular weight PEG in order to improve biocompatibility. To do this, the cleavable AMP L73 was synthesized with an N-terminal tetraglycine spacer to provide sufficient separation between polymer and cleavage site for enzymatic cleavage. Indeed, this spacer allowed for MMP-9 cleavage of the peptide after conjugation to 5, 10, and 22 kDa PEG. As in Chapter 2, the free peptide and its conjugates were inactive *in vitro* against pathogenic *S. aureus* until cleaved by MMP-9.

Promisingly, all three new conjugates displayed improved biocompatibility *in vitro* compared to the smaller $(PEG)_{2k}$-cL73, showing no influence on cytotoxicity or blood

compatibility up to a concentration of 63 μg/mL, or 8x the MIC of the cleaved, active peptide fragment. Furthermore, both free cG4-L73 and $(PEG)_{5k}$-cG4-L73 displayed some anti-inflammatory activity in a preliminary study of macrophage activation, the first experiment of its kind in regards to the immunomodulatory activity of peptide 73 derivatives, suggesting these compounds may also exert a protective effect during infection.

Ultimately, these results suggest the infection site-targeting platform developed in Chapter 2 was successfully translated to larger molecular weight PEG delivery vehicles in order to improve biocompatibility. In the future, this may allow for the MMP-cleavable AMP to be conjugated to other delivery systems, polymeric or otherwise, to best optimize activity, biocompatibility, and pharmacokinetics for effectively fighting bacterial infections.

Chapter 4: Conclusions and Future Work

4.1 Conclusions

If left unchecked, the continued rise in MDR pathogens will cause infection-related deaths to rise to levels not experienced in generations, where even small injuries might once again be fatal. AMPs, or HDPs, a diverse family of antimicrobial agents produced by virtually all domains of life, present a promising solution to these pathogens due to their high activity, low resistance generation, and, in some cases, auxiliary immunomodulatory properties that potentially provide a more robust response to infection. Unfortunately, however, the translation of AMPs as commercially available therapeutics has been greatly limited due to off-site toxicity and short biological half-lives. In fact, the majority of currently approved AMPs are limited to topical applications, which represent only a fraction of infections.

In attempts to reduce these unwanted properties, a number of mechanisms have been explored over the past decade. Direct chemical modification has generated stapled peptides or peptidomimetics with increased stability (generally accomplished by reducing proteolysis susceptibility), while delivery vehicle encapsulation or conjugation has produced formulations that generally display significant improvements in biocompatibility. However, particularly in the case of the latter, the modification of the AMP can greatly reduce or even abolish its antimicrobial activity, making the development of effective AMP therapeutics a challenging balancing act.

Here, an enzymatically cleavable AMP-PEG conjugation platform targeting host enzymes found at sites of infection was developed with the hope of combining the improved biocompatibility of the conjugated polymer with the unrestricted activity of the free peptide. In

Chapter 2, a model AMP, aurein 2.2-derived 73, was synthesized with an N- or C-terminal cleavage sequence susceptible to host infection-associated MMPs to determine which version best maintained antimicrobial activity upon cleavage. The N-terminal version proved to be the most effective, likely due to maintenance of its amidated C-terminus and higher positive charge, and was thus conjugated to low molecular weight PEG. Interestingly, MMP susceptibility remained upon conjugation to 2 kDa PEG, but was lost upon conjugation to 5 kDa PEG. Nevertheless, the bioconjugate displayed reductions in *in vitro* cytotoxicity relative to free peptide as well as good blood compatibility.

To confirm the designed system worked as intended, the MMP-cleavable AMP and AMP-PEG conjugate were tested for their efficacy in an abscess mouse model of high-density MRSA infection. Both compounds displayed strong activity, significantly reducing abscess size and bacterial load with only a single injection; furthermore, this activity was confirmed to be associated with host MMP activity, as non-cleavable counterparts of the compounds did not produce the same effect. In addition, activated MMPs were shown to accumulate at the abscess site throughout the period of infection as theorized, confirming their capacity to be used as targetable enzymes for infection site release.

Next, the releasable AMP was modified to enable translation of the system to larger PEG polymers to further improve the biocompatibility of the resulting conjugate. This was accomplished by incorporating a tetraglycine spacer between the polymer and the cleavage site of the AMP, which was thought could provide sufficient space between the two compounds to enable MMP binding. Indeed, this incorporated spacer allowed for cleavage of the AMP when conjugated to 5, 10, and 22 kDa PEG. In addition, these new bioconjugates displayed high blood compatibility, particularly improving hemolysis compared to the 2 kDa conjugate developed in

Chapter 2. Finally, the new AMP and its 5 kDa PEG conjugate were tested for their anti-inflammatory activity, where they showed significant reductions in the release of the cytokine TNF-α by LPS-stimulated macrophages, potentially signifying another benefit to using these compounds for the treatment of bacterial infection.

Altogether, this work details an enzyme-releasable platform for the targeted release of AMPs from PEG by infection site-associated host MMPs. By combining the enhanced biocompatibility of the polymer with the activity of the free peptide, a promising means for effectively targeting and treating infections within the body can be achieved. Though PEG was used as the model delivery vehicle here, this mechanism of AMP delivery has the potential to be translated to a wide array of carrier molecules, where stability, biocompatibility, and pharmacokinetics can be optimized, potentially facilitating the generation of efficacious AMP therapeutics for the future treatment of MDR pathogens.

4.2 Future Work

Developing this infection site-targeting platform has uncovered a number of avenues for further exploration. Firstly, as mentioned, additional delivery vehicles may be utilized for further improving the system's *in vivo* properties. Here, PEG was used as a proof-of-principle polymer, as it is readily available, well-studied, and one of the most established methods of improving the biocompatibility and pharmacokinetic profiles of bound drugs, garnering a great deal of success in pushing into clinical availability[173]. However, more recent reports have evidenced that anti-PEG antibodies may develop in patients treated with PEGylated therapeutics, resulting in losses in drug efficacy and in the potential advent of adverse effects[174]. These observations have called into question the long believed non-immunogenicity of PEG and its benefits in the development of novel therapeutics.

As such, alternatives to PEG have gained popularity in recent years. In particular, the tunable, multi-functional, highly biocompatible dendrimer-like polymer HPG has shown great potential for a number of biological applications, including the delivery of therapeutic agents[76] (Figure 4.1). Indeed, as mentioned in Chapter 1, ours labs previously used HPG to conjugate to aurein 2.2 and derivatives 73 and 77, which greatly improved the peptides' blood compatibility and reduced their toxicity profiles[36,78]. One of the most promising features of HPG is that multiple AMPs can be conjugated to a single molecule while still maintaining high biocompatibility, whereas only 1 or 2 AMPs can be attached to PEG, potentially allowing for improved efficacy. Indeed, the HPG-AMP conjugates showed decent antimicrobial activity *in vitro*, but this was lost when applied to the *in vivo* abscess model, making the MMP-releasable system developed here a perfect candidate for improving efficacy. A scheme for the potential synthesis of these conjugates is shown in Figure 4.1.

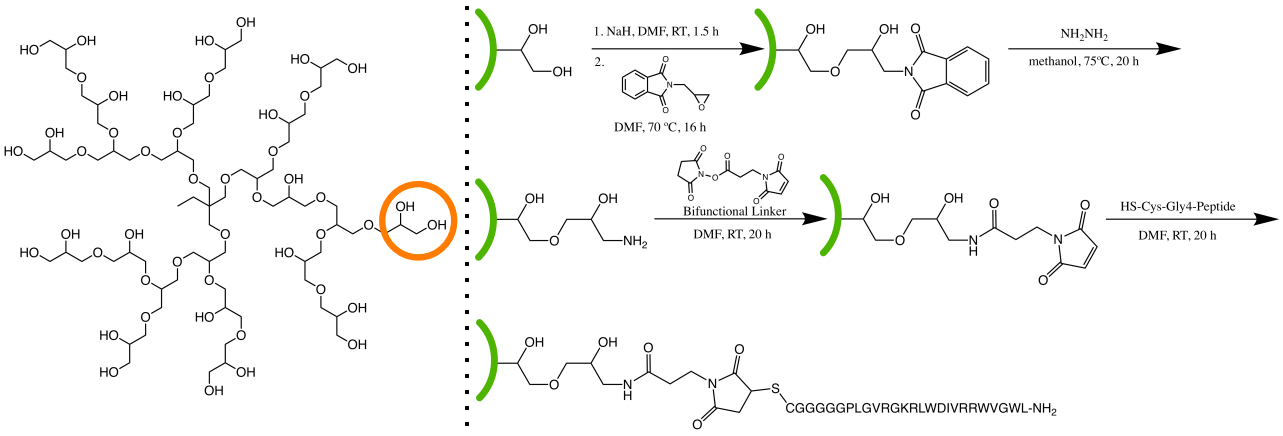

Figure 4.1. Schematic for the conjugation of the developed MMP-cleavable peptide with HPG. One terminal unit (circled in orange) is used to simplify the reaction scheme.

Secondly, it would be beneficial to assess the effectiveness of the developed conjugates (PEG, HPG, or otherwise) in treating bodily infections through systemic (e.g., intravenous)

administration. The abscess model utilized in this thesis provided an important means of confirming that MMPs accumulate at infection sites and therefore can be harnessed for AMP release, but proving that the conjugates can effectively treat infections systemically would significantly widen the applicability of the system. Further, the safety and pharmacokinetic parameters—particularly half-life, distribution, and release kinetics—of the conjugates would be important to test here. Fluorescent labeling of the AMP by, e.g., incorporating fluorescence resonance energy transfer (FRET) donor/acceptor fluorophores within the peptide could similarly be harnessed to measure accumulation at the infection site by producing a signal only when cleaved by targeted MMPs. Finally, the anti-inflammatory activity (and other immunomodulatory properties) of the conjugates hinted at in Chapter 3 could be further explored, as these properties may indicate a more robust and multimodal mechanism of antimicrobial activity that could potentially help to resolve inflammation and even treat serious immune system dysregulation (e.g., sepsis)[26,175].

In addition to furthering the study of the peptide 73-derived conjugates, it would also be fruitful to translate the system to other AMPs with higher initial biocompatibility than those developed here. This would minimize toxicity issues that might arise at the infection site due to long-term localized exposure to the peptide. The synthetic peptide IDR-1018, derived from a bovine neutrophil HDP, presents a good candidate for this purpose as it displays negligible toxicity *in vitro* and possesses a wide array of well-characterized protective properties, including immunomodulatory, anti-infective, anti-biofilm, and wound healing activities[176–178]. However, the activity of the peptide liberated upon MMP-9 cleavage would need to be tested on a case-by-case basis, as it is difficult to predict the effects the additional residues may have on the peptide's

properties. In this regard, it may be useful to test an array of AMPs containing the additional residues using, e.g., SPOT synthesis[179,180] to generate the most active peptides.

Ultimately, the studies suggested above aim to further characterize the safety and efficacy of the MMP-targeting platform developed in this thesis in order to widen its capabilities as an anti-infection treatment. By conjugating the developed AMP to HPG, the biocompatibility and pharmacokinetics of the conjugate may be tuned, potentially allowing for translation of the system as a systemically administered treatment where the infection site-targeting mechanism can particularly shine. Moreover, further exploration of the conjugates' anti-inflammatory properties may lead to additional avenues regarding the applications of the system. In the end, the hope remains that the work detailed here will provide a doorway toward the development of clinically available AMP therapeutics that can safely and effectively treat dangerous MDR pathogens.

References

(1) Aminov, R. I. A Brief History of the Antibiotic Era: Lessons Learned and Challenges for the Future. *Front. Microbiol.* **2010**, *1*, 1–7. DOI: 10.3389/fmicb.2010.00134

(2) Davies, J. Origins and Evolution of Antibiotic Resistance. *Microbiologia* **1996**, *12* (1), 9–16. DOI: 10.1128/mmbr.00016-10

(3) Ventola, C. L. The Antibiotic Resistance Crisis: Causes and Threats. *P. T. J.* **2015**, *40* (4), 277–283.

(4) Theuretzbacher, U.; Outterson, K.; Engel, A.; Karlén, A. The Global Preclinical Antibacterial Pipeline. *Nat. Rev. Microbiol.* **2019**, *18* (5), 275–285. DOI: 10.1038/s41579-019-0288-0

(5) Andrei, S.; Droc, G.; Stefan, G. FDA Approved Antibacterial Drugs: 2018-2019. *Discoveries* **2019**, *7* (4), e102. DOI: 10.15190/d.2019.15

(6) Shallcross, L. J.; Howard, S. J.; Fowler, T.; Davies, S. C. Tackling the Threat of Antimicrobial Resistance: From Policy to Sustainable Action. *Philos. Trans. R. Soc. B Biol. Sci.* **2015**, *370* (1670), 20140082. DOI: 10.1098/rstb.2014.0082

(7) Matsunaga, N.; Hayakawa, K. Estimating the Impact of Antimicrobial Resistance. *Lancet Glob. Heal.* **2018**, *6* (9), e934–e935. DOI: 10.1016/S2214-109X(18)30325-5

(8) Langford, B. J.; So, M.; Raybardhan, S.; Leung, V.; Westwood, D.; MacFadden, D. R.; Soucy, J. P. R.; Daneman, N. Bacterial Co-Infection and Secondary Infection in Patients with COVID-19: A Living Rapid Review and Meta-Analysis. *Clin. Microbiol. Infect.* **2020**, *26* (12), 1622–1629. DOI: 10.1016/j.cmi.2020.07.016

(9) Strathdee, S. A.; Davies, S. C.; Marcelin, J. R. Confronting Antimicrobial Resistance beyond the COVID-19 Pandemic and the 2020 US Election. *Lancet* **2020**, *396* (10257), 1050–1053. DOI: 10.1016/S0140-6736(20)32063-8

(10) Hsu, J. How Covid-19 Is Accelerating the Threat of Antimicrobial Resistance. *BMJ* **2020**, *369*, 1–2. DOI: 10.1136/bmj.m1983

(11) Coico, R. Gram Staining. *Curr. Protoc. Microbiol.* **2005**, Appendix 3–Appendix 3C. DOI: 10.1002/9780471729259.mca03cs00

(12) Silhavy, T. J.; Kahne, D.; Walker, S. The Bacterial Cell Envelope. *Cold Spring Harbor perspectives in biology*. **2010**, *2* (5): a000414. DOI: 10.1101/cshperspect.a000414

(13) Opal, S. M. Endotoxins and Other Sepsis Triggers. *Contrib. Nephrol.* **2010**, *167*, 14–24. DOI: 10.1159/000315915

(14) Swoboda, J. G.; Campbell, J.; Meredith, T. C.; Walker, S. Wall Teichoic Acid Function, Biosynthesis, and Inhibition. *ChemBioChem* **2010**, *11* (1), 35–45. DOI: 10.1002/cbic.200900557

(15) Sani, M. A.; Henriques, S. T.; Weber, D.; Separovic, F. Bacteria May Cope Differently from Similar Membrane Damage Caused by the Australian Tree Frog Antimicrobial Peptide Maculatin 1.1. *J. Biol. Chem.* **2015**, *290* (32), 19853–19862. DOI: 10.1074/jbc.M115.643262

(16) Rosenfeld, Y.; Shai, Y. Lipopolysaccharide (Endotoxin)-Host Defense Antibacterial Peptides Interactions: Role in Bacterial Resistance and Prevention of Sepsis. *Biochim. Biophys. Acta - Biomembr.* **2006**, *1758* (9), 1513–1522. DOI: 10.1016/j.bbamem.2006.05.017

(17) Kohanski, M. A.; Dwyer, D. J.; Collins, J. J. How Antibiotics Kill Bacteria: From Targets to Networks. *Nat. Rev. Microbiol.* **2010**, *8* (6), 423–435. DOI: 10.1038/nrmicro2333

(18) Hooper, D. C. Mechanisms of Action of Antimicrobials: Focus on Fluoroquinolones. *Clin. Infect. Dis.* **2001**, *32*, 9–15. DOI: 10.1086/319370

(19) Blair, J. M. A.; Webber, M. A.; Baylay, A. J.; Ogbolu, D. O.; Piddock, L. J. V. Molecular Mechanisms of Antibiotic Resistance. *Nat. Rev. Microbiol.* **2015**, *13* (1), 42–51. DOI: 10.1038/nrmicro3380

(20) Reygaert, W. C. An Overview of the Antimicrobial Resistance Mechanisms of Bacteria. *AIMS Microbiol.* **2018**, *4* (3), 482–501. DOI: 10.3934/microbiol.2018.3.482

(21) Czaplewski, L.; Bax, R.; Clokie, M.; Dawson, M.; Fairhead, H.; Fischetti, V. A.; Foster, S.; Gilmore, B. F.; Hancock, R. E. W.; Harper, D.; Henderson, I. R.; Hilpert, K.; Jones, B. V.; Kadioglu, A.; Knowles, D.; Ólafsdóttir, S.; Payne, D.; Projan, S.; Shaunak, S.; Silverman, J.; Thomas, C. M.; Trust, T. J.; Warn, P.; Rex, J. H. Alternatives to Antibiotics-a Pipeline Portfolio Review. *Lancet Infect. Dis.* **2016**, *16* (2), 239–251. DOI: 10.1016/S1473-3099(15)00466-1

(22) Theuretzbacher, U.; Piddock, L. J. V. Non-Traditional Antibacterial Therapeutic Options and Challenges. *Cell Host Microbe* **2019**, *26* (1), 61–72. DOI: 10.1016/j.chom.2019.06.004

(23) Magana, M.; Pushpanathan, M.; Santos, A. L.; Leanse, L.; Fernandez, M.; Ioannidis, A.; Giulianotti, M. A.; Apidianakis, Y.; Bradfute, S.; Ferguson, A. L.; Cherkasov, A.; Seleem, M. N.; Pinilla, C.; de la Fuente-Nunez, C.; Lazaridis, T.; Dai, T.; Houghten, R. A.; Hancock, R. E. W.; Tegos, G. P. The Value of Antimicrobial Peptides in the Age of Resistance. *Lancet Infect. Dis.* **2020**, *20* (9), e216–e230. DOI: 10.1016/S1473-

3099(20)30327-3

(24) Hancock, R. E. W.; Falla, T. J. Antimicrobial Peptides: Broad-Spectrum Antibiotics from Nature. *Clin. Microbiol. Infect.* **1996**, *1* (4), 226–229. DOI: 10.1111/j.1469-0691.1996.tb00566.x

(25) Hancock, R. E. W.; Sahl, H.-G. Antimicrobial and Host-Defense Peptides as New Anti-Infective Therapeutic Strategies. *Nat. Biotechnol.* **2006**, *24* (12), 1551–1557. DOI: 10.1038/nbt1267

(26) Alford, M. A.; Baquir, B.; Santana, F. L.; Haney, E. F.; Hancock, R. E. W. Cathelicidin Host Defense Peptides and Inflammatory Signaling: Striking a Balance. *Front. Microbiol.* **2020**, *11*, 1–18. DOI: 10.3389/fmicb.2020.01902

(27) Mahlapuu, M.; Håkansson, J.; Ringstad, L.; Björn, C. Antimicrobial Peptides: An Emerging Category of Therapeutic Agents. *Front. Cell. Infect. Microbiol.* **2016**, *6*, 1–12. DOI: 10.3389/fcimb.2016.00194

(28) Giuliani, A.; Pirri, G.; Nicoletto, S. F. Antimicrobial Peptides: An Overview of a Promising Class of Therapeutics. *Cent. Eur. J. Biol.* **2007**, *2*, 1–33. DOI: 10.2478/s11535-007-0010-5

(29) Kumar, P.; Kizhakkedathu, J. N.; Straus, S. K. Antimicrobial Peptides: Diversity, Mechanism of Action and Strategies to Improve the Activity and Biocompatibility in Vivo. *Biomolecules* **2018**, *8* (1), 4. DOI: 10.3390/biom8010004

(30) Raheem, N.; Kumar, P.; Lee, E.; Cheng, J. T. J.; Hancock, R. E. W.; Straus, S. K. Insights into the Mechanism of Action of Two Analogues of Aurein 2.2. *Biochim. Biophys. Acta - Biomembr.* **2020**, *1862* (6), 183262. DOI: 10.1016/j.bbamem.2020.183262

(31) Pan, Y.-L.; Cheng, T.-J..; Hale, J.; Pan, J.; Hancock, R. E. W.; Straus, S. K. Characterization of the Structure and Membrane Interaction of the Antimicrobial Peptides Aurein 2.2 and 2.3 from Australian Southern Bell Frogs. *Biophys. J.* **2007**, *92* (8), 2854–2864. DOI: 10.1529/biophysj.106.097238

(32) Cheng, T.-J.; Hale, J. D.; Elliot, M.; Hancock, R. E. W.; Straus, S. K. Effect of Membrane Composition on Antimicrobial Peptides Aurein 2.2 and 2.3 from Australian Southern Bell Frogs. *Biophys. J.* **2009**, *96* (2), 552–565. DOI: 10.1016/j.bpj.2008.10.012

(33) Cheng, J.-T.; Hale, J. D.; Elliott, M.; Hancock, R. E. W.; Straus, S. K. The Importance of Bacterial Membrane Composition in the Structure and Function of Aurein 2.2 and Selected Variants. *Biochim. Biophys. Acta - Biomembr.* **2011**, *1808* (3), 622–633. DOI: 10.1016/j.bbamem.2010.11.025

(34) Wenzel, M.; Senges, C. H. R.; Zhang, J.; Suleman, S.; Nguyen, M.; Kumar, P.; Chiriac, A. I.; Stepanek, J. J.; Raatschen, N.; May, C.; Krämer, U.; Sahl, H. G.; Straus, S. K.; Bandow, J. E. Antimicrobial Peptides from the Aurein Family Form Ion-Selective Pores in Bacillus Subtilis. *ChemBioChem* **2015**, *16* (7), 1101–1108. DOI: 10.1002/cbic.201500020

(35) Cheng, J.-T.; Hale, J. D.; Kindrachuk, J.; Jessen, H.; Elliott, M.; Hancock, R. E. W.; Straus, S. K. Importance of Residue 13 and the C-Terminus for the Structure and Activity of the Antimicrobial Peptide Aurein 2.2. *Biophys. J.* **2010**, *99* (9), 2926–2935. DOI: 10.1016/j.bpj.2010.08.077

(36) Kumar, P.; Takayesu, A.; Abbasi, U.; Kalathottukaren, M. T.; Abbina, S.; Kizhakkedathu, J. N.; Straus, S. K. Antimicrobial Peptide-Polymer Conjugates with High Activity: Influence of Polymer Molecular Weight and Peptide Sequence on Antimicrobial Activity, Proteolysis, and Biocompatibility. *ACS Appl. Mater. Interfaces* **2017**, *9* (43), 37575–37586. DOI: 10.1021/acsami.7b09471

(37) Haney, E. F.; Nguyen, L. T.; Schibli, D. J.; Vogel, H. J. Design of a Novel Tryptophan-Rich Membrane-Active Antimicrobial Peptide from the Membrane-Proximal Region of the HIV Glycoprotein, Gp41. *Beilstein J. Org. Chem.* **2012**, *8*, 1172–1184. DOI: 10.3762/bjoc.8.130

(38) Chan, D. I.; Prenner, E. J.; Vogel, H. J. Tryptophan- and Arginine-Rich Antimicrobial Peptides: Structures and Mechanisms of Action. *Biochimica et Biophysica Acta - Biomembranes*. **2006**, *1758* (9), 1184–1202. DOI: 10.1016/j.bbamem.2006.04.006

(39) Jing, W.; Demcoe, A. R.; Vogel, H. J. Conformation of a Bactericidal Domain of Puroindoline a: Structure and Mechanism of Action of a 13-Residue Antimicrobial Peptide. *J. Bacteriol.* **2003**, *185* (16), 4938-4947. DOI: 10.1128/JB.185.16.4938-4947.2003

(40) Vlieghe, P.; Lisowski, V.; Martinez, J.; Khrestchatisky, M. Synthetic Therapeutic Peptides: Science and Market. *Drug Discovery Today*. **2010**, *15* (1-2), 40–56. DOI: 10.1016/j.drudis.2009.10.009

(41) Haney, E. F.; Hancock, R. E. W. Peptide Design for Antimicrobial and Immunomodulatory Applications. *Biopolymers* **2013**, *100* (6), 572–583. DOI: 10.1002/bip.22250

(42) Jenssen, H.; Hamill, P.; Hancock, R. E. W. Peptide Antimicrobial Agents. *Clin. Microbiol. Rev.* **2006**, *19* (3), 491–511. DOI: 10.1128/CMR.00056-05

(43) Koo, H. B.; Seo, J. Antimicrobial Peptides under Clinical Investigation. *Pept. Sci.* **2019**,

111 (5). DOI: 10.1002/pep2.24122

(44) Zhao, Y.; Zhang, M.; Qiu, S.; Wang, J.; Peng, J.; Zhao, P.; Zhu, R.; Wang, H.; Li, Y.; Wang, K.; Yan, W.; Wang, R. Antimicrobial Activity and Stability of the D-Amino Acid Substituted Derivatives of Antimicrobial Peptide Polybia-MPI. *AMB Express* **2016**, *6* (1), 122. DOI: 10.1186/s13568-016-0295-8

(45) Jia, F.; Wang, J.; Peng, J.; Zhao, P.; Kong, Z.; Wang, K.; Yan, W.; Wang, R. D-Amino Acid Substitution Enhances the Stability of Antimicrobial Peptide Polybia-CP. *Acta Biochim. Biophys. Sin. (Shanghai).* **2017**, *49* (10), 916–925. DOI: 10.1093/abbs/gmx091

(46) Mourtada, R.; Herce, H. D.; Yin, D. J.; Moroco, J. A.; Wales, T. E.; Engen, J. R.; Walensky, L. D. Design of Stapled Antimicrobial Peptides That Are Stable, Nontoxic and Kill Antibiotic-Resistant Bacteria in Mice. *Nat. Biotechnol.* **2019**, *37* (10), 1186–1197. DOI: 10.1038/s41587-019-0222-z

(47) Nguyen, L. T.; Chau, J. K.; Perry, N. A.; de Boer, L.; Zaat, S. A. J.; Vogel, H. J. Serum Stabilities of Short Tryptophan- and Arginine-Rich Antimicrobial Peptide Analogs. *PLoS One* **2010**, *5* (9), 1–8. DOI: 10.1371/journal.pone.0012684

(48) Spokoyny, A. M.; Zou, Y.; Ling, J. J.; Yu, H.; Lin, Y. S.; Pentelute, B. L. A Perfluoroaryl-Cysteine SNAr Chemistry Approach to Unprotected Peptide Stapling. *J. Am. Chem. Soc.* **2013**, *135* (16), 5946–5949. DOI: 10.1021/ja400119t

(49) Lautrette, G.; Touti, F.; Lee, H. G.; Dai, P.; Pentelute, B. L. Nitrogen Arylation for Macrocyclization of Unprotected Peptides. *J. Am. Chem. Soc.* **2016**, *138* (27), 8340–8343. DOI: 10.1021/jacs.6b03757

(50) Migoń, D.; Neubauer, D.; Kamysz, W. Hydrocarbon Stapled Antimicrobial Peptides. *Protein J.* **2018**, *37* (1), 2–12. DOI: 10.1007/s10930-018-9755-0

(51) Molchanova, N.; Hansen, P. R.; Franzyk, H. Advances in Development of Antimicrobial Peptidomimetics as Potential Drugs. *Molecules* **2017**, *22* (9), 1430. DOI: 10.3390/molecules22091430

(52) Ghosh, C.; Sarkar, P.; Issa, R.; Haldar, J. Alternatives to Conventional Antibiotics in the Era of Antimicrobial Resistance. *Trends Microbiol.* **2019**, *27* (4), 323–338. DOI: 10.1016/j.tim.2018.12.010

(53) Kowalski, R. P.; Romanowski, E. G.; Yates, K. A.; Mah, F. S. An Independent Evaluation of a Novel Peptide Mimetic, Brilacidin (PMX30063), for Ocular Anti-Infective. *J. Ocul. Pharmacol. Ther.* **2016**, *32* (1), 23–27. DOI: 10.1089/jop.2015.0098

(54) Kuppusamy, R.; Willcox, M.; Black, D. S. C.; Kumar, N. Short Cationic Peptidomimetic

Antimicrobials. *Antibiotics* **2019**, *8* (2), 1–31. DOI: 10.3390/antibiotics8020044

(55) Luther, A.; Urfer, M.; Zahn, M.; Müller, M.; Wang, S. Y.; Mondal, M.; Vitale, A.; Hartmann, J. B.; Sharpe, T.; Monte, F. Lo; Kocherla, H.; Cline, E.; Pessi, G.; Rath, P.; Modaresi, S. M.; Chiquet, P.; Stiegeler, S.; Verbree, C.; Remus, T.; Schmitt, M.; Kolopp, C.; Westwood, M. A.; Desjonquères, N.; Brabet, E.; Hell, S.; LePoupon, K.; Vermeulen, A.; Jaisson, R.; Rithié, V.; Upert, G.; Lederer, A.; Zbinden, P.; Wach, A.; Moehle, K.; Zerbe, K.; Locher, H. H.; Bernardini, F.; Dale, G. E.; Eberl, L.; Wollscheid, B.; Hiller, S.; Robinson, J. A.; Obrecht, D. Chimeric Peptidomimetic Antibiotics against Gram-Negative Bacteria. *Nature* **2019**, *576* (7787), 452–458. DOI: 10.1038/s41586-019-1665-6

(56) Martin-Serrano, Á.; Gómez, R.; Ortega, P.; Mata, F. J. D. La. Nanosystems as Vehicles for the Delivery of Antimicrobial Peptides (AMPs). *Pharmaceutics* **2019**, *11* (9), 1–24. DOI: 10.3390/pharmaceutics11090448

(57) Makowski, M.; Silva, Í. C.; Do Amaral, C. P.; Gonçalves, S.; Santos, N. C. Advances in Lipid and Metal Nanoparticles for Antimicrobial Peptide Delivery. *Pharmaceutics* **2019**, *11* (11), 588. DOI: 10.3390/pharmaceutics11110588

(58) Rao, L.; Tian, R.; Chen, X. Cell-Membrane-Mimicking Nanodecoys against Infectious Diseases. *ACS Nano* **2020**, *14* (3), 2569–2574. DOI: 10.1021/acsnano.0c01665

(59) Kumar, P.; Pletzer, D.; Haney, E. F.; Rahanjam, N.; Cheng, J. T. J.; Yue, M.; Aljehani, W.; Hancock, R. E. W.; Kizhakkedathu, J. N.; Straus, S. K. Aurein-Derived Antimicrobial Peptides Formulated with Pegylated Phospholipid Micelles to Target Methicillin-Resistant Staphylococcus Aureus Skin Infections. *ACS Infect. Dis.* **2019**, *5* (3), 443–453. DOI: 10.1021/acsinfecdis.8b00319

(60) Rajchakit, U.; Sarojini, V. Recent Developments in Antimicrobial-Peptide-Conjugated Gold Nanoparticles. *Bioconjug. Chem.* **2017**, *28* (11), 2673–2686. DOI: 10.1021/acs.bioconjchem.7b00368

(61) Liu, L.; Yang, J.; Xie, J.; Luo, Z.; Jiang, J.; Yang, Y. Y.; Liu, S. The Potent Antimicrobial Properties of Cell Penetrating Peptide-Conjugated Silver Nanoparticles with Excellent Selectivity for Gram-Positive Bacteria over Erythrocytes. *Nanoscale* **2013**, *5* (9), 3834–3840. DOI: 10.1039/c3nr34254a

(62) Gao, J.; Na, H.; Zhong, R.; Yuan, M.; Guo, J.; Zhao, L.; Wang, Y.; Wang, L.; Zhang, F. One Step Synthesis of Antimicrobial Peptide Protected Silver Nanoparticles: The Core-Shell Mutual Enhancement of Antibacterial Activity. *Colloids Surfaces B Biointerfaces* **2020**, *186*, 110704. DOI: 10.1016/j.colsurfb.2019.110704

(63) Yeom, J. H.; Lee, B.; Kim, D.; Lee, J. kook; Kim, S.; Bae, J.; Park, Y.; Lee, K. Gold

Nanoparticle-DNA Aptamer Conjugate-Assisted Delivery of Antimicrobial Peptide Effectively Eliminates Intracellular Salmonella Enterica Serovar Typhimurium. *Biomaterials* **2016**, *104*, 43–51. DOI: 10.1016/j.biomaterials.2016.07.009

(64) Lee, B.; Park, J.; Ryu, M.; Kim, S.; Joo, M.; Yeom, J. H.; Kim, S.; Park, Y.; Lee, K.; Bae, J. Antimicrobial Peptide-Loaded Gold Nanoparticle-DNA Aptamer Conjugates as Highly Effective Antibacterial Therapeutics against Vibrio Vulnificus. *Sci. Rep.* **2017**, *7* (1), 1–10. DOI: 10.1038/s41598-017-14127-z

(65) Ekladious, I.; Colson, Y. L.; Grinstaff, M. W. Polymer–Drug Conjugate Therapeutics: Advances, Insights and Prospects. *Nat. Rev. Drug Discov.* **2019**, *18* (4), 273–294. DOI: 10.1038/s41573-018-0005-0

(66) Imura, Y.; Nishida, M.; Ogawa, Y.; Takakura, Y.; Matsuzaki, K. Action Mechanism of Tachyplesin I and Effects of PEGylation. *Biochim. Biophys. Acta - Biomembr.* **2007**, *1768* (5), 1160–1169. DOI: 10.1016/j.bbamem.2007.01.005

(67) Imura, Y.; Nishida, M.; Matsuzaki, K. Action Mechanism of PEGylated Magainin 2 Analogue Peptide. *Biochim. Biophys. Acta - Biomembr.* **2007**, *1768* (10), 2578–2585. DOI: 10.1016/j.bbamem.2007.06.013

(68) Singh, S.; Papareddy, P.; Mörgelin, M.; Schmidtchen, A.; Malmsten, M. Effects of PEGylation on Membrane and Lipopolysaccharide Interactions of Host Defense Peptides. *Biomacromolecules* **2014**, *15* (4), 1337–1345. DOI: 10.1021/bm401884e

(69) Morris, C. J.; Beck, K.; Fox, M. A.; Ulaeto, D.; Clark, G. C.; Gumbleton, M. Pegylation of Antimicrobial Peptides Maintains the Active Peptide Conformation, Model Membrane Interactions, and Antimicrobial Activity While Improving Lung Tissue Biocompatibility Following Airway Delivery. *Antimicrob. Agents Chemother.* **2012**, *56* (6), 3298–3308. DOI: 10.1128/AAC.06335-11

(70) Kaur, N.; Dilawari, R.; Kaur, A.; Sahni, G.; Rishi, P. Recombinant Expression, Purification and PEGylation of Paneth Cell Peptide (Cryptdin-2) with Value Added Attributes against Staphylococcus Aureus. *Sci. Rep.* **2020**, *10* (1), 12164. DOI: 10.1038/s41598-020-69039-2

(71) Makadia, H. K.; Siegel, S. J. Poly Lactic-Co-Glycolic Acid (PLGA) as Biodegradable Controlled Drug Delivery Carrier. *Polymers (Basel).* **2011**, *3* (3), 1377–1397. DOI: 10.3390/polym3031377

(72) Chereddy, K. K.; Her, C. H.; Comune, M.; Moia, C.; Lopes, A.; Porporato, P. E.; Vanacker, J.; Lam, M. C.; Steinstraesser, L.; Sonveaux, P.; Zhu, H.; Ferreira, L. S.; Vandermeulen, G.; Préat, V. PLGA Nanoparticles Loaded with Host Defense Peptide

LL37 Promote Wound Healing. *J. Control. Release* **2014**, *194*, 138–147. DOI: 10.1016/j.jconrel.2014.08.016

(73) Vijayan, A.; James, P. P.; Nanditha, C. K.; Vinod Kumar, G. S. Multiple Cargo Deliveries of Growth Factors and Antimicrobial Peptide Using Biodegradable Nanopolymer as a Potential Wound Healing System. *Int. J. Nanomedicine* **2019**, *14*, 2253–2263. DOI: 10.2147/IJN.S190321

(74) Water, J. J.; Smart, S.; Franzyk, H.; Foged, C.; Nielsen, H. M. Nanoparticle-Mediated Delivery of the Antimicrobial Peptide Plectasin against Staphylococcus Aureus in Infected Epithelial Cells. *Eur. J. Pharm. Biopharm.* **2015**, *92*, 65–73. DOI: 10.1016/j.ejpb.2015.02.009

(75) Casciaro, B.; D'Angelo, I.; Zhang, X.; Loffredo, M. R.; Conte, G.; Cappiello, F.; Quaglia, F.; Di, Y. P. P.; Ungaro, F.; Mangoni, M. L. Poly(Lactide-Co-Glycolide) Nanoparticles for Prolonged Therapeutic Efficacy of Esculentin-1a-Derived Antimicrobial Peptides against Pseudomonas Aeruginosa Lung Infection: In Vitro and in Vivo Studies. *Biomacromolecules* **2019**, *20* (5), 1876–1888. DOI: 10.1021/acs.biomac.8b01829

(76) Abbina, S.; Vappala, S.; Kumar, P.; Siren, E. M. J.; La, C. C.; Abbasi, U.; Brooks, D. E.; Kizhakkedathu, J. N. Hyperbranched Polyglycerols: Recent Advances in Synthesis, Biocompatibility and Biomedical Applications. *J. Mater. Chem. B* **2017**, *5* (47), 9249–9277. DOI: 10.1039/c7tb02515g

(77) Abbina, S.; Abbasi, U.; Gill, A.; Wong, K.; Kalathottukaren, M. T.; Kizhakkedathu, J. N. Design of Safe Nanotherapeutics for the Excretion of Excess Systemic Toxic Iron. *ACS Cent. Sci.* **2019**, *5* (5), 917–926. DOI: 10.1021/acscentsci.9b00284

(78) Kumar, P.; Shenoi, R. A.; Lai, B. F.; Nguyen, M.; Kizhakkedathu, J. N.; Straus, S. K. Conjugation of Aurein 2.2 to HPG Yields an Antimicrobial with Better Properties. *Biomacromolecules* **2015**, *16* (3), 913–923. DOI: 10.1021/bm5018244

(79) Haney, E. F.; Wuerth, K. C.; Rahanjam, N.; Nikouei, N. S.; Ghassemi, A.; Noghani, M. A.; Boey, A.; Hancock, R. E. W. Identification of an IDR Peptide Formulation Candidate That Prevents Peptide Aggregation and Retains Immunomodulatory Activity. *Pept. Sci.* **2019**, *111* (1), e24077. DOI: 10.1002/pep2.24077

(80) Petrin, T. H. C.; Fadel, V.; Martins, D. B.; Dias, S. A.; Cruz, A.; Sergio, L. M.; Arcisio-Miranda, M.; Castanho, M. A. R. B.; Dos Santos Cabrera, M. P. Synthesis and Characterization of Peptide-Chitosan Conjugates (PepChis) with Lipid Bilayer Affinity and Antibacterial Activity. *Biomacromolecules* **2019**, *20* (7), 2743–2753. DOI: 10.1021/acs.biomac.9b00501

(81) Almaaytah, A.; Mohammed, G. K.; Abualhaijaa, A.; Al-Balas, Q. Development of Novel Ultrashort Antimicrobial Peptide Nanoparticles with Potent Antimicrobial and Antibiofilm Activities against Multidrug-Resistant Bacteria. *Drug Des. Devel. Ther.* **2017**, *11*, 3159–3170. DOI: 10.2147/DDDT.S147450

(82) Sahariah, P.; Sørensen, K. K.; Hjálmarsdóttir, M. A.; Sigurjónsson, Ó. E.; Jensen, K. J.; Másson, M.; Thygesen, M. B. Antimicrobial Peptide Shows Enhanced Activity and Reduced Toxicity upon Grafting to Chitosan Polymers. *Chem. Commun.* **2015**, *51* (58), 11611–11614. DOI: 10.1039/c5cc04010h

(83) Hou, Z.; Shankar, Y. V.; Liu, Y.; Ding, F.; Subramanion, J. L.; Ravikumar, V.; Zamudio-Vázquez, R.; Keogh, D.; Lim, H.; Tay, M. Y. F.; Bhattacharjya, S.; Rice, S. A.; Shi, J.; Duan, H.; Liu, X. W.; Mu, Y.; Tan, N. S.; Tam, K. C.; Pethe, K.; Chan-Park, M. B. Nanoparticles of Short Cationic Peptidopolysaccharide Self-Assembled by Hydrogen Bonding with Antibacterial Effect against Multidrug-Resistant Bacteria. *ACS Appl. Mater. Interfaces* **2017**, *9* (44), 38288–38303. DOI: 10.1021/acsami.7b12120

(84) Piras, A. M.; Maisetta, G.; Sandreschi, S.; Gazzarri, M.; Bartoli, C.; Grassi, L.; Esin, S.; Chiellini, F.; Batoni, G. Chitosan Nanoparticles Loaded with the Antimicrobial Peptide Temporin B Exert a Long-Term Antibacterial Activity in Vitro against Clinical Isolates of Staphylococcus Epidermidis. *Front. Microbiol.* **2015**, *6*, 1–10. DOI: 10.3389/fmicb.2015.00372

(85) Shelke, N. B.; James, R.; Laurencin, C. T.; Kumbar, S. G. Polysaccharide Biomaterials for Drug Delivery and Regenerative Engineering. *Polym. Adv. Technol.* **2014**, *25* (5), 448–460. DOI: 10.1002/pat.3266

(86) Lee, H.; Lim, S. I.; Shin, S. H.; Lim, Y.; Koh, J. W.; Yang, S. Conjugation of Cell-Penetrating Peptides to Antimicrobial Peptides Enhances Antibacterial Activity. *ACS Omega* **2019**, *4* (13), 15694–15701. DOI: 10.1021/acsomega.9b02278

(87) Ho, P. L.; Ong, H. K.; Teo, J.; Ow, D. S. W.; Chao, S. H. HEXIM1 Peptide Exhibits Antimicrobial Activity against Antibiotic Resistant Bacteria through Guidance of Cell Penetrating Peptide. *Front. Microbiol.* **2019**, *10*, 1–10. DOI: 10.3389/fmicb.2019.00203

(88) Umstätter, F.; Domhan, C.; Hertlein, T.; Ohlsen, K.; Mühlberg, E.; Kleist, C.; Zimmermann, S.; Beijer, B.; Klika, K. D.; Haberkorn, U.; Mier, W.; Uhl, P. Vancomycin Resistance Is Overcome by Conjugation of Polycationic Peptides. *Angew. Chemie Int. Ed.* **2020**, 1–6. DOI: 10.1002/anie.202002727

(89) Siriwardena, T. N.; Capecchi, A.; Gan, B. H.; Jin, X.; He, R.; Wei, D.; Ma, L.; Köhler, T.; van Delden, C.; Javor, S.; Reymond, J. L. Optimizing Antimicrobial Peptide Dendrimers

in Chemical Space. *Angew. Chemie - Int. Ed.* **2018**, *57* (28), 8483–8487. DOI: 10.1002/anie.201802837

(90) Pini, A.; Falciani, C.; Mantengoli, E.; Bindi, S.; Brunetti, J.; Iozzi, S.; Rossolini, G. M.; Bracci, L. A Novel Tetrabranched Antimicrobial Peptide That Neutralizes Bacterial Lipopolysaccharide and Prevents Septic Shock in Vivo. *FASEB J.* **2010**, *24* (4), 1015–1022. DOI: 10.1096/fj.09-145474

(91) Brunetti, J.; Falciani, C.; Roscia, G.; Pollini, S.; Bindi, S.; Scali, S.; Arrieta, U. C.; Gomez-Vallejo, V.; Quercini, L.; Ibba, E.; Prato, M.; Rossolini, G. M.; Llop, J.; Bracci, L.; Pini, A. In Vitro and in Vivo Efficacy, Toxicity, Bio-Distribution and Resistance Selection of a Novel Antibacterial Drug Candidate. *Sci. Rep.* **2016**, *6*, 1–12. DOI: 10.1038/srep26077

(92) Falciani, C.; Lozzi, L.; Pollini, S.; Luca, V.; Carnicelli, V.; Brunetti, J.; Lelli, B.; Bindi, S.; Scali, S.; Di Giulio, A.; Rossolini, G. M.; Mangoni, M. L.; Bracci, L.; Pini, A. Isomerization of an Antimicrobial Peptide Broadens Antimicrobial Spectrum to Gram-Positive Bacterial Pathogens. *PLoS One* **2012**, *7* (10), 1–8. DOI: 10.1371/journal.pone.0046259

(93) Zurawski, D. V.; McLendon, M. K. Monoclonal Antibodies as an Antibacterial Approach against Bacterial Pathogens. *Antibiotics* **2020**, *9* (4), 1–12. DOI: 10.3390/antibiotics9040155

(94) Mariathasan, S.; Tan, M. W. Antibody–Antibiotic Conjugates: A Novel Therapeutic Platform against Bacterial Infections. *Trends Mol. Med.* **2017**, *23* (2), 135–149. DOI: 10.1016/j.molmed.2016.12.008

(95) Lehar, S. M.; Pillow, T.; Xu, M.; Staben, L.; Kajihara, K. K.; Vandlen, R.; DePalatis, L.; Raab, H.; Hazenbos, W. L.; Hiroshi Morisaki, J.; Kim, J.; Park, S.; Darwish, M.; Lee, B. C.; Hernandez, H.; Loyet, K. M.; Lupardus, P.; Fong, R.; Yan, D.; Chalouni, C.; Luis, E.; Khalfin, Y.; Plise, E.; Cheong, J.; Lyssikatos, J. P.; Strandh, M.; Koefoed, K.; Andersen, P. S.; Flygare, J. A.; Wah Tan, M.; Brown, E. J.; Mariathasan, S. Novel Antibody-Antibiotic Conjugate Eliminates Intracellular S. Aureus. *Nature* **2015**, *527* (7578), 323–328. DOI: 10.1038/nature16057

(96) Franzman, M. R.; Burnell, K. K.; Dehkordi-Vakil, F. H.; Guthmiller, J. M.; Dawson, D. V.; Brogden, K. A. Targeted Antimicrobial Activity of a Specific IgG-SMAP28 Conjugate against Porphyromonas Gingivalis in a Mixed Culture. *Int. J. Antimicrob. Agents* **2009**, *33* (1), 14–20. DOI: 10.1016/j.ijantimicag.2008.05.021

(97) Touti, F.; Lautrette, G.; Johnson, K. D.; Delaney, J. C.; Wollacott, A.; Tissire, H.;

Viswanathan, K.; Shriver, Z.; Mong, S. K.; Mijalis, A. J.; Plante, O. J.; Pentelute, B. L. Antibody–Bactericidal Macrocyclic Peptide Conjugates To Target Gram-Negative Bacteria. *ChemBioChem* **2018**, *19* (19), 2039–2044. DOI: 10.1002/cbic.201800295

(98) Gautam, S.; Kim, T.; Lester, E.; Deep, D.; Spiegel, D. A. Wall Teichoic Acids Prevent Antibody Binding to Epitopes within the Cell Wall of Staphylococcus Aureus. *ACS Chem. Biol.* **2016**, *11* (1), 25–30. DOI: 10.1021/acschembio.5b00439

(99) Madhanagopal, B. R.; Zhang, S.; Demirel, E.; Wady, H.; Chandrasekaran, A. R. DNA Nanocarriers: Programmed to Deliver. *Trends Biochem. Sci.* **2018**, *43* (12), 997–1013. DOI: 10.1016/j.tibs.2018.09.010

(100) Obuobi, S.; Tay, H. K. L.; Tram, N. D. T.; Selvarajan, V.; Khara, J. S.; Wang, Y.; Ee, P. L. R. Facile and Efficient Encapsulation of Antimicrobial Peptides via Crosslinked DNA Nanostructures and Their Application in Wound Therapy. *J. Control. Release* **2019**, *313*, 120–130. DOI: 10.1016/j.jconrel.2019.10.013

(101) Mela, I.; Endo, M.; Sugiyama, H.; Henderson, R. M.; Kaminski, C. F. DNA Origami as a Tool in the Targeted Destruction of Bacteria. *Biophys. J.* **2019**, *116* (3), 324a. DOI: 10.1016/j.bpj.2018.11.1759

(102) Gao, W.; Thamphiwatana, S.; Angsantikul, P.; Zhang, L. Nanoparticle Approaches against Bacterial Infections. *Wiley Interdiscip. Rev. Nanomed. Nanobiotechnol.* **2014**, *6* (6), 532–547. DOI: 10.1002/wnan.1282

(103) Azzopardi, E. A.; Ferguson, E. L.; Thomas, D. W. The Enhanced Permeability Retention Effect: A New Paradigm for Drug Targeting in Infection. *J. Antimicrob. Chemother.* **2013**, *68* (2), 257–274. DOI: 10.1093/jac/dks379

(104) Lee, W. L.; Liles, W. C. Endothelial Activation, Dysfunction and Permeability during Severe Infections. *Curr. Opin. Hematol.* **2011**, *18* (3), 191–196. DOI: 10.1097/MOH.0b013e328345a3d1

(105) Boerman, O. C.; Storm, G.; Oyen, W. J. G.; Van Bloois, L.; Van der Meer, J. W. M.; Claessens, R. A. M. J.; Crommelin, D. J. A.; Corstens, F. H. M. Sterically Stabilized Liposomes Labeled with Indium-111 to Image Focal Infection. *J. Nucl. Med.* **1995**, *36* (9), 1639–1644.

(106) Boerman, O. C.; Oyen, W. J. G.; Van Bloois, L.; Koenders, E. B.; Van Der Meer, J. W. M.; Corstens, F. H. M.; Storm, G. Optimization of Technetium-99m-Labeled PEG Liposomes to Image Focal Infection: Effects of Particle Size and Circulation Time. *J. Nucl. Med.* **1997**, *38* (3), 489–493.

(107) Laverman, P.; Dams, E. T. M.; Storm, G.; Hafmans, T. G.; Croes, H. J.; Oyen, W. J. G.; Corstens, F. H. M.; Boerman, O. C. Microscopic Localization of PEG-Liposomes in a Rat Model of Focal Infection. *J. Control. Release* **2001**, *75* (3), 347–355. DOI: 10.1016/S0168-3659(01)00402-3

(108) Kell, A. J.; Stewart, G.; Ryan, S.; Peytavi, R.; Boissinot, M.; Huletsky, A.; Bergeron, M. G.; Simard, B. Vancomycin-Modified Nanoparticles for Efficient Targeting and Preconcentration of Gram-Positive and Gram-Negative Bacteria. *ACS Nano* **2008**, *2* (9), 1777–1788. DOI: 10.1021/nn700183g

(109) Chen, M.; Xie, S.; Wei, J.; Song, X.; Ding, Z.; Li, X. Antibacterial Micelles with Vancomycin-Mediated Targeting and pH/Lipase-Triggered Release of Antibiotics. *ACS Appl. Mater. Interfaces* **2018**, *10* (43), 36814–36823. DOI: 10.1021/acsami.8b16092

(110) Meeker, D. G.; Jenkins, S. V.; Miller, E. K.; Beenken, K. E.; Loughran, A. J.; Powless, A.; Muldoon, T. J.; Galanzha, E. I.; Zharov, V. P.; Smeltzer, M. S.; Chen, J. Synergistic Photothermal and Antibiotic Killing of Biofilm-Associated Staphylococcus Aureus Using Targeted Antibiotic-Loaded Gold Nanoconstructs. *ACS Infect. Dis.* **2016**, *2* (4), 241–250. DOI: 10.1021/acsinfecdis.5b00117

(111) Chen, J.; Zhang, C.; Liu, Q.; Shao, X.; Feng, C.; Shen, Y.; Zhang, Q.; Jiang, X. Solanum Tuberosum Lectin-Conjugated PLGA Nanoparticles for Nose-to-Brain Delivery: In Vivo and in Vitro Evaluations. *J. Drug Target.* **2012**, *20* (2), 174–184. DOI: 10.3109/1061186X.2011.622396

(112) Umamaheshwari, R. B.; Jain, N. K. Receptor Mediated Targeting of Lectin Conjugated Gliadin Nanoparticles in the Treatment of Helicobacter Pylori. *J. Drug Target.* **2003**, *11* (7), 415–424. DOI: 10.1080/10611860310001647771

(113) Mura, S.; Nicolas, J.; Couvreur, P. Stimuli-Responsive Nanocarriers for Drug Delivery. *Nat. Mater.* **2013**, *12* (11), 991–1003. DOI: 10.1038/nmat3776

(114) Radovic-Moreno, A. F.; Lu, T. K.; Puscasu, V. A.; Yoon, C. J.; Langer, R.; Farokhzad, O. C. Surface Charge-Switching Polymeric Nanoparticles for Bacterial Cell Wall-Targeted Delivery of Antibiotics. *ACS Nano* **2012**, *6* (5), 4279–4287. DOI: 10.1021/nn3008383

(115) Wu, J.; Li, F.; Hu, X.; Lu, J.; Sun, X.; Gao, J.; Ling, D. Responsive Assembly of Silver Nanoclusters with a Biofilm Locally Amplified Bactericidal Effect to Enhance Treatments against Multi-Drug-Resistant Bacterial Infections. *ACS Cent. Sci.* **2019**, *5* (8), 1366–1376. DOI: 10.1021/acscentsci.9b00359

(116) Gupta, A.; Das, R.; Yesilbag Tonga, G.; Mizuhara, T.; Rotello, V. M. Charge-Switchable Nanozymes for Bioorthogonal Imaging of Biofilm-Associated Infections. *ACS Nano*

2018, *12* (1), 89–94. DOI: 10.1021/acsnano.7b07496

(117) Alfadda, A. A.; Sallam, R. M. Reactive Oxygen Species in Health and Disease. *J. Biomed. Biotechnol.* **2012**, *2012*, 936486. DOI: 10.1155/2012/936486

(118) Vanlaere, I.; Libert, C. Matrix Metalloproteinases as Drug Targets in Infections Caused by Gram-Negative Bacteria and in Septic Shock. *Clin. Microbiol. Rev.* **2009**, *22* (2), 224–239. DOI: 10.1128/CMR.00047-08

(119) Chaplin, D. D. Overview of the Immune Response. *J. Allergy Clin. Immunol.* **2010**, *125* (2 SUPPL. 2), S3–S23. DOI: 10.1016/j.jaci.2009.12.980

(120) Peyron, P.; Maridonneau-Parini, I.; Stegmann, T. Fusion of Human Neutrophil Phagosomes with Lysosomes in Vitro: Involvement of Tyrosine Kinases of the Src Family and Inhibition by Mycobacteria. *J. Biol. Chem.* **2001**, *276* (38), 35512–35517. DOI: 10.1074/jbc.M104399200

(121) Kamaruzzaman, N. F.; Kendall, S.; Good, L. Targeting the Hard to Reach: Challenges and Novel Strategies in the Treatment of Intracellular Bacterial Infections. *Br. J. Pharmacol.* **2017**, *174* (14), 2225–2236. DOI: 10.1111/bph.13664

(122) Xiong, M. H.; Li, Y. J.; Bao, Y.; Yang, X. Z.; Hu, B.; Wang, J. Bacteria-Responsive Multifunctional Nanogel for Targeted Antibiotic Delivery. *Adv. Mater.* **2012**, *24* (46), 6175–6180. DOI: 10.1002/adma.201202847

(123) Hou, X.; Zhang, X.; Zhao, W.; Zeng, C.; Deng, B.; McComb, D. W.; Du, S.; Zhang, C.; Li, W.; Dong, Y. Vitamin Lipid Nanoparticles Enable Adoptive Macrophage Transfer for the Treatment of Multidrug-Resistant Bacterial Sepsis. *Nat. Nanotechnol.* **2020**, *15* (1), 41–46. DOI: 10.1038/s41565-019-0600-1

(124) Canaparo, R.; Foglietta, F.; Giuntini, F.; Pepa, C. Della; Dosio, F.; Serpe, L. Recent Developments in Antibacterial Therapy: Focus on Stimuli-Responsive Drug-Delivery Systems and Therapeutic Nanoparticles. *Molecules* **2019**, *24* (10), 1991. DOI: 10.3390/molecules24101991

(125) Dong, P.; Zhou, Y.; He, W.; Hua, D. A Strategy for Enhanced Antibacterial Activity against Staphylococcus Aureus by the Assembly of Alamethicin with a Thermo-Sensitive Polymeric Carrier. *Chem. Commun.* **2016**, *52* (5), 896–899. DOI: 10.1039/c5cc07054f

(126) Mohapatra, A.; Harris, M. A.; LeVine, D.; Ghimire, M.; Jennings, J. A.; Morshed, B. I.; Haggard, W. O.; Bumgardner, J. D.; Mishra, S. R.; Fujiwara, T. Magnetic Stimulus Responsive Vancomycin Drug Delivery System Based on Chitosan Microbeads Embedded with Magnetic Nanoparticles. *J. Biomed. Mater. Res. - Part B Appl. Biomater.*

2018, *106* (6), 2169–2176. DOI: 10.1002/jbm.b.34015

(127) Maleki, H.; Rai, A.; Pinto, S.; Evangelista, M.; Cardoso, R. M. S.; Paulo, C.; Carvalheiro, T.; Paiva, A.; Imani, M.; Simchi, A.; Durães, L.; Portugal, A.; Ferreira, L. High Antimicrobial Activity and Low Human Cell Cytotoxicity of Core-Shell Magnetic Nanoparticles Functionalized with an Antimicrobial Peptide. *ACS Appl. Mater. Interfaces* **2016**, *8* (18), 11366–11378. DOI: 10.1021/acsami.6b03355

(128) Gross, J.; Lapiere, C. M. Collagenolytic Activity in Amphibian Tissues: A Tissue Culture Assay. *Proc. Natl. Acad. Sci. U. S. A.* **1962**, *48* (6), 1014–1022. DOI: 10.1073/pnas.48.6.1014

(129) Cui, N.; Hu, M.; Khalil, R. A. Biochemical and Biological Attributes of Matrix Metalloproteinases. *Prog. Mol. Biol. Transl. Sci.* **2017**, *147*, 1–73. DOI: 10.1016/bs.pmbts.2017.02.005

(130) Glasheen, B. M.; Kabra, A. T.; Page-McCaw, A. Distinct Functions for the Catalytic and Hemopexin Domains of a Drosophila Matrix Metalloproteinase. *Proc. Natl. Acad. Sci. U. S. A.* **2009**, *106* (8), 2659–2664. DOI: 10.1073/pnas.0804171106

(131) Löffek, S.; Schilling, O.; Franzke, C. W. Biological Role of Matrix Metalloproteinases: A Critical Balance. *Eur. Respir. J.* **2011**, *38* (1), 191–208. DOI: 10.1183/09031936.00146510

(132) Elkington, P. T. G.; O'Kane, C. M.; Friedland, J. S. The Paradox of Matrix Metalloproteinases in Infectious Disease. *Clin. Exp. Immunol.* **2005**, *142* (1), 12–20. DOI: 10.1111/j.1365-2249.2005.02840.x

(133) Smigiel, K. S.; Parks, W. C. Matrix Metalloproteinases and Leukocyte Activation. *Prog. Mol. Biol. Transl. Sci.* **2017**, *147*, 167–195. DOI: 10.1016/bs.pmbts.2017.01.003

(134) Browne, K.; Chakraborty, S.; Chen, R.; Willcox, M. D. P.; Black, D. S.; Walsh, W. R.; Kumar, N. A New Era of Antibiotics: The Clinical Potential of Antimicrobial Peptides. *Int. J. Mol. Sci.* **2020**, *21* (19), 1–23. DOI: 10.3390/ijms21197047

(135) Chen, C. H.; Lu, T. K. Development and Challenges of Antimicrobial Peptides for Therapeutic Applications. *Antibiotics* **2020**, *9* (1), 24. DOI: 10.3390/antibiotics9010024

(136) Eckhard, U.; Huesgen, P. F.; Schilling, O.; Bellac, C. L.; Butler, G. S.; Cox, J. H.; Dufour, A.; Goebeler, V.; Kappelhoff, R.; auf dem Keller, U.; Klein, T.; Lange, P. F.; Marino, G.; Morrison, C. J.; Prudova, A.; Rodriguez, D.; Starr, A. E.; Wang, Y.; Overall, C. M. Active Site Specificity Profiling of the Matrix Metalloproteinase Family: Proteomic Identification of 4300 Cleavage Sites by Nine MMPs Explored with Structural and Synthetic Peptide

Cleavage Analyses. *Matrix Biol.* **2016**, *49* (2016), 37–60. DOI: 10.1016/j.matbio.2015.09.003

(137) Chakrabarti, S.; Zee, J. M.; Patel, K. D. Regulation of Matrix Metalloproteinase-9 (MMP-9) in TNF-Stimulated Neutrophils: Novel Pathways for Tertiary Granule Release. *J. Leukoc. Biol.* **2006**, *79* (1), 214–222. DOI: 10.1189/jlb.0605353

(138) Ardi, V. C.; Kupriyanova, T. A.; Deryugina, E. I.; Quigley, J. P. Human Neutrophils Uniquely Release TIMP-Free MMP-9 to Provide a Potent Catalytic Stimulator of Angiogenesis. *Proc. Natl. Acad. Sci. U. S. A.* **2007**, *104* (51), 20262–20267. DOI: 10.1073/pnas.0706438104

(139) Hasty, K. A.; Hibbs, M. S.; Kang, A. H.; Mainardi, C. L. Secreted Forms of Human Neutrophil Collagenase. *J. Biol. Chem.* **1986**, *261* (12), 5645–5650.

(140) Rossi, N. A. A.; Constantinescu, I.; Kainthan, R. K.; Brooks, D. E.; Scott, M. D.; Kizhakkedathu, J. N. Red Blood Cell Membrane Grafting of Multi-Functional Hyperbranched Polyglycerols. *Biomaterials* **2010**, *31* (14), 4167–4178. DOI: 10.1016/j.biomaterials.2010.01.137

(141) Ahmed, M.; Lai, B. F. L.; Kizhakkedathu, J. N.; Narain, R. Hyperbranched Glycopolymers for Blood Biocompatibility. *Bioconjug. Chem.* **2012**, *23* (5), 1050–1058. DOI: 10.1021/bc3000723

(142) Imran Ul-Haq, M.; Hamilton, J. L.; Lai, B. F. L.; Shenoi, R. A.; Horte, S.; Constantinescu, I.; Leitch, H. A.; Kizhakkedathu, J. N. Design of Long Circulating Nontoxic Dendritic Polymers for the Removal of Iron in Vivo. *ACS Nano* **2013**, *7* (12), 10704–10716. DOI: 10.1021/nn4035074

(143) Pletzer, D.; Mansour, S. C.; Wuerth, K.; Rahanjam, N.; Hancock, R. E. W. New Mouse Model for Chronic Infections by Gram-Negative Bacteria Enabling the Study of Anti-Infective Efficacy and Host-Microbe Interactions. *MBio* **2017**, *8* (1), 1–16. DOI: 10.1128/mBio.00140-17

(144) Lee, A.; Kim, S. H.; Lee, H.; Kim, B.; Kim, Y. S.; Key, J. Visualization of MMP-2 Activity Using Dual-Probe Nanoparticles to Detect Potential Metastatic Cancer Cells. *Nanomaterials* **2018**, *8* (2), 1–12. DOI: 10.3390/nano8020119

(145) Loynachan, C. N.; Soleimany, A. P.; Dudani, J. S.; Lin, Y.; Najer, A.; Bekdemir, A.; Chen, Q.; Bhatia, S. N.; Stevens, M. M. Renal Clearable Catalytic Gold Nanoclusters for in Vivo Disease Monitoring. *Nat. Nanotechnol.* **2019**, *14* (9), 883–890. DOI: 10.1038/s41565-019-0527-6

(146) Li, J.; Ge, Z.; Liu, S. PEG-Sheddable Polyplex Micelles as Smart Gene Carriers Based on MMP-Cleavable Peptide-Linked Block Copolymers. *Chem. Commun.* **2013**, *49* (62), 6974–6976. DOI: 10.1039/c3cc43576h

(147) Bremer, C.; Tung, C. H.; Weissleder, R. In Vivo Molecular Target Assessment of Matrix Metalloproteinase Inhibition. *Nat. Med.* **2001**, *7* (6), 743–748. DOI: 10.1038/89126

(148) Borregaard, N. Neutrophils, from Marrow to Microbes. *Immunity* **2010**, *33* (5), 657–670. DOI: 10.1016/j.immuni.2010.11.011

(149) Sheshachalam, A.; Srivastava, N.; Mitchell, T.; Lacy, P.; Eitzen, G. Granule Protein Processing and Regulated Secretion in Neutrophils. *Front. Immunol.* **2014**, *5*, 1–11. DOI: 10.3389/fimmu.2014.00448

(150) Ong, C. W. M.; Pabisiak, P. J.; Brilha, S.; Singh, P.; Roncaroli, F.; Elkington, P. T.; Friedland, J. S. Complex Regulation of Neutrophil-Derived MMP-9 Secretion in Central Nervous System Tuberculosis. *J. Neuroinflammation* **2017**, *14* (1), 1–12. DOI: 10.1186/s12974-017-0801-1

(151) Rosales, C. Neutrophil: A Cell with Many Roles in Inflammation or Several Cell Types? *Front. Physiol.* **2018**, *9*, 1–17. DOI: 10.3389/fphys.2018.00113

(152) McQuibban, G. A.; Gong, J. H.; Wong, J. P.; Wallace, J. L.; Clark-Lewis, I.; Overall, C. M. Matrix Metalloproteinase Processing of Monocyte Chemoattractant Proteins Generates CC Chemokine Receptor Antagonists with Anti-Inflammatory Properties in Vivo. *Blood* **2002**, *100* (4), 1160–1167. DOI: 10.1182/blood.v100.4.1160.h81602001160_1160_1167

(153) McQuibban, G. A.; Gong, J. H.; Tam, E. M.; McCulloch, C. A. G.; Clark-Lewis, I.; Overall, C. M. Inflammation Dampened by Gelatinase a Cleavage of Monocyte Chemoattractant Protein-3. *Science.* **2000**, *289* (5482), 1202–1206. DOI: 10.1126/science.289.5482.1202

(154) Houghton, A. M. G.; Hartzell, W. O.; Robbins, C. S.; Gomis-Rüth, F. X.; Shapiro, S. D. Macrophage Elastase Kills Bacteria within Murine Macrophages. *Nature* **2009**, *460* (7255), 637–641. DOI: 10.1038/nature08181

(155) Lin, M.; Jackson, P.; Tester, A. M.; Diaconu, E.; Overall, C. M.; Blalock, J. E.; Pearlman, E. Matrix Metalloproteinase-8 Facilitates Neutrophil Migration through the Corneal Stromal Matrix by Collagen Degradation and Production of the Chemotactic Peptide Pro-Gly-Pro. *Am. J. Pathol.* **2008**, *173* (1), 144–153. DOI: 10.2353/ajpath.2008.080081

(156) Holinstat, M. Normal Platelet Function. *Cancer Metastasis Rev.* **2017**, *36* (2), 195–198. DOI: 10.1007/s10555-017-9677-x

(157) Shenoi, R. A.; Kalathottukaren, M. T.; Travers, R. J.; Lai, B. F. L. L.; Creagh, A. L.; Lange, D.; Yu, K.; Weinhart, M.; Chew, B. H.; Du, C.; Brooks, D. E.; Carter, C. J.; Morrissey, J. H.; Haynes, C. A.; Kizhakkedathu, J. N. Affinity-Based Design of a Synthetic Universal Reversal Agent for Heparin Anticoagulants. *Sci. Transl. Med.* **2014**, *6* (260), 260ra150. DOI: 10.1182/blood-2014-05-577932

(158) Forde, E. Novel Host Defence Peptide Prodrugs for Use in Cystic Fibrosis. Ph.D. Thesis, Royal College of Surgeons in Ireland, **2015**. DOI: 10.25419/rcsi.10808747.v1

(159) Forde, E.; Devocelle, M. Pro-Moieties of Antimicrobial Peptide Prodrugs. *Molecules* **2015**, *20* (1), 1210–1227. DOI: 10.3390/molecules20011210

(160) Svenson, J.; Brandsdal, B. O.; Stensen, W.; Svendsen, J. S. Albumin Binding of Short Cationic Antimicrobial Micropeptides and Its Influence on the in Vitro Bactericidal Effect. *J. Med. Chem.* **2007**, *50* (14), 3334–3339. DOI: 10.1021/jm0703542

(161) Sivertsen, A.; Isaksson, J.; Leiros, H. K. S.; Svenson, J.; Svendsen, J. S.; Brandsdal, B. O. Synthetic Cationic Antimicrobial Peptides Bind with Their Hydrophobic Parts to Drug Site II of Human Serum Albumin. *BMC Struct. Biol.* **2014**, *14* (1), 4. DOI: 10.1186/1472-6807-14-4

(162) Kolar, S. L.; Liu, G. Y. Targeting Bacterial Abscess Formation. *EBioMedicine* **2016**, *12*, 16–17. DOI: 10.1016/j.ebiom.2016.10.017

(163) Mansour, S. C.; Pletzer, D.; de la Fuente-Núñez, C.; Kim, P.; Cheung, G. Y. C.; Joo, H. S.; Otto, M.; Hancock, R. E. W. Bacterial Abscess Formation Is Controlled by the Stringent Stress Response and Can Be Targeted Therapeutically. *EBioMedicine* **2016**, *12*, 219–226. DOI: 10.1016/j.ebiom.2016.09.015

(164) Stearne, L. E. T.; Kooi, C.; Goessens, W. H. F.; Bakker-Woudenberg, I. A. J. M.; Gyssens, I. C. In Vitro Activity of Trovafloxacin against Bacteroides Fragilis in Mixed Culture with Either Escherichia Coli or a Vancomycin-Resistant Strain of Enterococcus Faecium Determined by an Anaerobic Time-Kill Technique. *Antimicrob. Agents Chemother.* **2001**, *45* (1), 243–251. DOI: 10.1128/AAC.45.1.243-251.2001

(165) Kerschenmeyer, A.; Arlov, Ø.; Malheiro, V.; Steinwachs, M.; Rottmar, M.; Maniura-Weber, K.; Palazzolo, G.; Zenobi-Wong, M. Anti-Oxidant and Immune-Modulatory Properties of Sulfated Alginate Derivatives on Human Chondrocytes and Macrophages. *Biomater. Sci.* **2017**, *5* (9), 1756–1765. DOI: 10.1039/c7bm00341b

(166) Chen, X.; Zaro, J. L.; Shen, W. C. Fusion Protein Linkers: Property, Design and Functionality. *Adv. Drug Deliv. Rev.* **2013**, *65* (10), 1357–1369. DOI: 10.1016/j.addr.2012.09.039

(167) Van Rosmalen, M.; Krom, M.; Merkx, M. Tuning the Flexibility of Glycine-Serine Linkers to Allow Rational Design of Multidomain Proteins. *Biochemistry* **2017**, *56* (50), 6565–6574. DOI: 10.1021/acs.biochem.7b00902

(168) Banerjee, S. S.; Aher, N.; Patil, R.; Khandare, J. Poly(Ethylene Glycol)-Prodrug Conjugates: Concept, Design, and Applications. *J. Drug Deliv.* **2012**, *2012*, 1–17. DOI: 10.1155/2012/103973

(169) Dhara, D.; Chatterji, P. R. Electrophoretic Transport of Poly(Ethylene Glycol) Chains through Poly(Acrylamide) Gel. *J. Phys. Chem. B* **1999**, *103* (40), 8458–8461. DOI: 10.1021/jp990443t

(170) Schumacher, F. F.; Sanchania, V. A.; Tolner, B.; Wright, Z. V. F.; Ryan, C. P.; Smith, M. E. B.; Ward, J. M.; Caddick, S.; Kay, C. W. M.; Aeppli, G.; Chester, K. A.; Baker, J. R. Homogeneous Antibody Fragment Conjugation by Disulfide Bridging Introduces "Spinostics." *Sci. Rep.* **2013**, *3*, 1–8. DOI: 10.1038/srep01525

(171) Sun, Y.; Shang, D. Inhibitory Effects of Antimicrobial Peptides on Lipopolysaccharide-Induced Inflammation. *Mediators Inflamm.* **2015**, *2015*, 167572. DOI: 10.1155/2015/167572

(172) Pulido, D.; Nogús, M. V.; Boix, E.; Torrent, M. Lipopolysaccharide Neutralization by Antimicrobial Peptides: A Gambit in the Innate Host Defense Strategy. *J. Innate Immun.* **2012**, *4* (4), 327–336. DOI: 10.1159/000336713

(173) Swierczewska, M.; Lee, K. C.; Lee, S. What Is the Future of PEGylated Therapies? *Expert Opin. Emerg. Drugs* **2015**, *20* (4), 531–536. DOI: 10.1517/14728214.2015.1113254

(174) Huckaby, J. T.; Jacobs, T. M.; Li, Z.; Perna, R. J.; Wang, A.; Nicely, N. I.; Lai, S. K. Structure of an Anti-PEG Antibody Reveals an Open Ring That Captures Highly Flexible PEG Polymers. *Commun. Chem.* **2020**, *3* (1), 1–8. DOI: 10.1038/s42004-020-00369-y

(175) Li, L. H.; Ju, T. C.; Hsieh, C. Y.; Dong, W. C.; Chen, W. T.; Hua, K. F.; Chen, W. J. A Synthetic Cationic Antimicrobial Peptide Inhibits Inflammatory Response and the NLRP3 Inflammasome by Neutralizing LPS and ATP. *PLoS One* **2017**, *12* (7), 1–17. DOI: 10.1371/journal.pone.0182057

(176) Steinstraesser, L.; Hirsch, T.; Schulte, M.; Kueckelhaus, M.; Jacobsen, F.; Mersch, E. A.; Stricker, I.; Afacan, N.; Jenssen, H.; Hancock, R. E. W.; Kindrachuk, J. Innate Defense Regulator Peptide 1018 in Wound Healing and Wound Infection. *PLoS One* **2012**, *7* (8), 1–7. DOI: 10.1371/journal.pone.0039373

(177) Mansour, S. C.; De La Fuente-Núñez, C.; Hancock, R. E. W. Peptide IDR-1018:

Modulating the Immune System and Targeting Bacterial Biofilms to Treat Antibiotic-Resistant Bacterial Infections. *J. Pept. Sci.* **2015**, *21* (5), 323–329. DOI: 10.1002/psc.2708

(178) Freitas, C. G.; Lima, S. M. F.; Freire, M. S.; Cantuária, A. P. C.; Júnior, N. G. O.; Santos, T. S.; Folha, J. S.; Ribeiro, S. M.; Dias, S. C.; Rezende, T. M. B.; Albuquerque, P.; Nicola, A. M.; De La Fuente-Núñez, C.; Hancock, R. E. W.; Franco, O. L.; Felipe, M. S. S. An Immunomodulatory Peptide Confers Protection in an Experimental Candidemia Murine Model. *Antimicrob. Agents Chemother.* **2017**, *61* (8), 1–11. DOI: 10.1128/AAC.02518-16

(179) Hilpert, K.; Winkler, D. F. H.; Hancock, R. E. W. Peptide Arrays on Cellulose Support: SPOT Synthesis, a Time and Cost Efficient Method for Synthesis of Large Numbers of Peptides in a Parallel and Addressable Fashion. *Nat. Protoc.* **2007**, *2* (6), 1333–1349. DOI: 10.1038/nprot.2007.160

(180) Frank, R. Spot-Synthesis: An Easy Technique for the Positionally Addressable, Parallel Chemical Synthesis on a Membrane Support. *Tetrahedron* **1992**, *48* (42), 9217–9232. DOI: 10.1016/S0040-4020(01)85612-X

Appendices

Appendix A

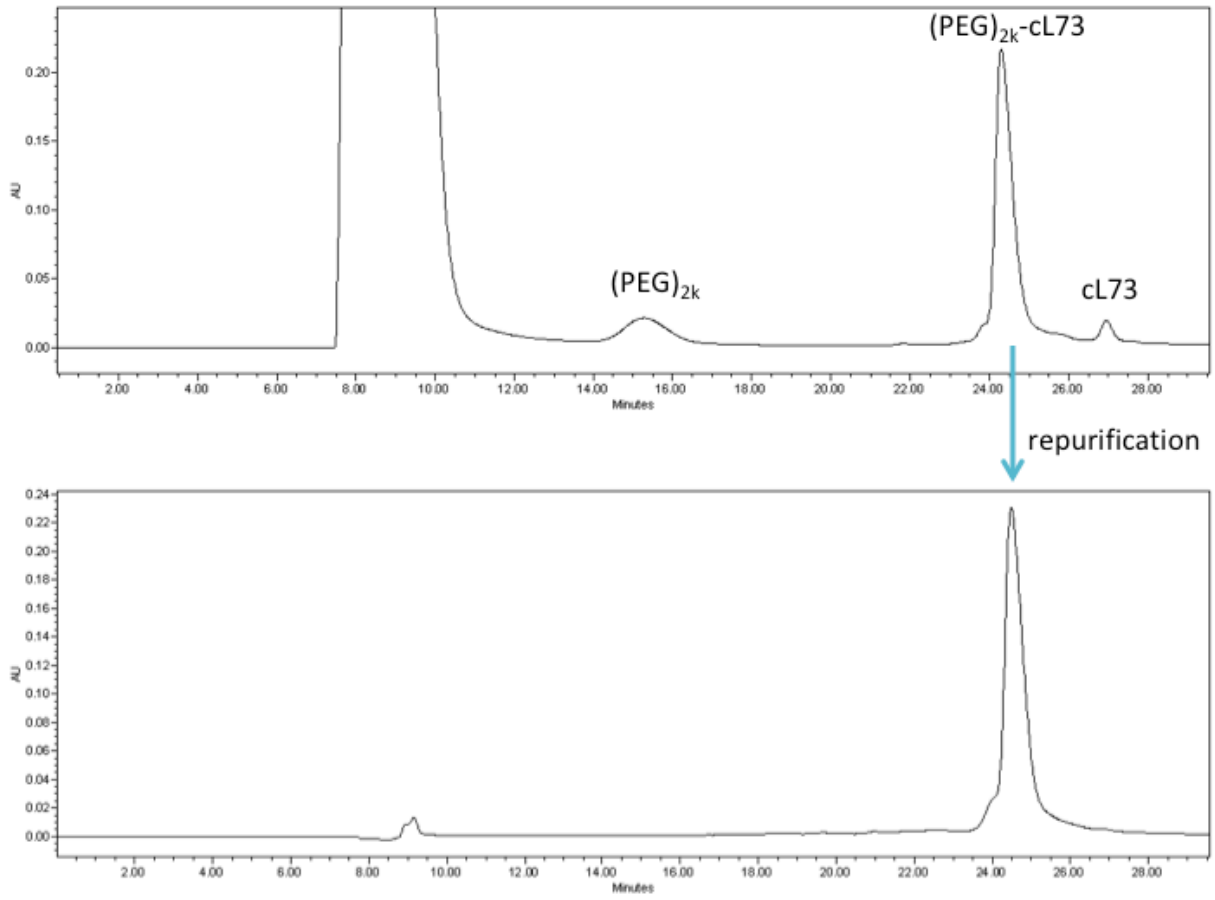

Figure A1. Confirmation of the purity of the PEGylated cL73 and 73Lc conjugates by HPLC. Top HPLC chromatogram of the conjugation mixture displays additional peaks for unreacted 2 kDa mPEG-maleimide and peptide cL73, while the bottom HPLC chromatogram of the repurified $(PEG)_{2k}$-cL73 bioconjugate does not. A large DMF solvent peak between 7.00 and 11.00 min can be seen in the top trace due to its presence in the conjugation mixture.

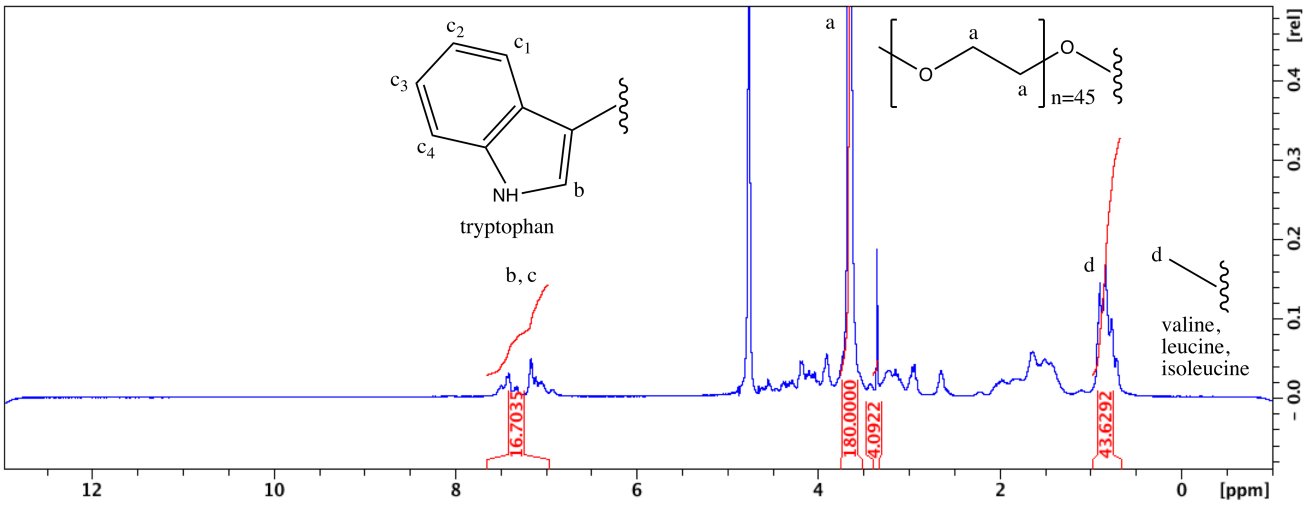

Figure A2. ^{1}H NMR spectrum of $(PEG)_{2k}$-cL73 (in D_2O). Using the integration of the H_a protons in 2 kDa mPEG (45 monomers x 4 H_a = 180 H_a), the number of aromatic protons from tryptophan residues was calculated to be 16.7 (theoretical: 15 assuming 1:1 PEG:peptide molar ratio) and the number of methyl protons from valine, leucine, and isoleucine residues was calculated to be 43.6 (theoretical: 42).

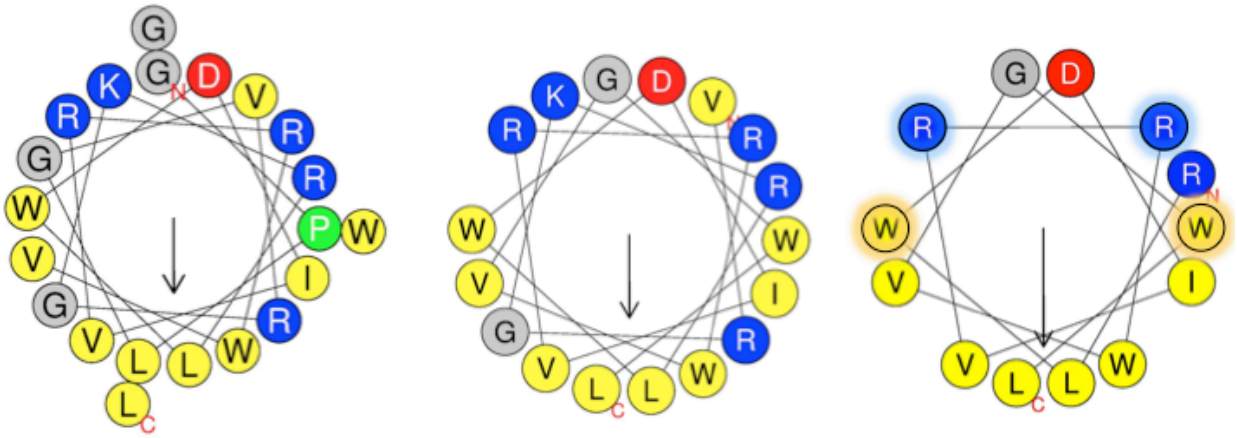

Figure A3. Helical wheel representations of peptides L73, MMP-cleaved L73, and 73. Cationic, anionic, and hydrophobic residues are displayed as blue, red, and yellow circles, respectively. Proline is shown in green. The hydrophobic moment is given as <μH>. Figures generated using: http://heliquest.ipmc.cnrs.fr/cgi-bin/ComputParams.py

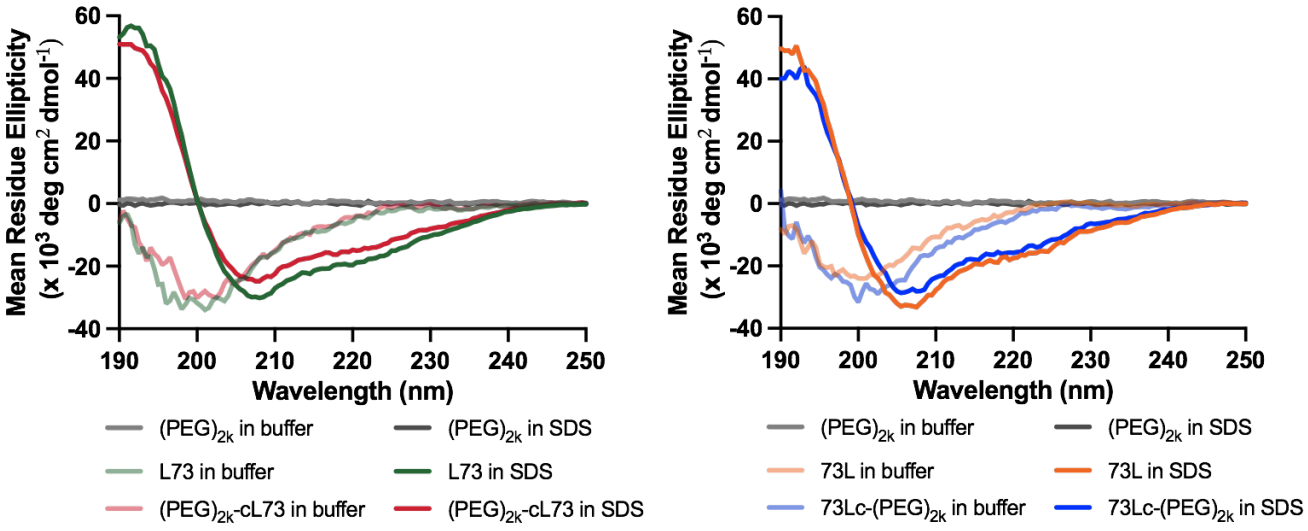

Figure A4. Circular dichroism spectra of L73 and 73L and their $(PEG)_{2k}$ conjugates in phosphate buffer or in the presence of SDS micelles.

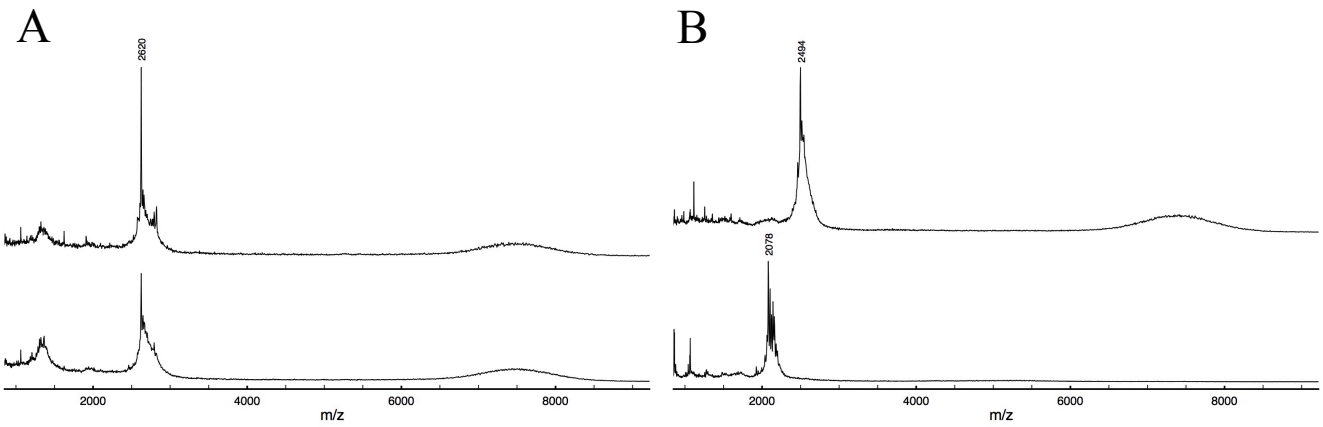

Figure A5. MALDI-TOF mass spectra of $(PEG)_{5k}$-cL73 (A) and 73Lc-$(PEG)_{5k}$ (B) before (top) and after (bottom) incubation with activated MMP-9.

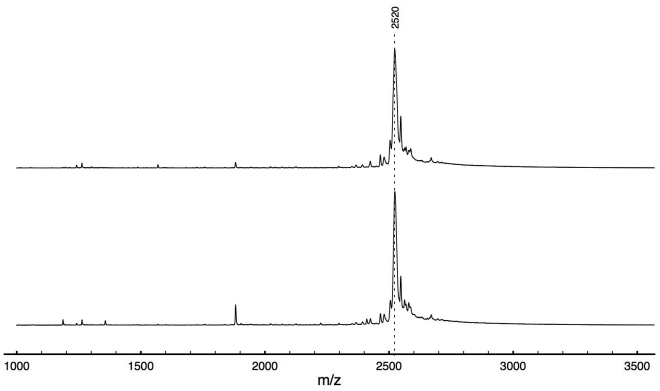

Figure A6. MALDI-TOF mass spectra of MMP-resistant D-L73 before (top) and after (bottom) incubation with activated MMP-9.

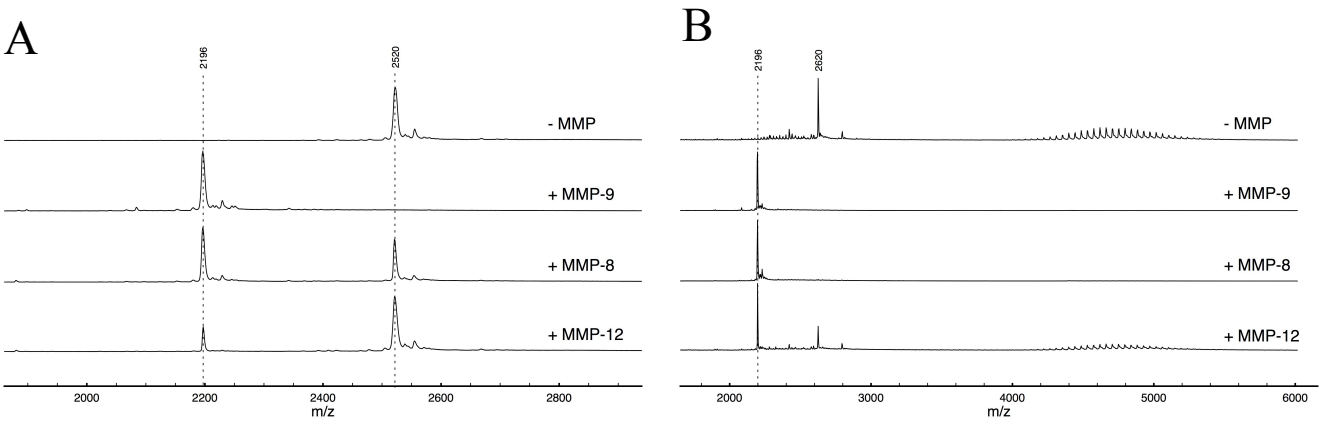

Figure A7. MALDI-TOF mass spectra of L73 (A) and $(PEG)_{2k}$-cL73 (B) before and after incubation with activated MMP-9, MMP-8 or MMP-12 catalytic domain.

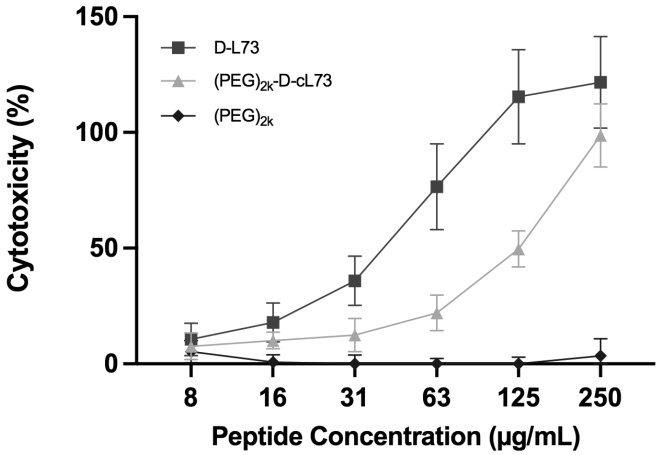

Figure A8. PBMC cytotoxicity upon exposure to the non-cleavable D-L73 and its corresponding conjugate, $(PEG)_{2k}$-D-cL73.

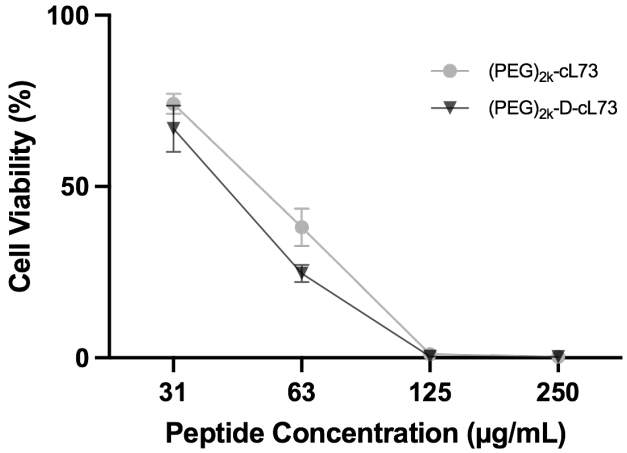

Figure A9. Cell viability of EA.hy926 endothelial cells after 48 h treatment with cleavable and non-cleavable conjugates in high serum (10% FBS) conditions.

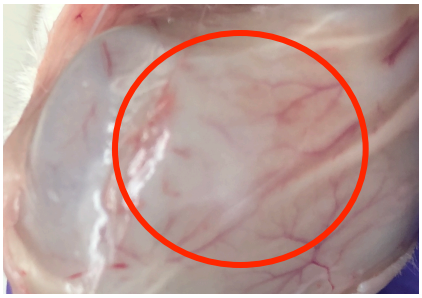

Figure A10. Image displaying the *in vivo* aggregation of L73 under the skin (circled in red) when injected at 15 mg/kg.

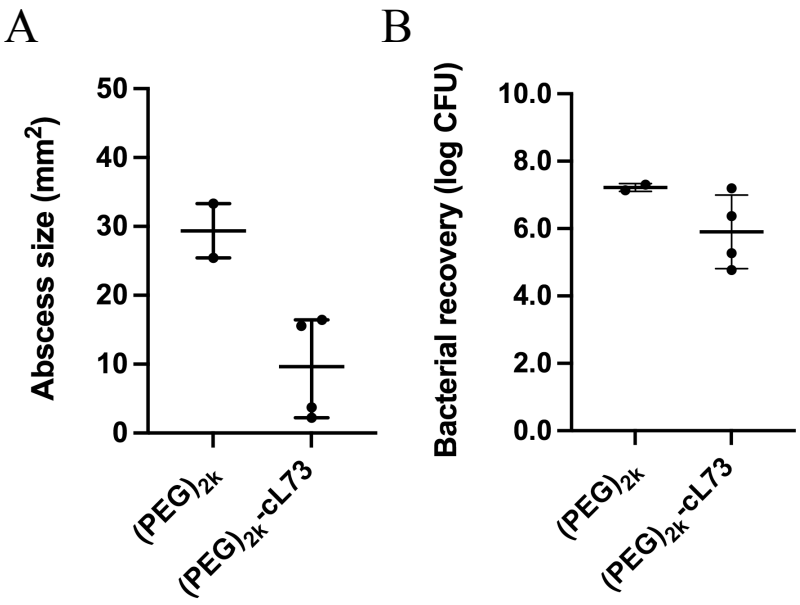

Figure A11. Efficacy of the $(PEG)_{2k}$-cL73 conjugate in a mouse infection abscess model at 50 mg/kg (28 mg/kg peptide concentration). Plots of abscess size (A) and bacterial load (B) are displayed.

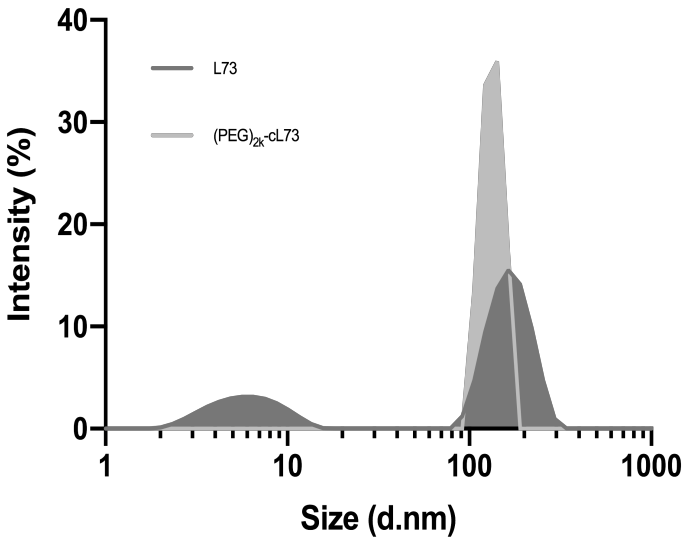

Figure A12. Aggregation profiles of the constructs in PBS as determined by DLS.

.

Appendix B

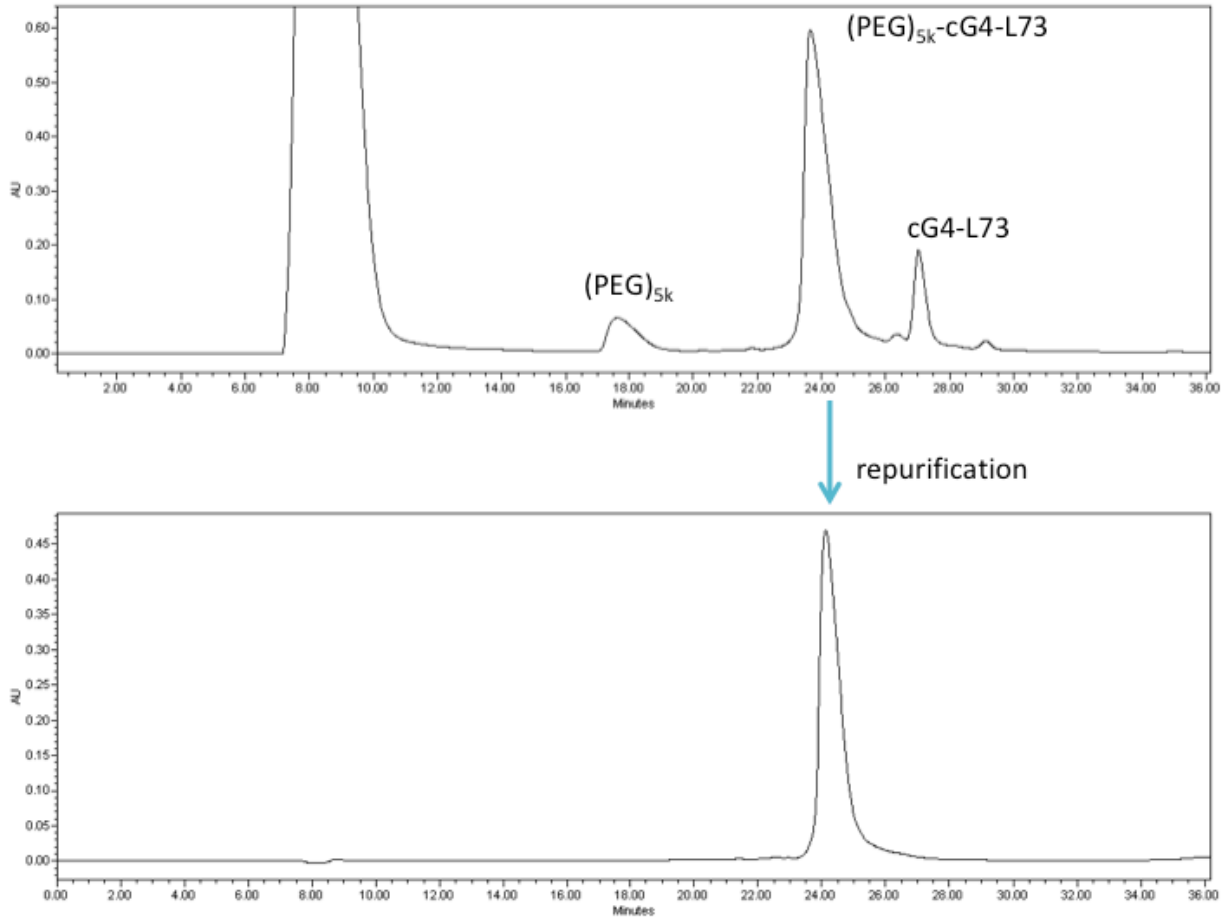

Figure B1. Confirmation of the purity of the PEGylated cG4-L73 conjugates by HPLC. Top HPLC chromatogram of the conjugation mixture displays additional peaks for unreacted 5 kDa mPEG-maleimide and peptide cG4-L73, while the bottom HPLC chromatogram of the repurified bioconjugate $(PEG)_{5k}$-cG4-L73 does not. A large DMF solvent peak between 7.00 and 11.00 min can be seen in the top trace due to its presence in the conjugation mixture. Analogous traces were obtained for the 10 and 22 kDa conjugates.